For assistance in accessing this document, please contact ghgreporting@epa.gov.

Subpart RR Monitoring, Reporting, and Verification (MRV) Plan
Mongoose AGI No. 1

Mitchell County, TX

Prepared for *Bayswater Operating Company LLC*
Denver, CO

By

Lonquist Sequestration, LLC
Austin, TX

Version 4.0
August 2024

INTRODUCTION

Bayswater Operating Company LLC (Bayswater) currently has a Class II acid gas injection (AGI) permit, issued by the Texas Railroad Commission (TRRC) for the Mongoose AGI No. 1 well (Mongoose), API No. 42-335-36013. The permit was issued March 10, 2023. This permit authorizes Bayswater to inject up to 6.9 million standard cubic feet per day (MMscf/D) of carbon dioxide (CO_2) and hydrogen sulfide (H_2S) into the Ellenburger formation at a depth of 8,300 feet (ft) to 9,000 ft with a maximum allowable surface pressure of 2,500 pounds per square inch gauge (psig). The Mongoose is a new well and is associated with the Mongoose Amine Treating Facility (the Plant) located in a rural area of Mitchell County, Texas, as shown in Figure 1.

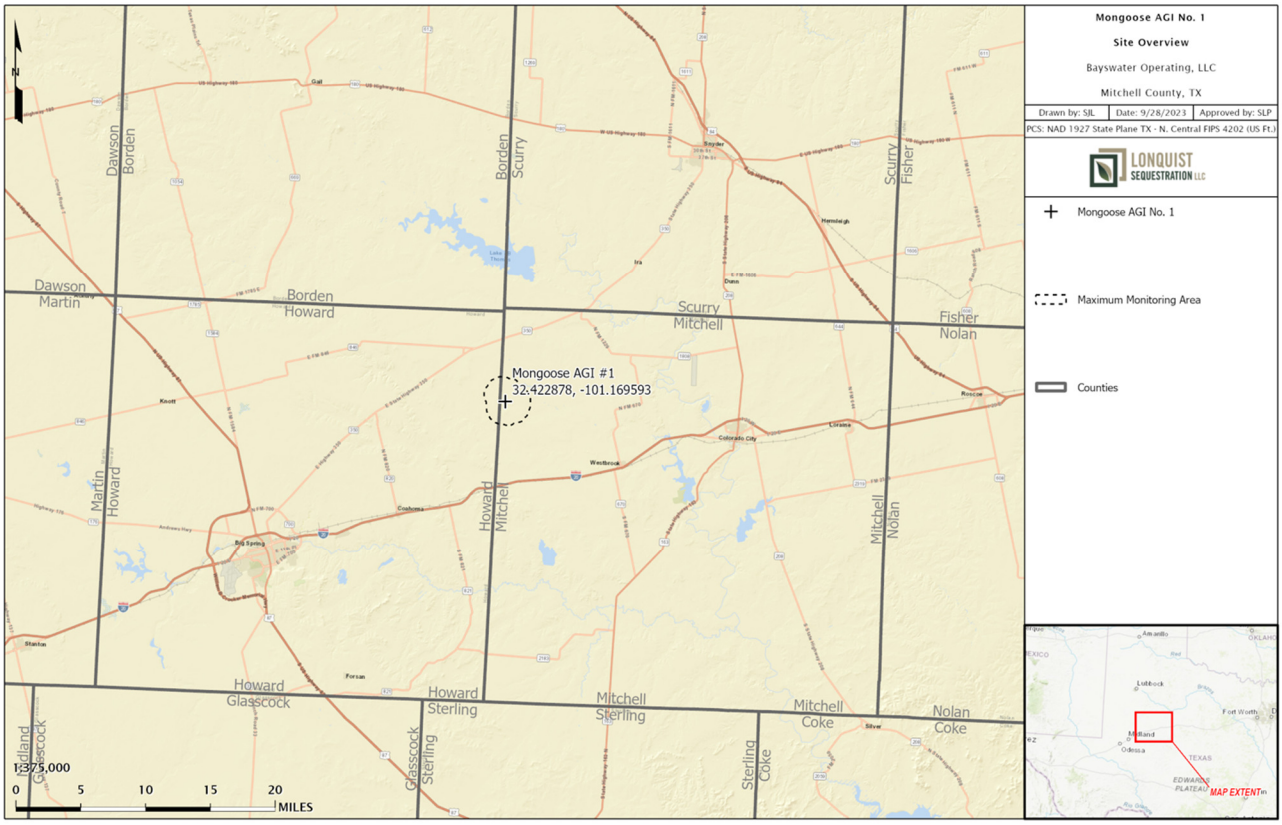

Figure 1 – Location of Mongoose AGI No. 1 Well

Bayswater is submitting this Monitoring, Reporting, and Verification (MRV) Plan to the Environmental Protection Agency (EPA) for approval under Title 40, U.S. Code of Federal Regulations (40 CFR) **98.440(a)**, Subpart RR, of the Greenhouse Gas Reporting Program (GHGRP). In addition to submitting this MRV plan to the EPA, Bayswater is also seeking TRRC approval to amend the existing Mongoose permit by increasing the permitted maximum quantity of injected treated acid gas (TAG) from 6.9 MMscf/D to 19.5 MMscf/D. Bayswater is planning to construct additional plant capacity coinciding with future production growth. Bayswater intends to inject into this well for approximately 40 years up to a maximum of 19.5 MMscf/D. The primary source of this injected CO_2 gas is the Mongoose Amine Treating Facility. Table 1 shows the expected composition of the gas stream to be sequestered. Table 2 shows the expected average daily volume of acid gas.

Table 1 – Expected Gas Composition

Component	Mol Percent
Carbon Dioxide	41.2%
Hydrogen Sulfide	58.8%

Table 2 – Expected Sequestered Gas Volumes

Contract Status	Avg. Rate (MMscf/D)
Committed	6.9
Proposed	12.6
Total	19.5

ACRONYMS AND ABBREVIATIONS

%	Percent (Percentage)
°C	Degrees Celsius
°F	Degrees Fahrenheit
AMA	Active Monitoring Area
BCF	Billion Cubic Feet
CH_4	Methane
CMG	Computer Modelling Group
CO_2	Carbon Dioxide (may also refer to other Carbon Oxides)
E	East
EOS	Equation of State
EPA	U.S. Environmental Protection Agency
ESD	Emergency Shutdown
FG	Fracture Gradient
ft	Foot (Feet)
GAPI	Gamma Units of the American Petroleum Institute
GAU	Groundwater Advisory Unit
GEM	Computer Modelling Group's GEM 2023.2
GHG	Greenhouse Gas
GHGRP	Greenhouse Gas Reporting Program
GL	Ground Level Elevation
H_2S	Hydrogen Sulfide
JPHIE	Effective Porosity (corrected for clay content)
mD	Millidarcy
mi	Mile(s)
MIT	Mechanical Integrity Test
MM	Million
MMA	Maximum Monitoring Area
MCF	Thousand Cubic Feet

MMcf	Million Cubic Feet
MMscf	Million Standard Cubic Feet
Mscf/D	Thousand Standard Cubic Feet per Day
MMscf/D	Million Standard Cubic Feet per Day
MRV	Monitoring, Reporting, and Verification
ν	Poisson's Ratio
N	North
NAD	North American Datum
NW	Northwest
OBG	Overburden Gradient
OSHA	Occupational Safety and Health Administration
PG	Pore Gradient
pH	Scale of Acidity
PISC	Post Injection Site Care
ppm	Parts per Million
psi	Pounds per Square Inch
psig	Pounds per Square Inch Gauge
S	South
SE	Southeast
SF	Safety Factor
SWD	Saltwater Disposal
TAC	Texas Administrative Code
TAG	Treated Acid Gas
TOC	Total Organic Carbon
TRRC	Texas Railroad Commission
UCZ	Upper Confining Zone
UIC	Underground Injection Control
USDW	Underground Source of Drinking Water
W	West

TABLE OF CONTENTS

Figures

Tables

Appendices

SECTION 1 – UIC INFORMATION

This section contains key information regarding the Underground Injection Control (UIC) Permit.

1.1 Underground Injection Control Permit Class: Class II

The TRRC regulates oil and gas activities in Texas and has primacy to implement the UIC Class II program. The TRRC classifies Mongoose AGI No. 1 as a UIC Class II well. A Class II permit was issued to Bayswater on March 10, 2023, under TRRC Rule 9 (Disposal into Non-Productive Formations) and Rule 36 (Oil, Gas, or Geothermal Resource Operation in Hydrogen Sulfide Areas).

1.2 UIC Well Identification Number

Mongoose AGI No. 1, API No. 42-335-36013, UIC No. 000125803

1.3 Reporter Number

- Facility Name: Mongoose Amine Treating Facility
- Greenhouse Gas Reporting Program ID: 586481
  - Currently reporting under Subpart UU
- Operator: Bayswater Operating Company LLC

1.4 Facility Address

Mongoose Amine Treating Facility
1625 County Road 280
Westbrook, Texas 79565

Coordinates in North American Datum of 1983 (NAD 83) for this facility:

Latitude: 32.4225396641
Longitude: -101.1714709142

SECTION 2 – PROJECT DESCRIPTION

This section discusses the geologic setting, planned injection process and volumes, and the reservoir and plume modeling performed for the Mongoose AGI No. 1 well.

The Mongoose injects both H_2S and CO_2 into Ellenburger formation at a depth of 8,300 ft to 9,000 ft, and approximately 7,825 ft below the base of the Underground Source of Drinking Water (USDW). Therefore, the well and the facility are designed to protect against the leakage out of the injection interval, to protect against contaminating other subsurface formations, and most critically to prevent surface releases.

2.1 Regional Geology

The Mongoose is located on the Eastern Shelf, as shown in the area map in Figure 2, within the greater Permian Basin of west Texas and New Mexico. The Permian Basin covers more than 86,000 square miles extending across an area approximately 250 miles wide and 300 miles long. The TRRC cites that the greater Permian Basin accounts for close to 40% of all oil production within the United States and nearly 15% of natural gas production. A general cross section of the basin is presented in Figure 3.

The ancestral Tobosa Basin was formed by structural flexure in the Precambrian basement at the southern margin of the North American Craton, or Laurentian Plate, during the Proterozoic (Popova, 2020). The modern form of the Permian Basin was shaped during the Carboniferous period due to the collision between Laurasia and Gondwana forming the supercontinent Pangea. The following uplift of the Central Basin Platform differentiated the greater basin into the Delaware Basin in the west, and the Midland Basin in the east along with its surrounding shelf margins (Popova, 2020).

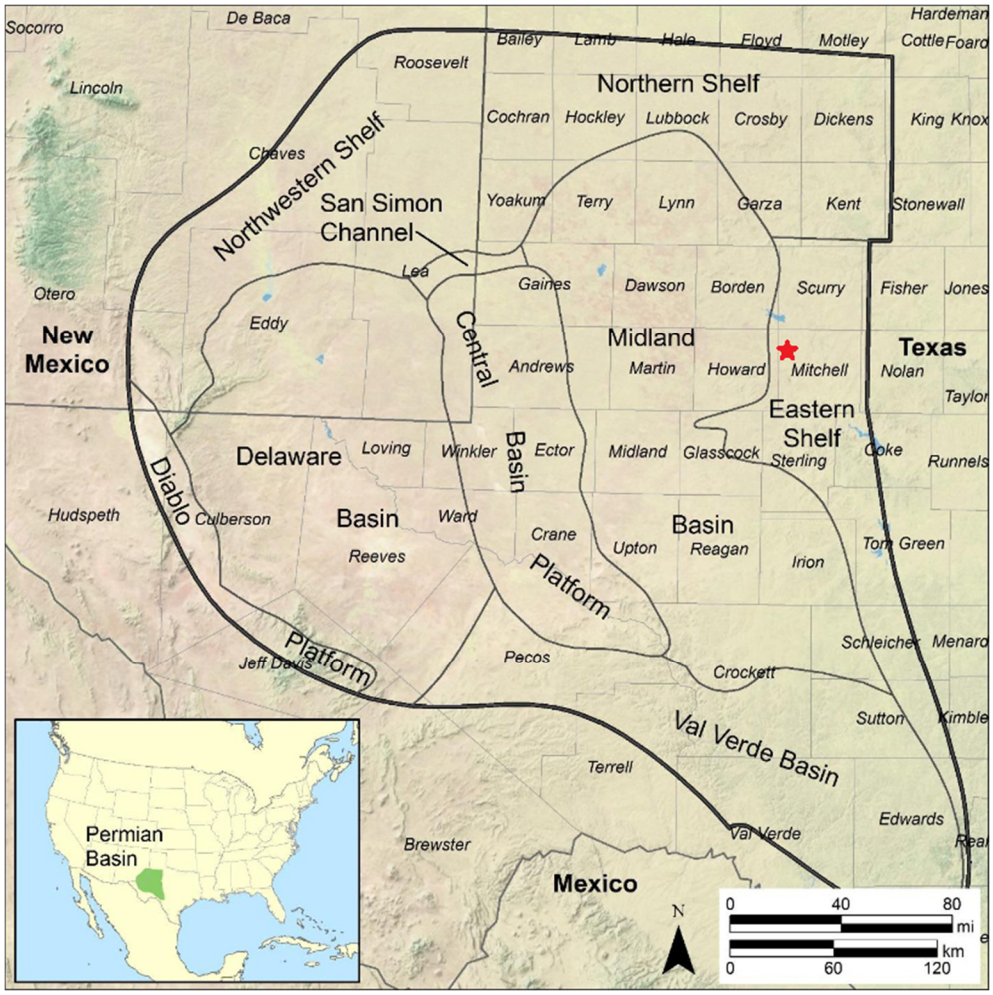

Figure 2 – Overview map of the Permian Basin including subregion names and counties. The red star represents the approximate location of the Mongoose AGI No. 1 (Scanlon, Reedy, Male, & Walsh).

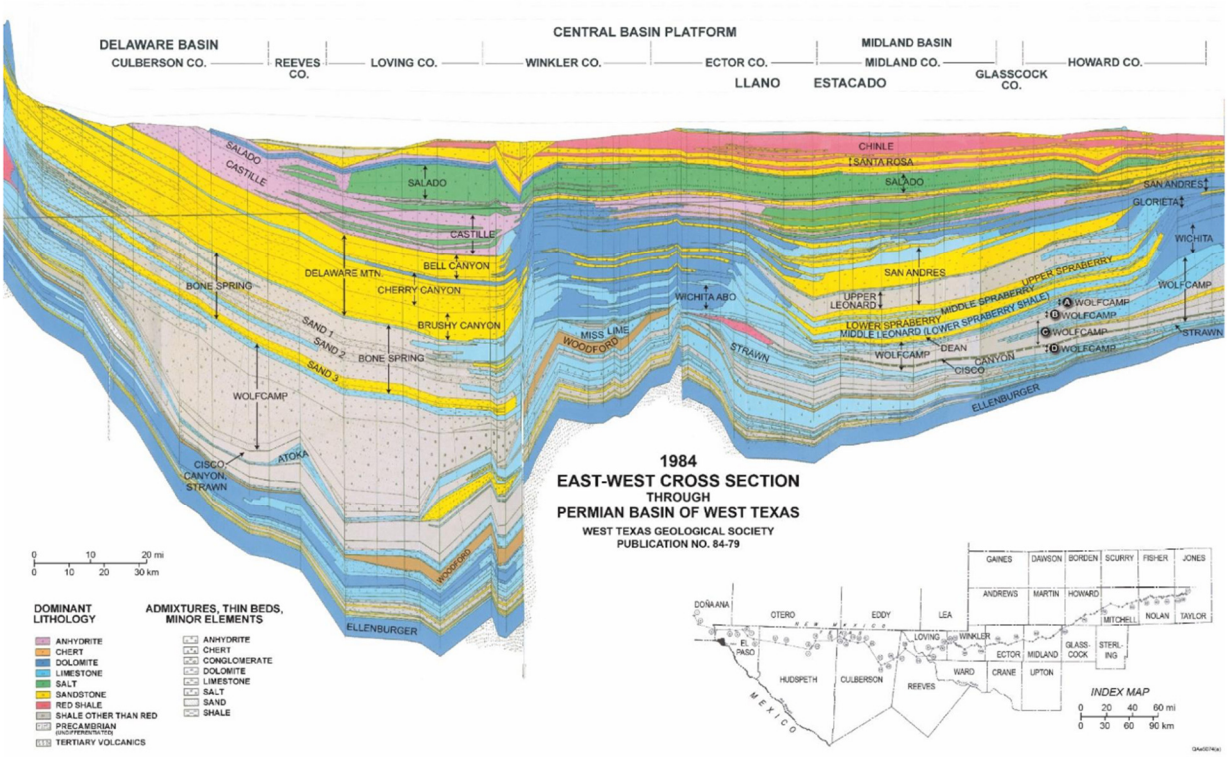

Figure 3 – Permian Basin East—West Cross Section (Scanlon, Reedy, Male, & Walsh)

The target injection interval for the Mongoose is the Ellenburger formation. The Ellenburger Group is part of an extensive shallow water carbonate platform known as the Great American Carbonate Bank, which covered much of the Laurentian landmass during the lower Ordovician (Sanchez, Loughry, & Coringrato, 2019). The Ellenburger is of lower Ordovician age and underlies the Woodford formation on the Eastern Shelf. The contact between the Ellenburger and Woodford represents an angular unconformity separated by roughly 110 million years of erosion and halted deposition (Sanchez, Loughry, & Coringrato, 2019). Many formations that are present within the Midland Basin are eroded and not seen upon reaching the Eastern Shelf. A cross section showing these truncations is displayed in Figure 5.

A generalized stratigraphic column of the Eastern Shelf is shown in Figure 4, with the target-injection formation indicated by the red star and historically productive formations indicated in the green stars. The Ellenburger formation is roughly 900 ft thick on the Eastern Shelf as shown by the isopach thickness map in Figure 6 (Loucks, Review of the Lower Ordovician Ellenburger Group of the Permian Basin, West Texas, 2006). On the Eastern Shelf, the Ellenburger formation dips to the west-southwest, towards the Midland Basin, and its subsea depth is roughly 6,000 ft (Sanchez, Loughry, & Coringrato, 2019). Figure 7 displays a structure map of the Ellenburger formation. Being far from any major sources of terrigenous clastic sediment input and at a time of a greenhouse climate leading to warm waters created an ideal setting primed for massive carbonate production during the Ellenburger deposition (Waite, 2021). The depositional facies associated with the Ellenburger on the Eastern Shelf is primarily within the restricted shelf depositional setting. Predominant pore types of this group determined by Holtz and Kerans are “ooid grainstone; ooid-peloid packstone-grainstone”

and reservoirs tend to be of good porosity and moderate permeability (Loucks, Review of the Lower Ordovician Ellenburger Group of the Permian Basin, West Texas, 2006).

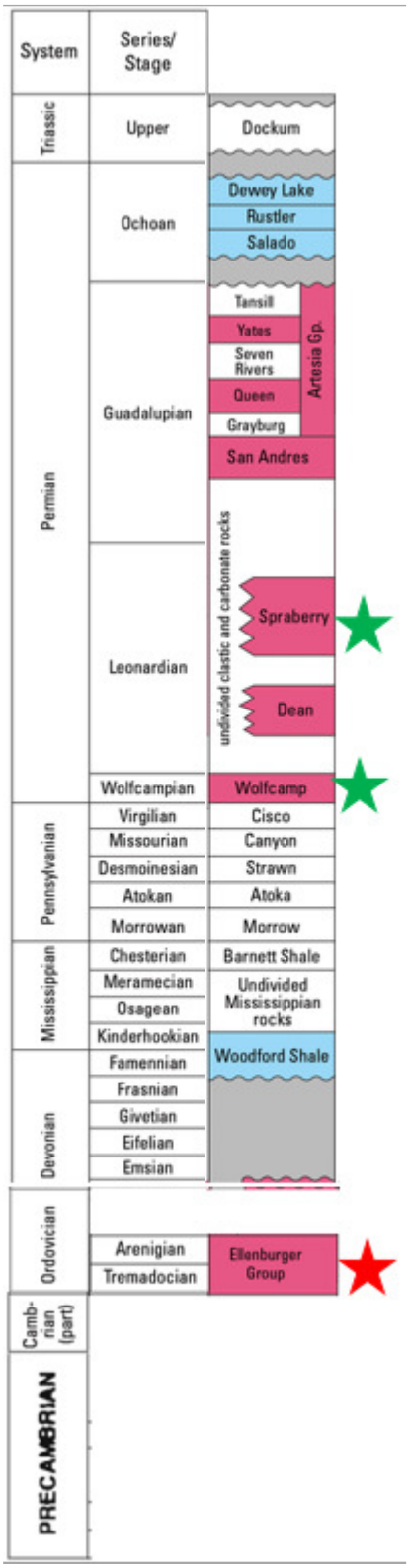

Figure 4 – Generalized Stratigraphic Column of the Eastern Shelf

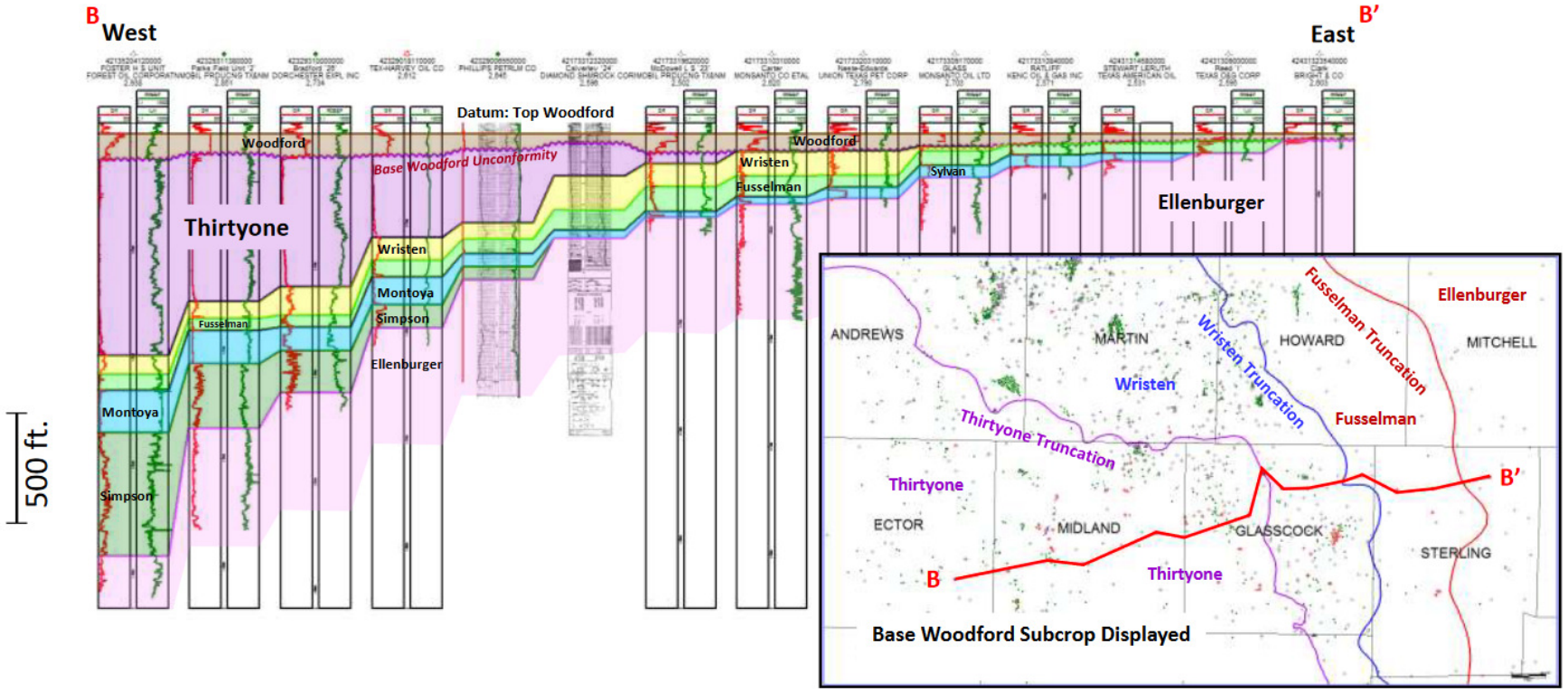

Figure 5 – Cross section indicating formation truncations when approaching the Eastern Shelf (Waite, 2021).

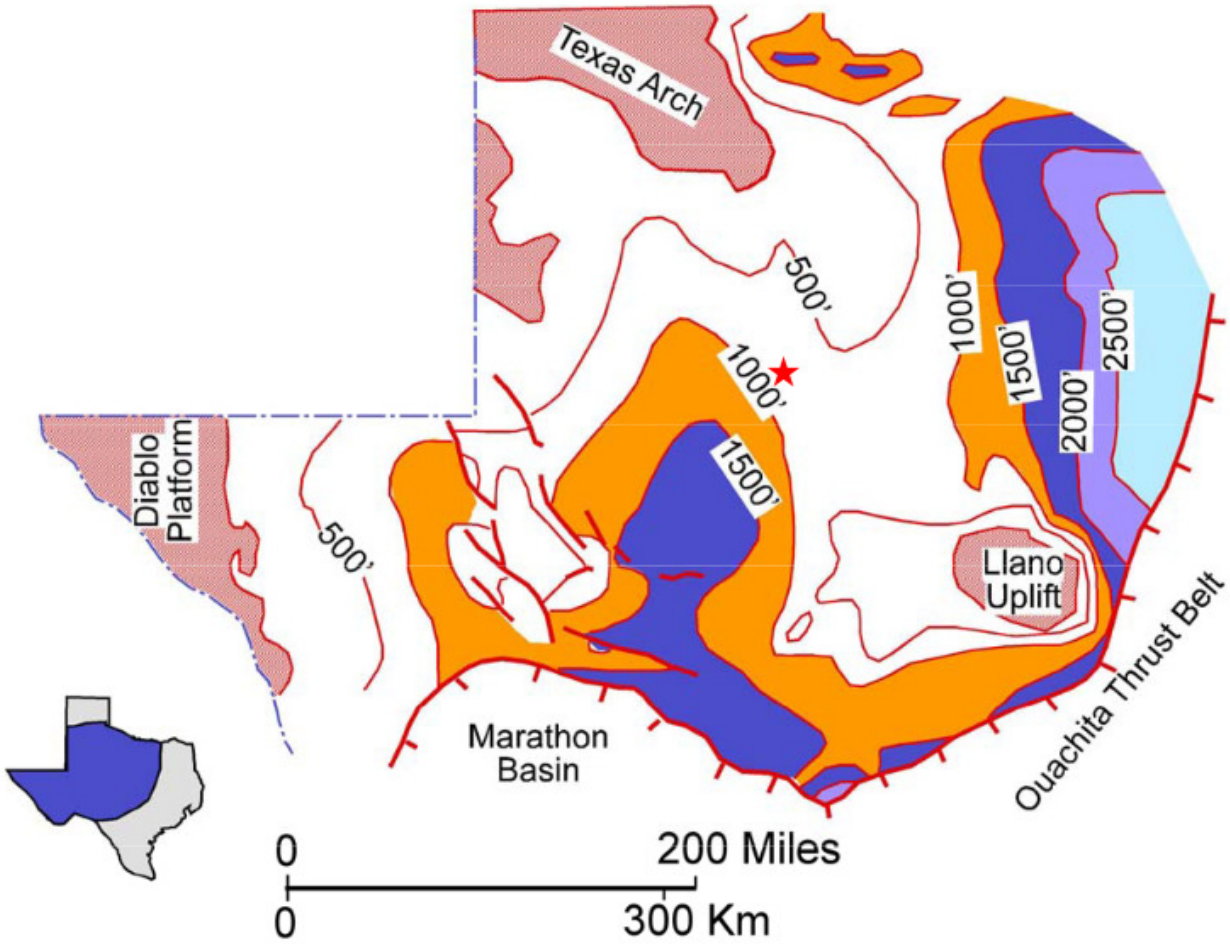

Figure 6 – Ellenburger Group Isopach Map (Loucks, Review of the Lower Ordovician Ellenburger Group of the Permian Basin, West Texas, 2006)

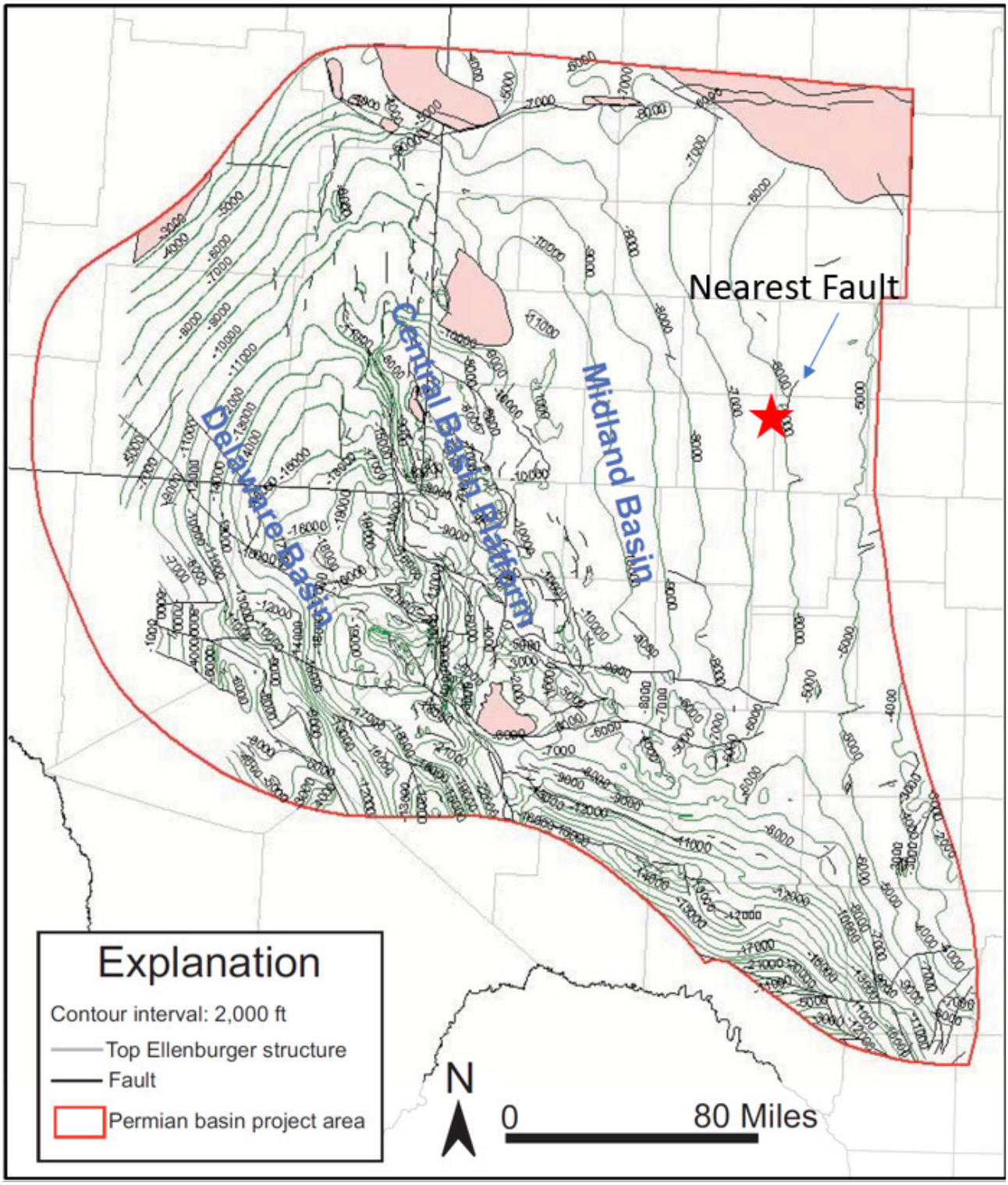

Figure 7 – Structure map referencing the top of the Ellenburger formation at subsea depth.

The lower Ordovician period on the Eastern Shelf was characterized by a restricted and low-energy shelf environment. The shelf was composed of a consistent sequence of gray to dark-gray dolomite, which had a fine to medium crystalline texture. Within this dolomite, there were irregular mottling patterns, likely indicative of bioturbation structures. Mudstone and peloid-wackestone, although in

smaller quantities, were also observed in the area (Kerans, 1990). To visually represent these different depositional environments and their corresponding lithologies, a map is presented in Figure 8. Due to a decrease in sea levels and subsequent exposure to air, a large portion of the Ellenburger formation underwent significant "karsting" and dolomitization. This karsting process resulted in the formation of extensive paleocave systems within the Ellenburger, which later collapsed and led to the creation of widespread brecciated and fractured carbonates. These formations are responsible for the occurrence of many Ellenburger reservoirs, according to Loucks (2006).

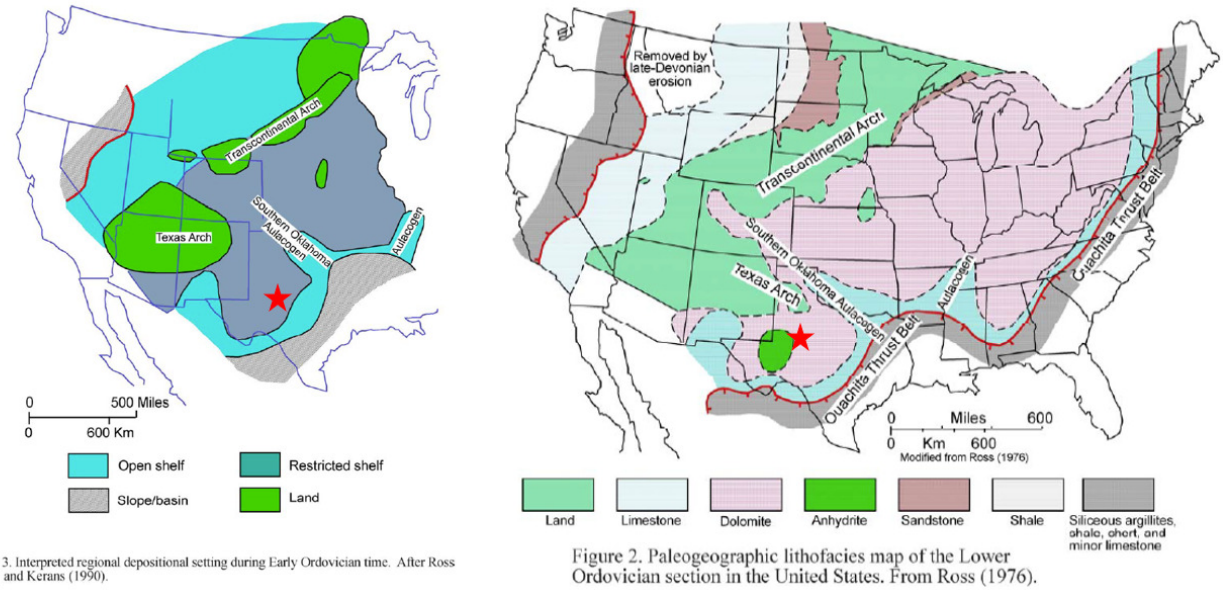

Figure 8 – Depositional Environments of the Lower Ordovician and Associated Lithofacies (Loucks, 2003)

In their research on saltwater disposal (SWD) injection into the Ellenburger, Pioneer Natural Resources describes three distinct facies within the formation as noted in the Figure 9 type log. The upper and middle facies are composed of fracture breccia, breccia fabrics, and matrix-supported breccia, which coincide with collapsed paleo cave facies as described by Loucks. The lower unit does not exhibit these characteristics but shows a high volume of small vugs (inch-scale) and large-dissolution features (foot-scale) and represents an area of the Ellenburger with elevated porosity and permeability (Sanchez, Loughry, & Coringrato, 2019).

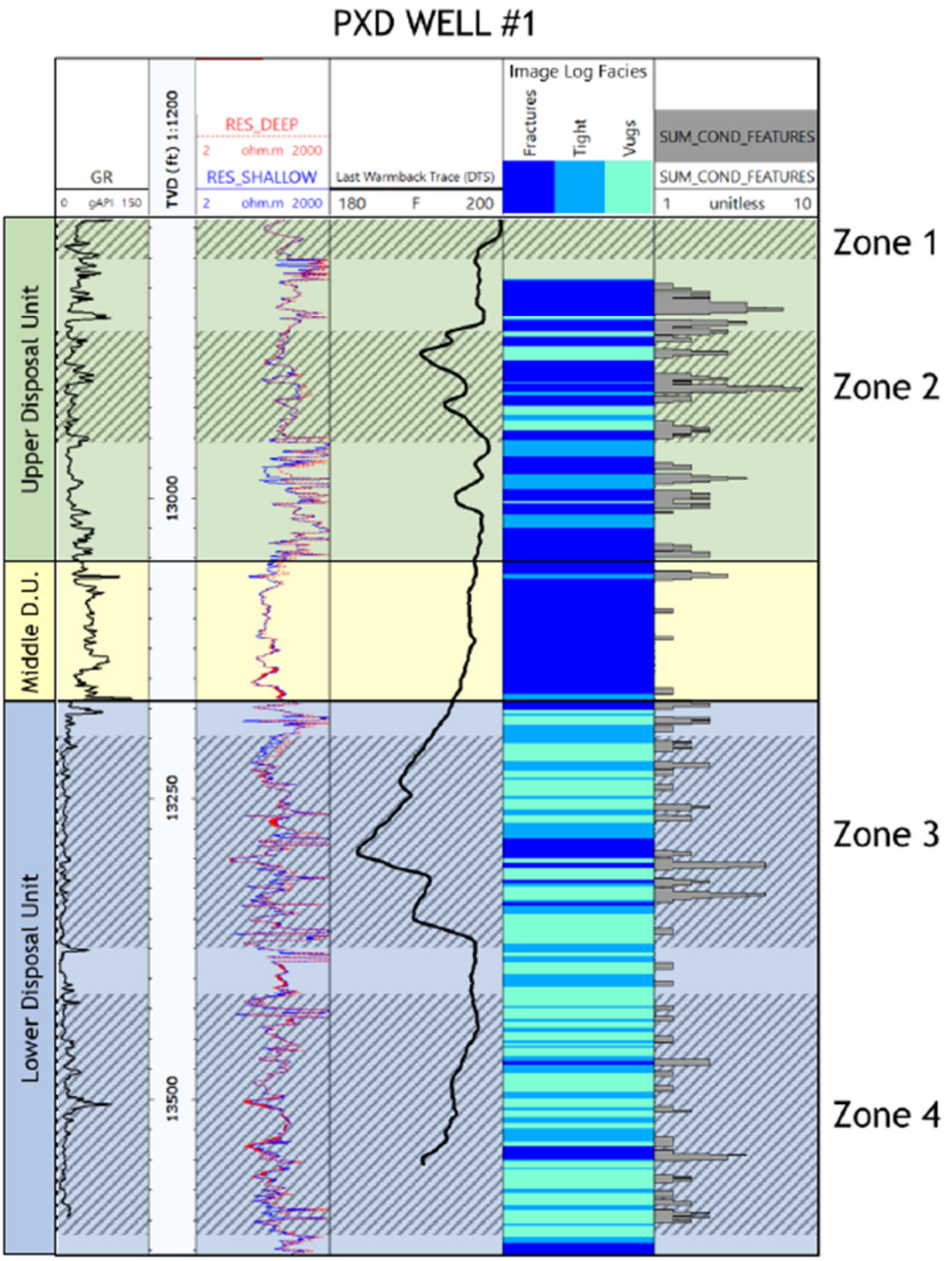

Figure 9 – Type Log and Disposal Units and Zones from PXD Well No. 1 (Sanchez, Loughry, & Coringrato, 2019)

2.1.1 Regional Faulting

The modeled area near the Mongoose does not show any faults. However, there is one fault interpreted northeast of the Mongoose location that lies outside the modeled area. This fault trend runs north-south in parallel with the dip. Figure 7 displayed this fault trend, which is the only example of such a trend within the area. Apart from this, the basin area is structurally inactive.

2.2 Site Characterization

The following section discusses site-specific geological characteristics of the Mongoose.

2.2.1 Stratigraphy and Lithologic Characteristics

Figure 10 shows an annotated well log for Mongoose that goes from the surface to the total depth. It indicates the injection and primary upper confining units with regional formation tops.

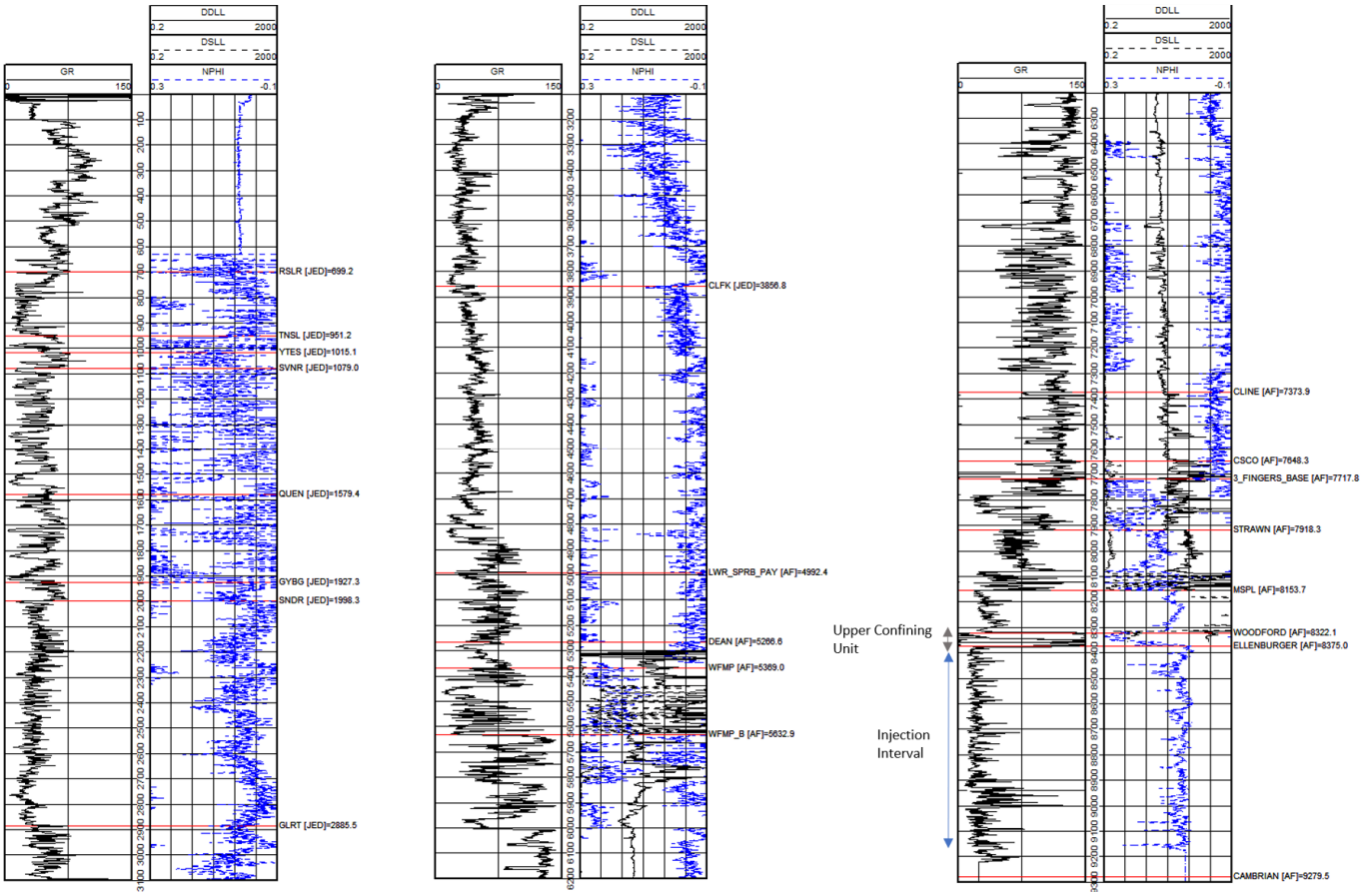

Figure 10 – Mongoose AGI No. 1 Type Log

2.2.2 Upper Confining Zone – Woodford Shale

The upper confining unit is the Upper Devonian age Woodford formation. The Woodford Shale, a late Devonian-aged organic-rich rock, was created through a widespread marine transgression. The deposition of the Woodford spread across a large area of the Permian Basin, producing a low-relief blanket of shale. The Woodford formation is an organic-rich petroleum source rock comprised of uncharacteristically highly radioactive, dark fissile shale and siltstone (Merril et al., 2015). Not only is the Woodford Shale a source of oil and gas, but it also acts as the primary source and sealant for the Wristen Group (Comer, 1991). As shown in Figure 5, the Wristen Group is a formation that lies directly below the Woodford to the west of the Mongoose location. The Wristen Group pinches out and is not found at the Mongoose location. However, the sealing nature of the Woodford, as described by Comer (1991), also provides confinement for the Ellenburger at this location. The Woodford formation overlies both unconformably and is diachronous to the underlying Ellenburger formation at the Mongoose location. The U.S. Geological Survey (USGS) CO_2 Storage Assessment defines the Woodford Shale as an appropriate seal due to its composition and regional extent for the Lower Paleozoic composite storage assessment unit (SAU) (Merril et al., 2015).

Rotary sidewall cores were taken from the offset well Buchanan 3111 #1XD (42-227-41307) in support of the acid-gas injection operations within the Mongoose. The Buchanan 3111 #1XD is approximately 10.4 mi. from the Mongoose as depicted in Figure 11. Figure 12 is a stratigraphic cross section showing the correlating cored Woodford formation (pink triangles representing cored intervals) in the Buchanan 3111 #1XD and the Mongoose wells. Routine core analysis, rock mechanics, and threshold entry pressure tests were performed on the core samples from the Woodford formation.

Core photos of the samples taken and analyzed within the Woodford are shown in Figure 13. The black shale unit exemplifies a well cemented unit with little to no fracturing. Routine core analysis was performed on these two samples, which includes bulk density, matrix permeability (as received and as under dry and Dean Stark extracted conditions), gas-filled porosity, gas saturation, grain density, porosity, oil saturation, and water saturation. The results are shown in Figure 14, with the footnotes at the base giving details on the testing processes of each value.

Under the dry and Dean Stark extracted conditions, permeability values of 2.2E-07 millidarcy (mD) were observed with even lower values of 4.87E-07 mD in the as-received samples. Porosities within the same sample were 1.3% when dried and .25% when gas-filled. These permeability and porosity values reflect optimal confining characteristics and validate the USGS assessment of an appropriate sealing formation for CO_2 storage.

To ensure these sealant properties would not be compromised by pressure influence of the injected fluid, a threshold entry pressure test was examined on these Woodford core samples. Figure 15 depicts a graph of permeability vs. pressure showing that, even with pressure increases up to 2,000 pounds per square inch (psi), permeability readings are still in the nano-darcy range. These values are shown in table form in Figure 16 against the pressures administered on the core, with the highest pressure being 2,000 psi. Given that permeability values were lowest (4.03E-07 mD) at 2,000 psi, it can be assumed that the threshold entry pressure of the Woodford formation was not met and

would be greater than 2,000 psi. Additionally, a table summary is depicted in Figure 17. These characteristics gathered from the Buchanan core provide a high level of detail into the confining nature of the Woodford Shale and alleviate any concerns of transmissibility through the confining unit.

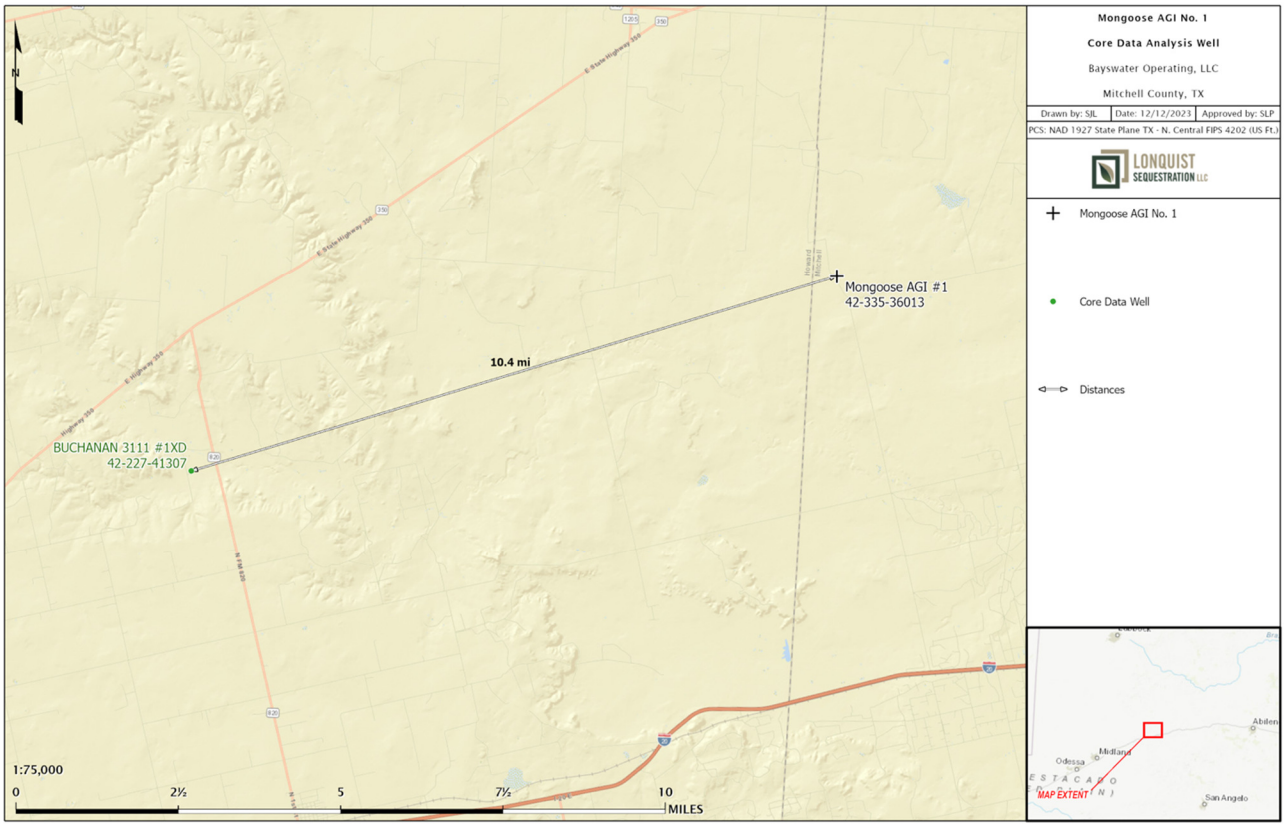

Figure 11 – Buchanan 3111 #XD location -- Offset well for Core Data

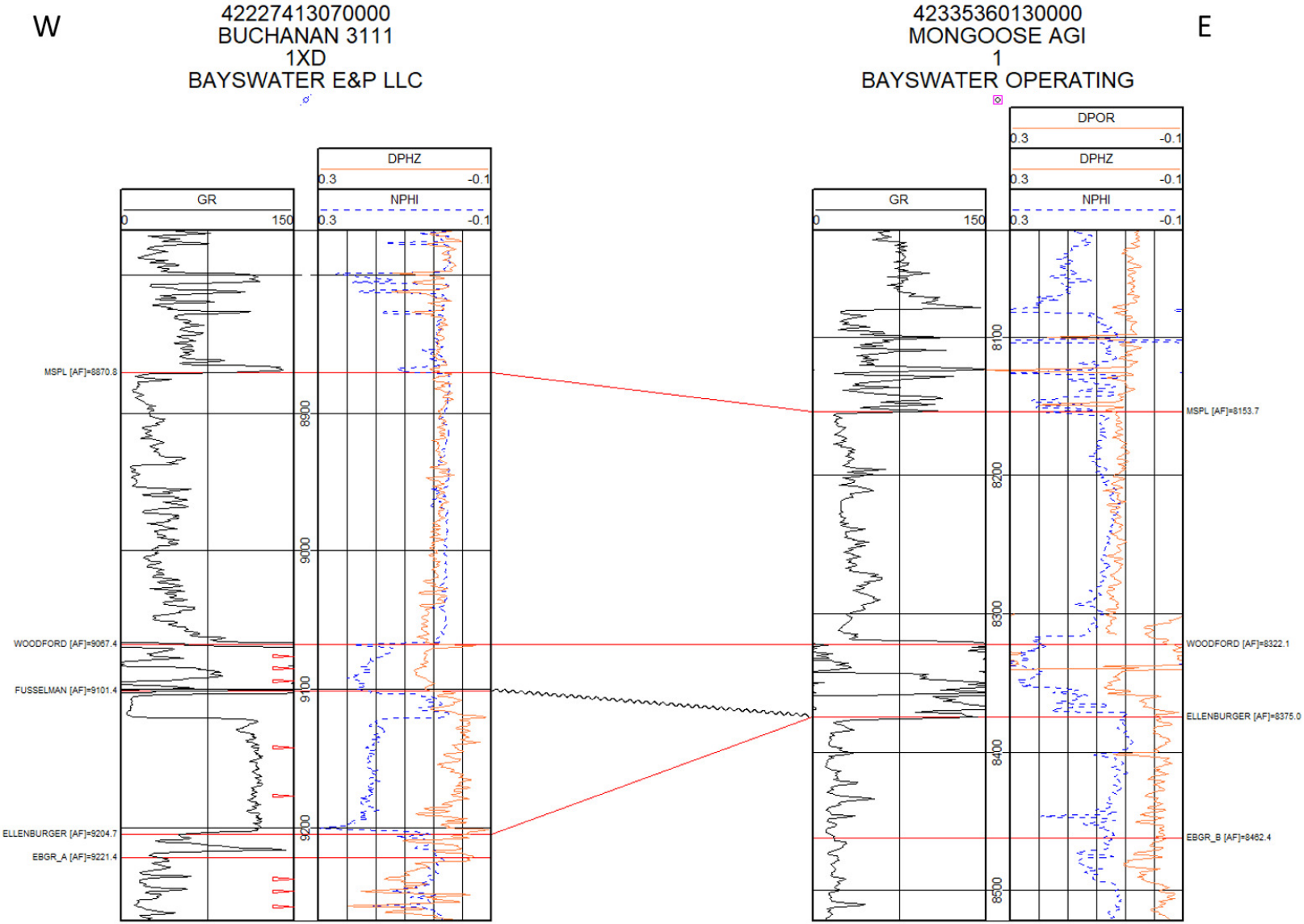

Figure 12 – Stratigraphic cross section of Mongoose AGI No. 1 and Buchanan 3111 #1XD depicting the Woodford and sidewall cores.

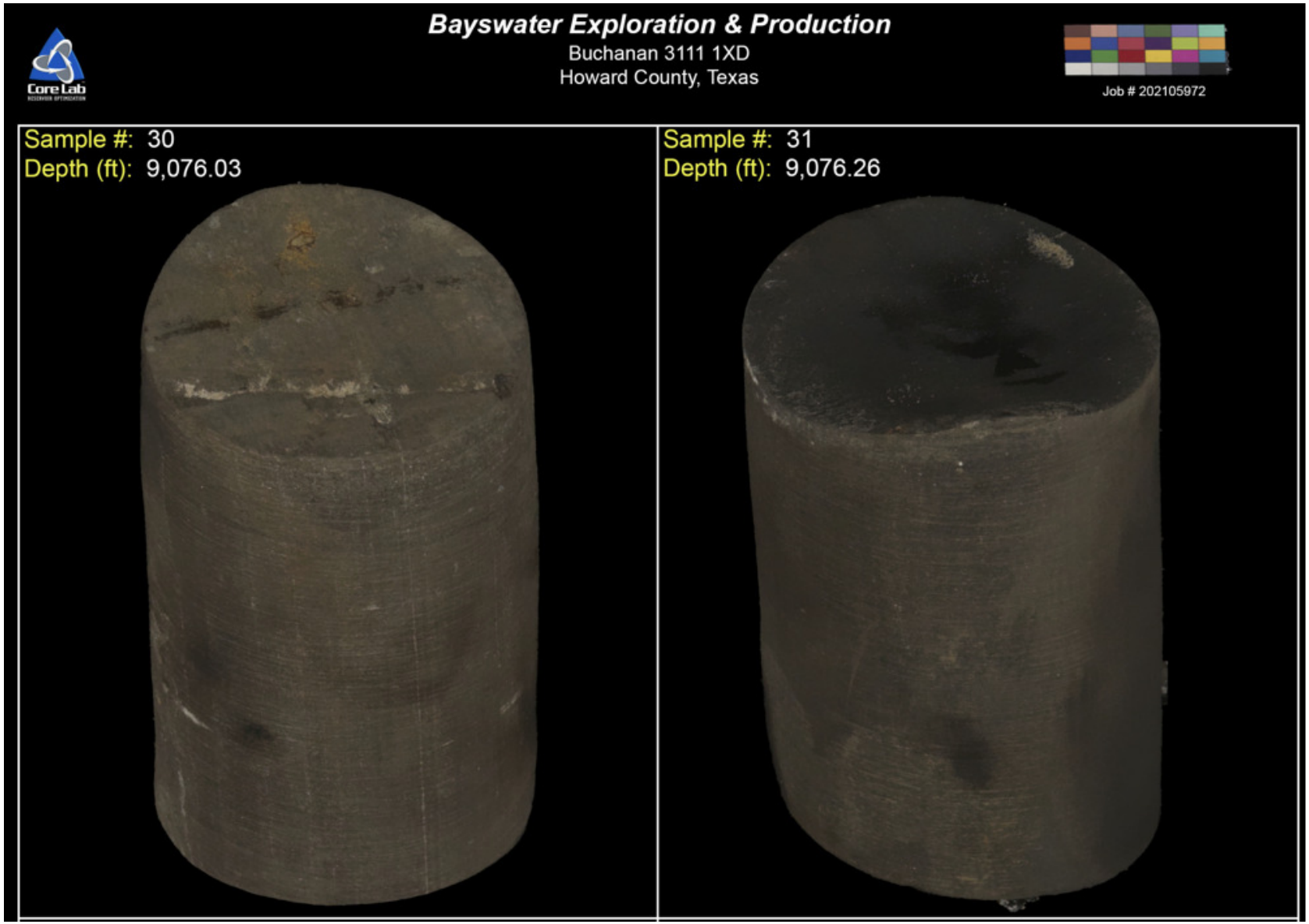

Figure 13 – Core Photo of Samples Within the Woodford Formation

Bayswater Exploration & Production
Buchanan 3111 1XD
Spraberry
Howard County, Texas

CL File No.: 202105972
Date: February 04, 2022
Analyst(s): MP

Shale Core Analysis (Rotary Sidewall Cores)

		As received				Dry & Dean Stark Extracted Conditions [2]				
Sample	Depth (ft)	Bulk Density (g/cc)	Matrix Permeability [1] (mD)	Gas-filled Porosity (%)	Gas Saturation (%)	Grain Density (g/cc)	Matrix Permeability [5] (mD)	Porosity (%)	Oil Saturation [3] (%)	Water Saturation [4] (%)
30,31	9076.03 - 9076.26	2.601	4.87E-09	0.25	18.9	2.624	2.22E-07	1.30	3.3	77.8

Footnotes:

Each sample is a composite of several rotary sidewall cores.

(1) Matrix Permeability is an effective Kg determined from pressure decay results on the fresh, crushed, 20/35 mesh size equivalent sample.
(2) Dean Stark extracted sample (20/35 mesh size) dried at 110 °C. Porosity and saturations are relative to total interconnected pore space.
(3) Oil volume computed assuming an oil density of 0.844 g/cc
(4) Water volume corrected assuming a brine concentration of 80000 ppm NaCl with an ambient density of 1.054 g/cc
(5) Matrix Permeability is an absolute Kg determined from pressure decay results on the clean and dry 20/35 mesh size equivalent sample.

Reference: "Development of Laboratory and Petrophysical Techniques for Evaluating Shale Reservoirs", GRI-95/0496, Gas Research Institute, April 1996

Figure 14 – Routine Core Analysis Within the Woodford Formation

THRESHOLD ENTRY PRESSURE ANALYSIS

Net Confining Stress: 2960 psi Temperature: 68°F

Fluid: 80,000 ppm NaCl

PETROLEUM SERVICES

Company: Bayswater Exploration & Production

Well: Buchanan 3111 1XD

Field: Spraberry

Location: Howard County, Texas

File: HOU-2105972

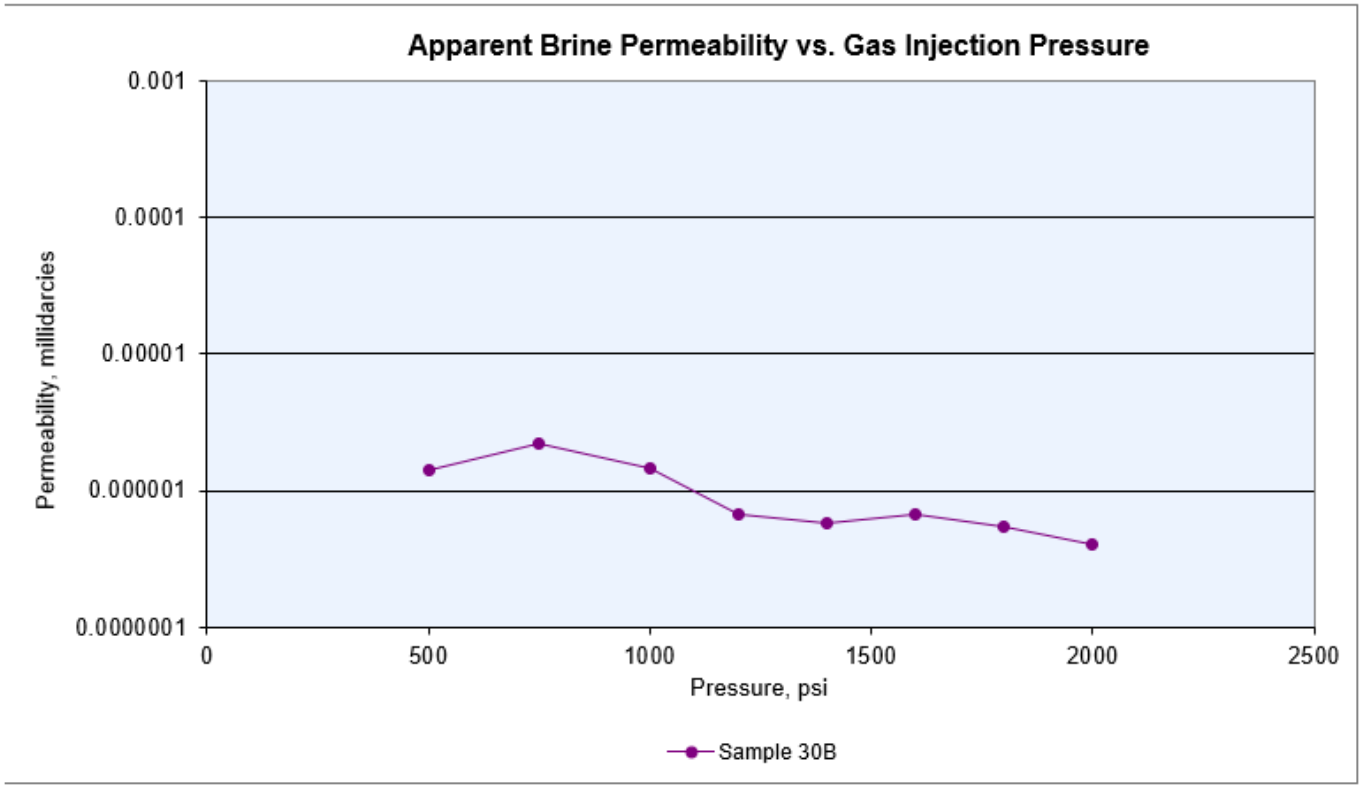

Figure 15 – Graph of Threshold Entry Pressure Within the Woodford Formation

THRESHOLD ENTRY PRESSURE ANALYSIS

Net Confining Stress: 2960 psi Temperature: 68°F
Fluid: 80,000 ppm NaCl

PETROLEUM SERVICES

Company: Bayswater Exploration & Production
Well: Buchanan 3111 1XD
Field: Spraberry
Location: Howard County, Texas

File: HOU-2105972

Sample 30B	
Gas Injection Pressure, psi	Permeability to Brine*, mD
500	1.44E-06
750	2.20E-06
1000	1.46E-06
1200	6.73E-07
1400	5.77E-07
1600	6.72E-07
1800	5.39E-07
2000	4.03E-07

Figure 16 – Tabular Data of the Threshold Entry Pressure Analysis Within the Woodford Formation

SUMMARY OF THRESHOLD ENTRY PRESSURE RESULTS

Net Confining Stress: 2960 psi Temperature: 68°F
Fluid: 80,000 ppm NaCl

PETROLEUM SERVICES

Company: Bayswater Exploration & Production
Well: Buchanan 3111 1XD
Field: Spraberry
Location: Howard County, Texas

File: HOU-2105972

Sample Number	Depth, feet	Length, cm	Diameter, cm	Final Permeability to Brine*, millidarcies	Threshold Entry Pressure, psi
30B	9076.03	2.67	2.54	4.03E-07	TEP>2000

* Apparent permeability to brine with humidified nitrogen displacing water

Figure 17 – Summary of Threshold Entry Pressure Analysis Within the Woodford Formation

2.2.3 Injection Interval – Ellenburger

2.2.3.1 Ellenburger

As described in the Regional Geology section, the Ellenburger at the Mongoose location is a widespread lower Ordovician carbonate deposited over the entire Permian area, indicating a relatively uniform depositional condition (Hendricks, 1964). However, post-depositional sequences have highly altered the section. These sequences have a large influence on the development of the reservoir quality within the injection interval and its ability to accept the proposed injectate. Further analysis based on regional and site-specific data was analyzed, as discussed below, to better understand the reservoir conditions at and around the Mongoose well location.

2.2.3.2 Ellenburger Porosity/Permeability Development

Facies in the low-energy, restricted shelf setting exhibit extensive dolomitization and are characterized by significant bioturbation, resulting in mottling patterns (Loucks, 2003). This dolomitization process has facilitated porosity development within the Ellenburger formation, accompanied by diagenetic leaching processes and the formation of secondary porosity features, including karsts and vugs. These same features were interpreted from the openhole logs in the Mongoose well and core from the Buchanan 3111 #1XD well. A total of 23 sidewall cores were taken within the Ellenburger formation in the Buchanan 3111 #1XD well, with 12 of those having routine core analysis performed on them. Figure 18 shows the results of the analysis.

Porosity values were primarily derived from offset openhole porosity logs within the Ellenburger section. Petrophysical analysis was performed on the offset logs to calculate an effective porosity curve, the porosity of a rock that is available to contribute to fluid flow, to better estimate porosity ranges with regards to injection within the Ellenburger. This is done by accounting for clay content and matrix lithology to better understand the varying porosity within the injection interval and how it relates to injection capacity. The ranges of effective porosity within the modeled wells are 0 to 39.4% with the mean being 4.6%. Figure 19 is a histogram depicting these porosity distributions within the seven modeled wells. These values are validated through similar ranges seen in the core results. The logical inference would be that, as the effective porosity increases, the reservoir quality for injection improves and the associated porosity increment leads to a rise in permeability.

A porosity to permeability relationship was created from this data with the outliers and non-applicable samples redacted. Additional regional data from Loucks (2003) was incorporated into the relationship to assist with the higher permeability ranges, to ensure that overestimates of permeability were not calculated. The data from Loucks (2003) is exemplified in Figure 20. A two-function porosity-permeability curve was developed from the regional and local core data. Figure 21 shows the equations and relationships where:

If Effective Porosity (Φeff) < 6.5%: $K(mD) = 7\ \ -08e^{3.3028*\Phi\text{eff}}$

If Effective Porosity (Φeff) > 6.5%: $K(mD) = 277.39\ln(\Phi e\quad) - 380.58$

These equations were extrapolated to all the wells within the model including the Mongoose. In Figure 22, the cross section of the Mongoose and Buchanan well is depicted. This illustration showcases the Ellenburger formation, with the sidewall cores from the Buchanan well represented by pink triangles. The calculated permeability curves resulting from the equations mentioned earlier are shown in red, while green represents the effective porosity. High permeability and porosity sections can be seen in both wells, most likely reflecting strata that had prolonged subaerial exposure creating the karst and vug features that will be targeted and utilized for injection. Figure 23 is a core photo from the Buchanan well depicting an example of what a vug feature within the Ellenburger can look like. These features will be taking the bulk of the injection and will be modeled within the area based on openhole log analysis.

Permeability ranges within the seven wells utilized in the model vary from 0 mD to 638 mD, with the mean being 40.822 mD. A histogram representing these ranges and distributions within the seven modeled wells is displayed in Figure 24. This range corroborates with Loucks (2003) and data recovered from the Buchanan well, and it can be concluded that the process used to determine the permeability distributions within the injection interval is valid.

Bayswater Exploration & Production
Buchanan 3111 1XD
Spraberry
Howard County, Texas

CL File No.: 202105972
Date: March 31, 2022
Analyst(s): MP

CMS-300 ROTARY SIDEWALL ANALYSIS

Sample Number	Depth (ft)	Net Confining Stress (psig)	Porosity (%)	Permeability Klinkenberg (md)	Permeability Kair (md)	b(air) psi	Beta ft(-1)	Alpha (microns)	Saturation Oil % Pore Volume	Saturation Water % Pore Volume	Grain Density (g/cm3)	Footnote
23	9236.98	2960	25.81	.259	.389	11.97	3.27E+09	2.75E+00	0.0	94.7	2.666	
21	9257.01	2960	4.77	.002	.009	104.71	2.14E+15	1.48E+04	1.2	66.1	2.746	(1)
19	9363.99	2960	5.23	5.17	5.81	2.07	1.75E+12	2.93E+04	4.1	66.9	2.800	(6)
15	9485.99	2960	3.41	.005	.016	62.63	3.24E+13	5.63E+02	2.3	64.6	2.838	(6)
13	9549.48	Ambient	1.55	N/A	N/A	N/A	N/A	N/A	1.9	44.7	2.829	(5)
12	9604.98	2960	1.63	.00006	.001	354.43	2.46E+18	5.38E+05	2.6	54.0	2.842	(1)
10	9712.03	Ambient	1.28	N/A	N/A	N/A	N/A	N/A	1.2	74.3	2.758	(5)
7	9835.05	2960	2.28	.001	.004	155.69	2.03E+16	4.48E+04	1.5	81.1	2.701	
6	9868.97	2960	3.43	.001	.003	166.37	3.03E+16	5.46E+04	0.9	81.6	2.827	
5	9892.03	2960	3.46	.001	.005	132.61	8.12E+15	2.84E+04	2.1	91.6	2.809	
4	9914.00	2960	5.46	659	669	0.18	1.07E+09	2.29E+03	0.7	58.7	2.835	(6)
3	9969.01	Ambient	11.18	N/A	N/A	N/A	N/A	N/A	1.7	42.9	2.846	(5),(6)

Figure 18 – Geologic and Petrophysical Parameters of the Ellenburger (Loucks, 2003)

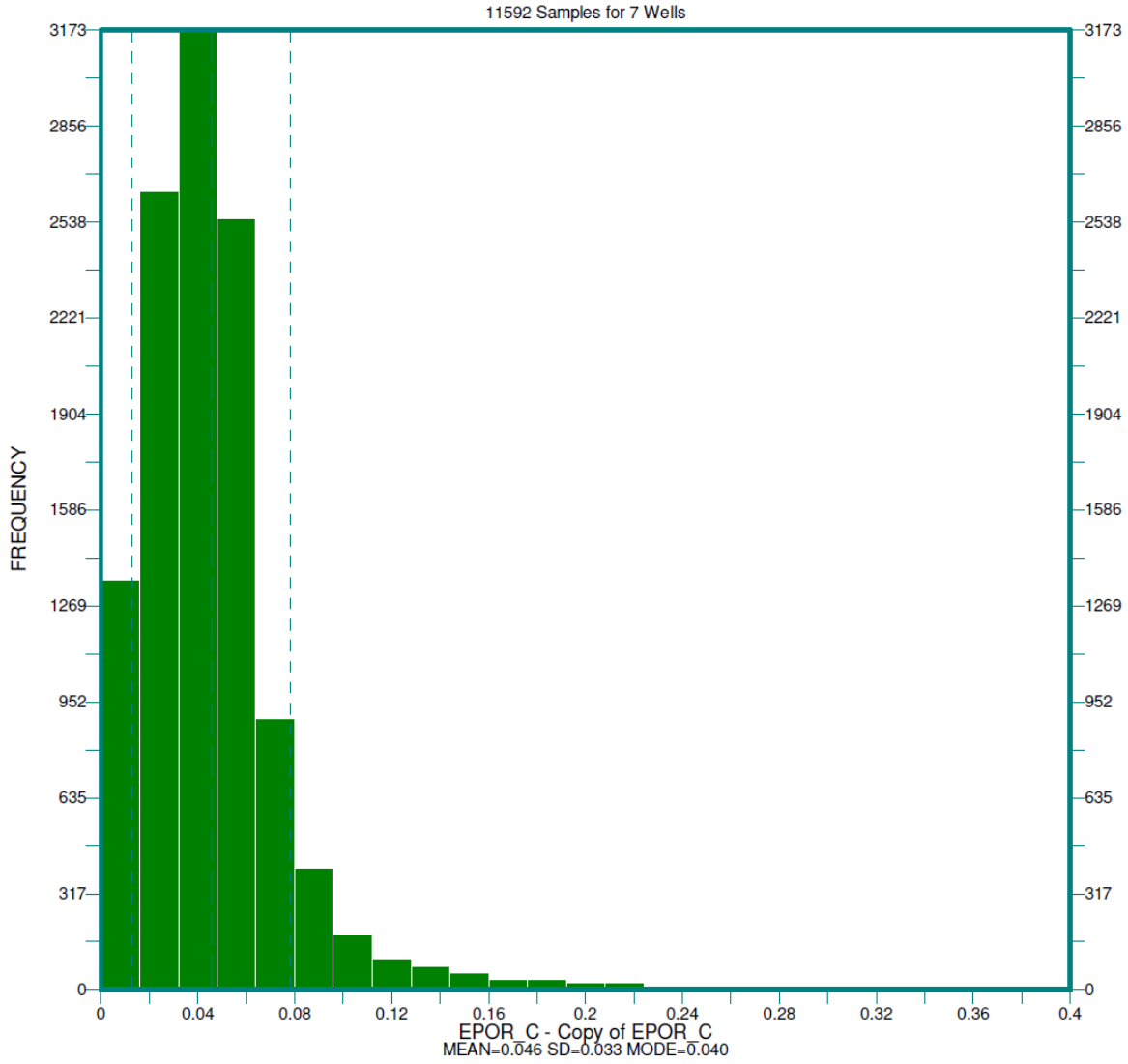

Figure 19 – Histogram of the Effective Porosity Distributions with the Seven Modeled Offset Wells

	Karst Modified	Ramp Carbonate	Tectonically Fractured Dolostone
Lithology	Dolostone	Dolostone	Dolostone
Depositional setting	Inner ramp	Mid- to outer ramp	Inner ramp
Karst facies	Extensive sub-Middle Ordovician	Sub-Middle Ordovician, sub-Silurian/Devonian, sub-Mississippian, sub-Permian/ Pennsylvanian	Variable intra-Ellenburger, sub-Middle Ordovician
Fault-related fracturing	Subsidiary	Subsidiary	Locally extensive
Dominant pore type	Karst-related fractures and interbreccia	Intercrystalline in dolomite	Fault-related fractures
Dolomitization	Pervasive	Partial, stratigraphic and fracture-controlled	Pervasive

Parameter	Karst Modified	Ramp Carbonate	Tectonically Fractured Dolostone
Net pay (ft)	Avg. = 181, Range = 20 - 410	Avg. = 43 Range = 4 - 223	Avg. = 293, Range = 7 - 790
Porosity (%)	Avg. = 3 Range = 1.6 - 7	Avg. = 14 Range = 2 - 14	Avg. = 4 Range = 1 - 8
Permeability (md)	Avg. = 32 Range = 2 - 750	Avg. = 12 Range = 0.8 - 44	Avg. = 4 Range = 1 - 100
Initial water saturation (%)	Avg. = 21 Range = 4 - 54	Avg. = 32 Range = 20 - 60	Avg. = 22, Range = 10 - 35
Residual oil saturation (%)	Avg. = 31 Range = 20 - 44	Avg. = 36 Range = 25 - 62	NA

Figure 20 – Regional Geologic and Petrophysical Parameters of the Ellenburger (Loucks, 2003)

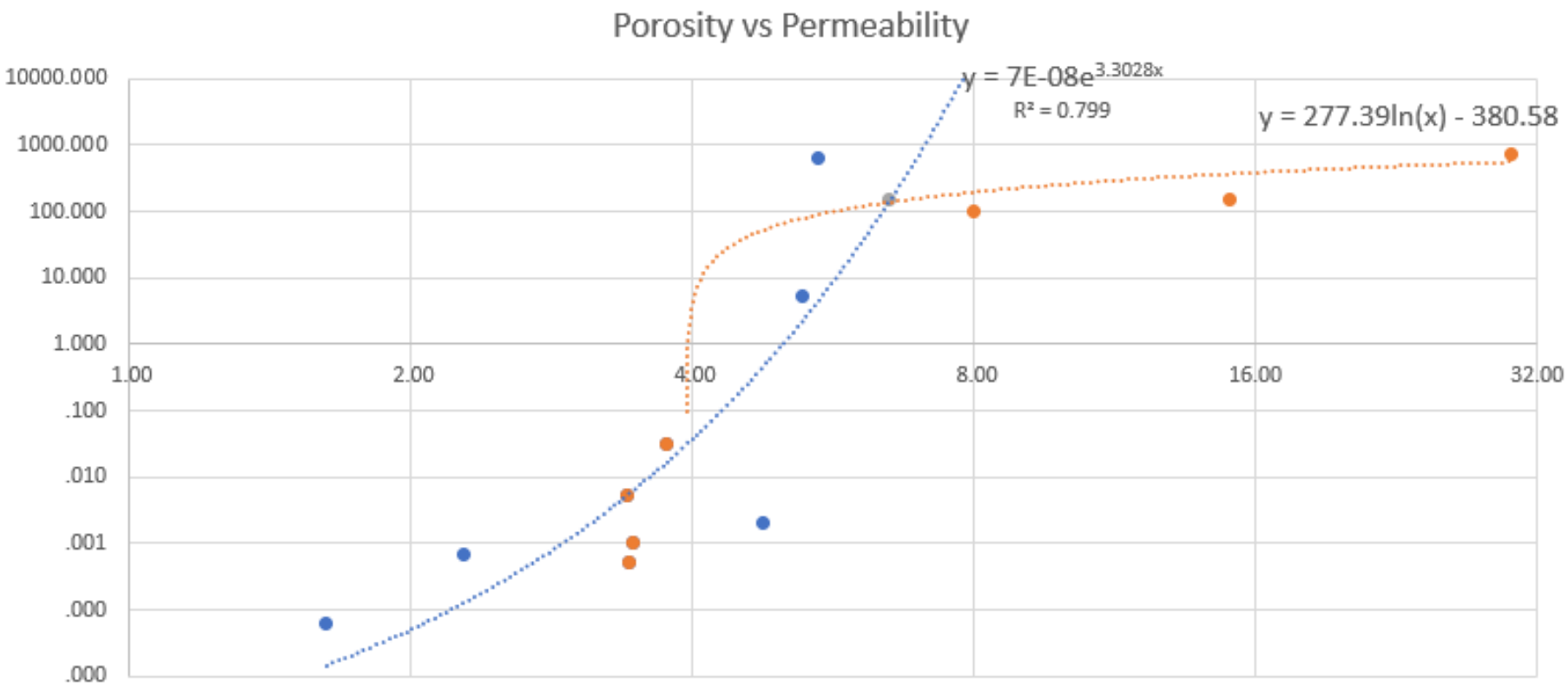

Figure 21 – Two-Function Porosity vs. Permeability Relationship Utilizing Local and Regional Core Data

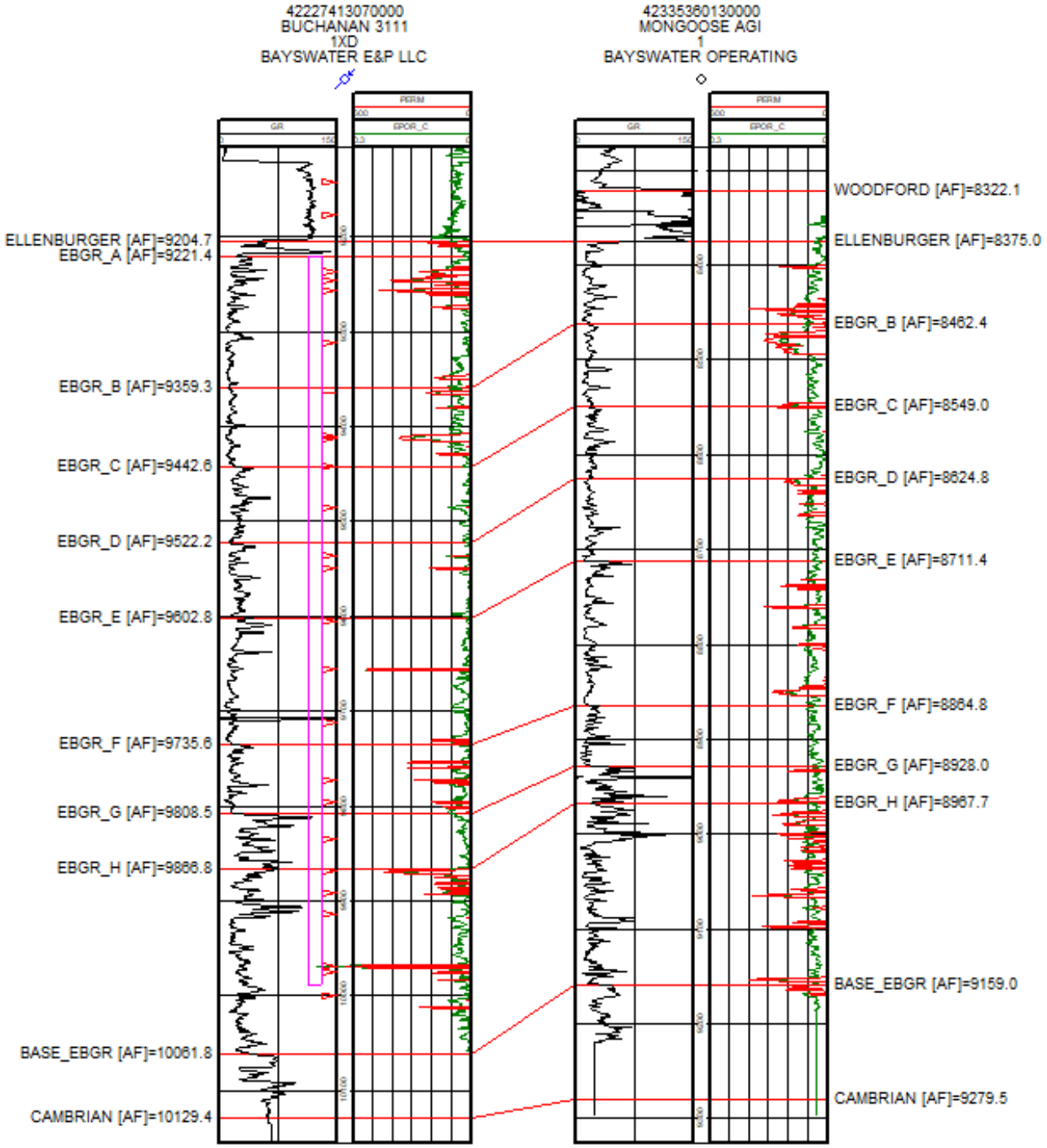

Figure 22 – Stratigraphic cross section of Mongoose AGI No. 1 and Buchanan 3111 #1XD depicting the Ellenburger formation and sidewall cores.

Figure 23 – Core photo of Ellenburger sample displaying vug features.

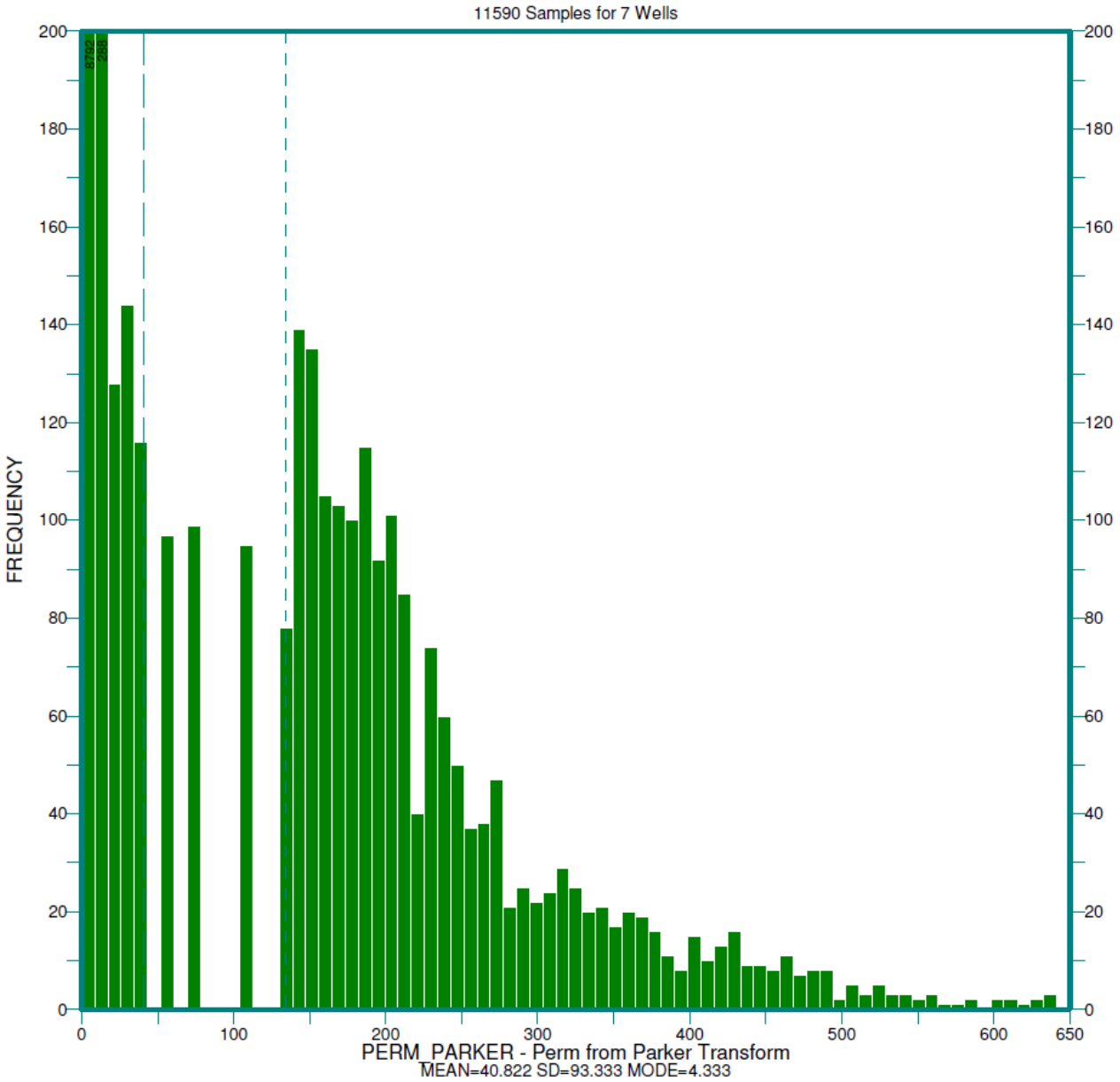

Figure 24 – Histogram of the Permeability Distributions with the Seven Modeled Offset Wells

2.2.3.3 Formation Fluid

Two wells were identified within approximately 30 miles of the Mongoose through a review of oil-field brine compositions of the Ellenburger formation from the USGS National Produced Waters Geochemical Database (ver. 2.3). The location of these wells is shown in Figure 25. Results from the synthesis of this data are provided in Table 3. The fluids have higher than 20,000 parts per million (ppm) total dissolved solids (TDS). Therefore, these aquifers are considered saline. These analyses indicate that the in situ reservoir fluid of the Ellenburger formation is compatible with the proposed injection fluids.

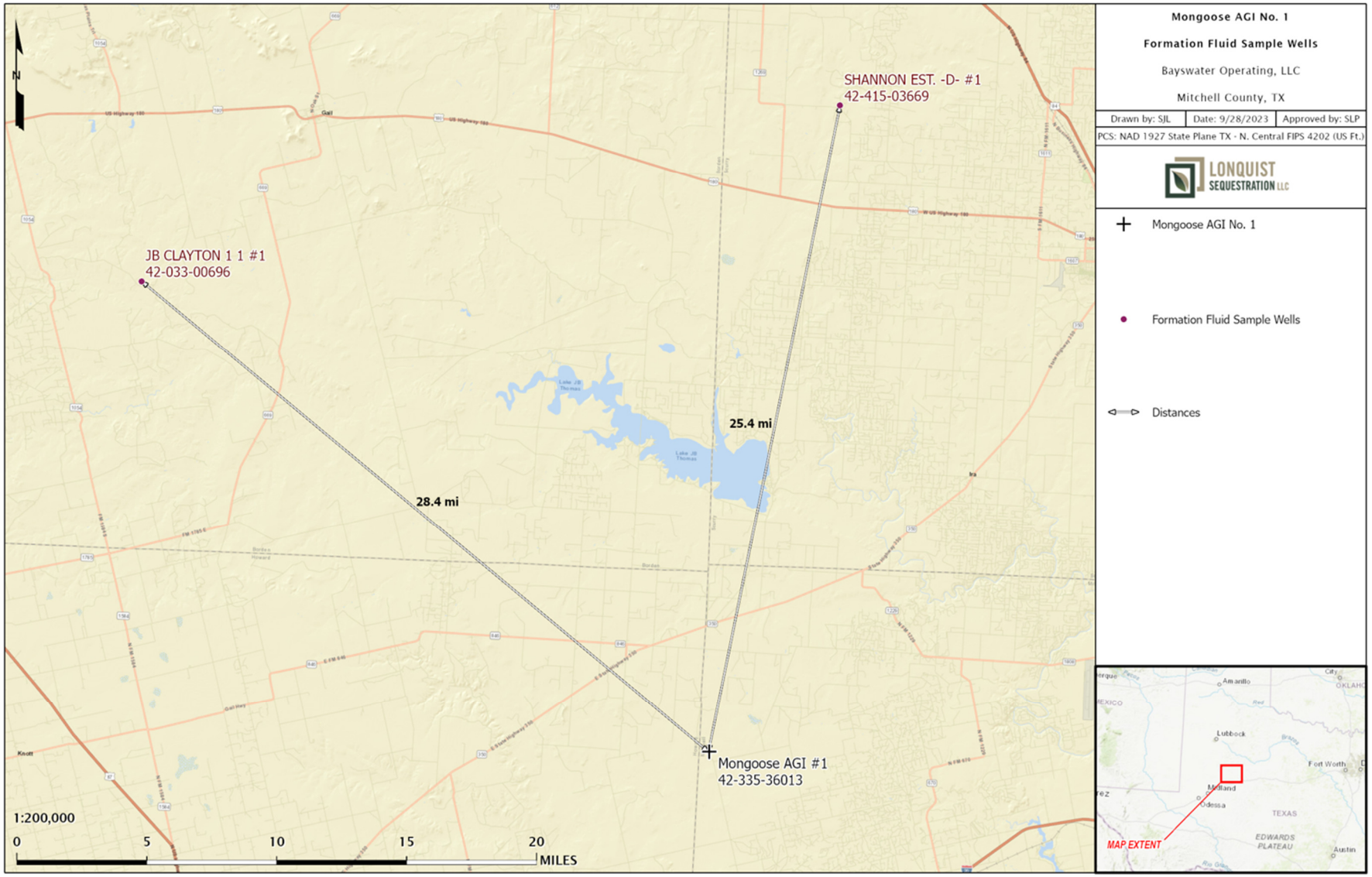

Figure 25 – Offset wells used for formation fluid characterization.

Table 3 – Analysis of Ordovician Age Formation Fluids from Nearby Oil-Field Brine Samples

	Average	Low	High
Total Dissolved Solids (ppm*)	47,427	42,014	52,840
pH	7	7	7
Sodium (ppm)	16,384	15,000	17,767
Chlorides (ppm)	27,590	24,900	30,281

*ppm – parts per million

2.2.4 Lower Confining Zone – Precambrian-age Formations

In the Permian Basin area, Precambrian-age formations are not normally specifically named in scientific literature. For the purposes of this MRV, these formations will just be referred to as the "Precambrian." Due to the lack of well penetrations and samples within the Precambrian, most compositions and interpretations of the Precambrian are sourced from outcrops in central Texas and the Trans-Pecos region of Texas and central New Mexico. Penetrations within the Precambrian are minimal and, when present, only penetrate a few feet into the section (Adams & Keller, 1996).

Adams and Keller conducted a geophysical analysis in 1996 to enhance the understanding of Precambrian rock types and their distribution in the Permian Basin. The study incorporated gravity modeling and magnetic and gravity anomalies, as well as rock data from Precambrian outcrops and drills to interpret the upper crustal geology of the area. Figure 26 displays the map resulting from their investigation, revealing that batholiths are likely present in the Precambrian basement rock at the Mongoose well location. Additionally, samples collected from offset wells displayed predominantly felsic rocks, which led to the interpretation of "granitic bodies in the upper crust" (Adams & Keller, 1996).

Offset Ellenburger injector wells were drilled through the Ellenburger section and reached total depths near the Precambrian. Log characteristics of strata near the total depth of the wells display gamma ray responses well above 90 gamma units of the American Petroleum Institute (GAPI), which is indicative of a high radioactive response. Additionally, the effective porosity curve near the base of the log shows little to no porosity, which represents a tight granitic rock that would act as an ideal lower confining zone. Due to the buoyancy of the injected gas in relation to the connate fluid within the Ellenburger, it is unlikely that the injectate will ever encounter the lower confining zone.

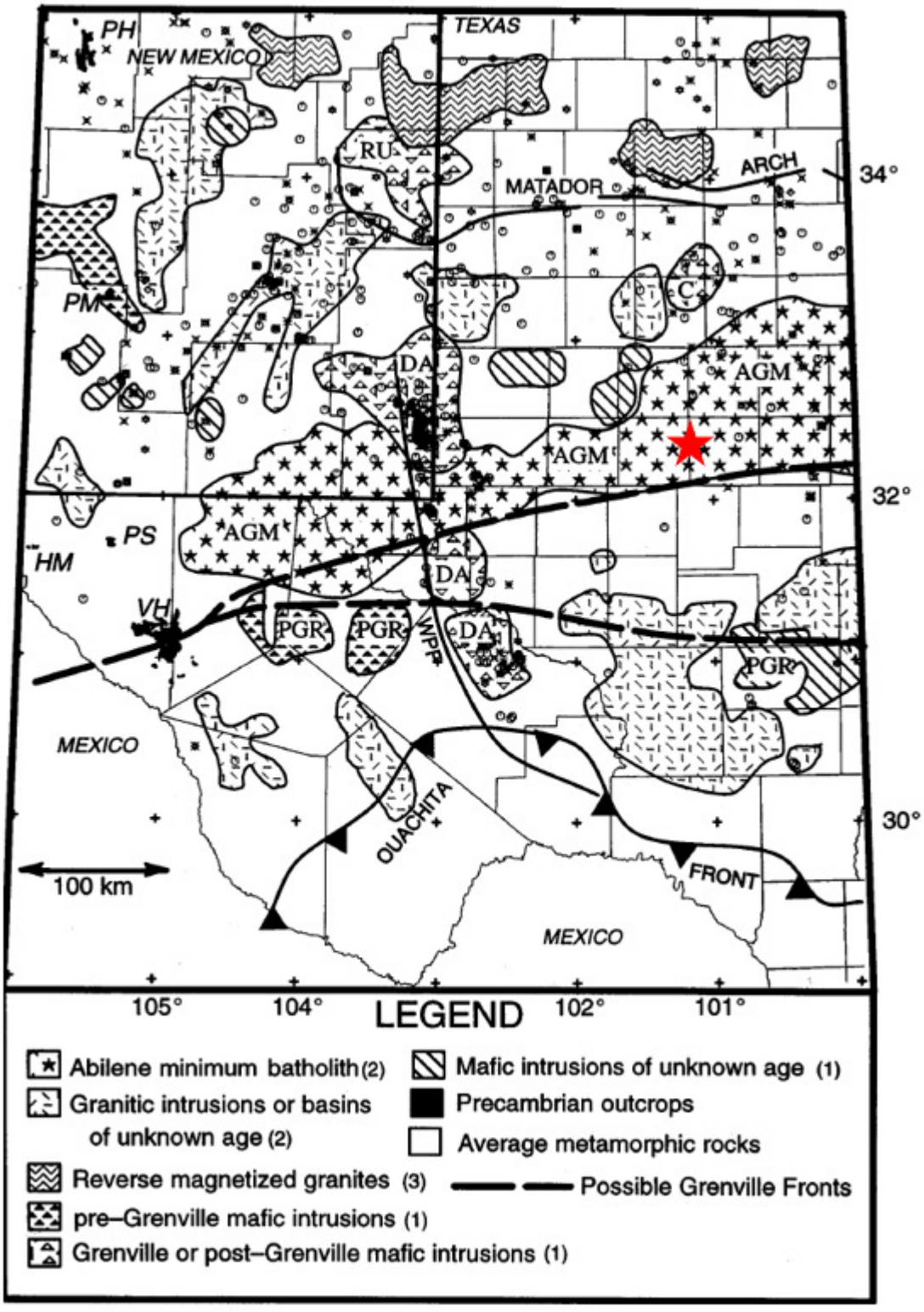

Figure 26 – Pre-Cambrian Distribution Map (Adams and Keller, 1996)

2.3 Geomechanics

2.3.1 Determination of Vertical Stress (S_v) from Density Measurements

The vertical stress can be characterized by the pressure exerted on a formation at a given depth due to the total weight of the rocks and fluids above that depth (Aird, 2019). The average bulk density of the upper and lower confining and injection zones was calculated from log data at the Buchanan 3111 #1XD (API No. 42-227-41307) offset well. The overburden gradient and vertical stress at the top of each zone were calculated by integrating the bulk density from surface to the formation depth in half-foot intervals. Table 4 shows the overburden gradient, vertical stress, and bulk densities of the top confining, injection, and lower confining zones.

Table 4 – Calculated Vertical Stresses

Formation	Depth (ft)	Bulk Density (g/cm^3)	Bulk Density (lb/ft^3)	Vertical Stress (psi)	Overburden Gradient (psi/ft)
Woodford	8,322	2.63	164.1	8,563	1.029
Ellenburger	8,375	2.75	171.2	8,635	1.031
Precambrian	9,500*	2.83	176.7	9,937	1.046

*Estimated

2.3.2 Elastic Moduli and Fracture Gradient

The fracture pressure gradient was estimated using Eaton's equation. Eaton's equation is commonly accepted as the standard practice for the determination of fracture gradients. The calculation requires Poisson's ratio (v), overburden gradient (OBG), and pore gradient (PG) in order to determine the required pressure to fracture the formation. These variables can be changed to match the site-specific injection zone.

A thorough review of log data, available literature, and industry standards indicate a 0.465 psi/ft pore gradient should be assumed when there are no site-specific numbers available. Poisson's ratio was calculated for the upper confining and injection zones using a sonic log that was run at the Buchanan 3111 #1XD. The calculation was performed using the equation below for log data points at half-foot depth intervals. The results were then averaged for the depth range of each zone. This resulted in a Poisson's ratio of 0.261 for the upper confining zone and 0.273 for the injection zone.

$$\nu = \frac{\frac{1}{2}\left(\frac{v_p}{v_s}\right)^2 - 1}{\left(\frac{v_p}{v_s}\right)^2 - 1}$$

Where:

ν = Poisson's Ratio
v_p = Compressional Velocity
v_s = Shear Velocity

Log data was unavailable for the lower confining zone, therefore the Poisson's ratio for this zone was estimated through a review of available literature. The lower confining zone consists of granite, which has been observed to have a Poisson's ratio ranging from 0.19 to 0.35 with a mean value of 0.28 (Domede, 2017). Based on this research, an average value of 0.28 was assumed. Using these values in the equation below, a fracture gradient of 0.664 psi/ft was calculated for the upper confining zone. A 10% safety factor was applied to this number resulting in a maximum allowed bottomhole pressure of 0.598 psi/ft. This zone had the lowest fracture gradient of the confining and injection zones. It was used to define the maximum allowable pressure to ensure that the injection pressure would not exceed the fracture pressure of any of the three zones. The resulting fracture gradients are displayed in Table 5.

Example Fracture Gradient Calculation for Upper Confining Zone

$$FG = \frac{\nu}{1-\nu}(OBG - PG) + PG$$

$$FG = \frac{0.261}{1-0.261}(1.029 - 0.465) + 0.465 = 0.664\ psi/\ t$$

$$FG\ with\ SF = 0.689\ \times 90\% = \mathbf{0.598\ psi/ft}$$

Table 5 – Fracture Gradient Calculation Inputs and Results

Depth (ft)	Zone	Member	Overburden Stress (psi)	Pore Pressure (psi)	Poisson's Ratio	Fracture Gradient (psi/ft)
8,322	Upper Confining	Woodford	1.029	0.465	0.261	0.664
8,375	Injection	Ellenburger	1.031	0.465	0.273	0.678
9,500*	Lower Confining	Precambrian	1.046	0.465	0.28	0.691

*Estimated

2.4 Local Structure

The area surrounding the Mongoose well is characterized by a monoclinal dip from east to west that is influenced by a shallow westward slope towards the Midland Basin and an upward slope to the east towards the Eastern Shelf. No evidence of structural faulting was found in this specific region that could have affected the geological trend. Figure 27 shows the topography of the Ellenburger formation, with the Mongoose well marked by a black star.

Subsurface interpretations of the Ellenburger formation heavily relied on well data and 3D seismic coverage in the area. The black boundary in Figure 27 represents the extent of the seismic coverage. Within the mapped area, approximately 100 wells have penetrated the Ellenburger formation. However, only seven of these wells fully penetrated the entire Ellenburger section. The remaining 93 wells only reached the top of the Ellenburger formation. These wells are plotted on the map and cover four counties. In addition to the Mongoose well, six other wells located offset of the Mongoose were used for the model build and are indicated by red stars.

Figure 28 is a structural cross section through the seven wells, modeled as depicted by the blue line on the Ellenburger structure map. The Ellenburger was broken down into eight subsections labeled Ellenburger A through H. Figure 29 is a stratigraphic cross section flattened on the Ellenburger that better illustrates these subtops.

The cross sections reveal the regional unconformity in the area when moving east from the Midland Basin. As we go farther updip and to the east, the Fusselman section gradually erodes. While there is also thinning in the Woodford, the cross section shows that the Woodford is present throughout the modeled area, creating a continuous seal above the plume.

With no major structural or stratigraphic features within the injection interval in the Mongoose area, there is little to no concern of geologic conduits outside of the injection interval. General flow trends will follow dip and optimal reservoir features within the Ellenburger. Large scale versions of Figures 28 and 29 are provided in *Appendix D*.

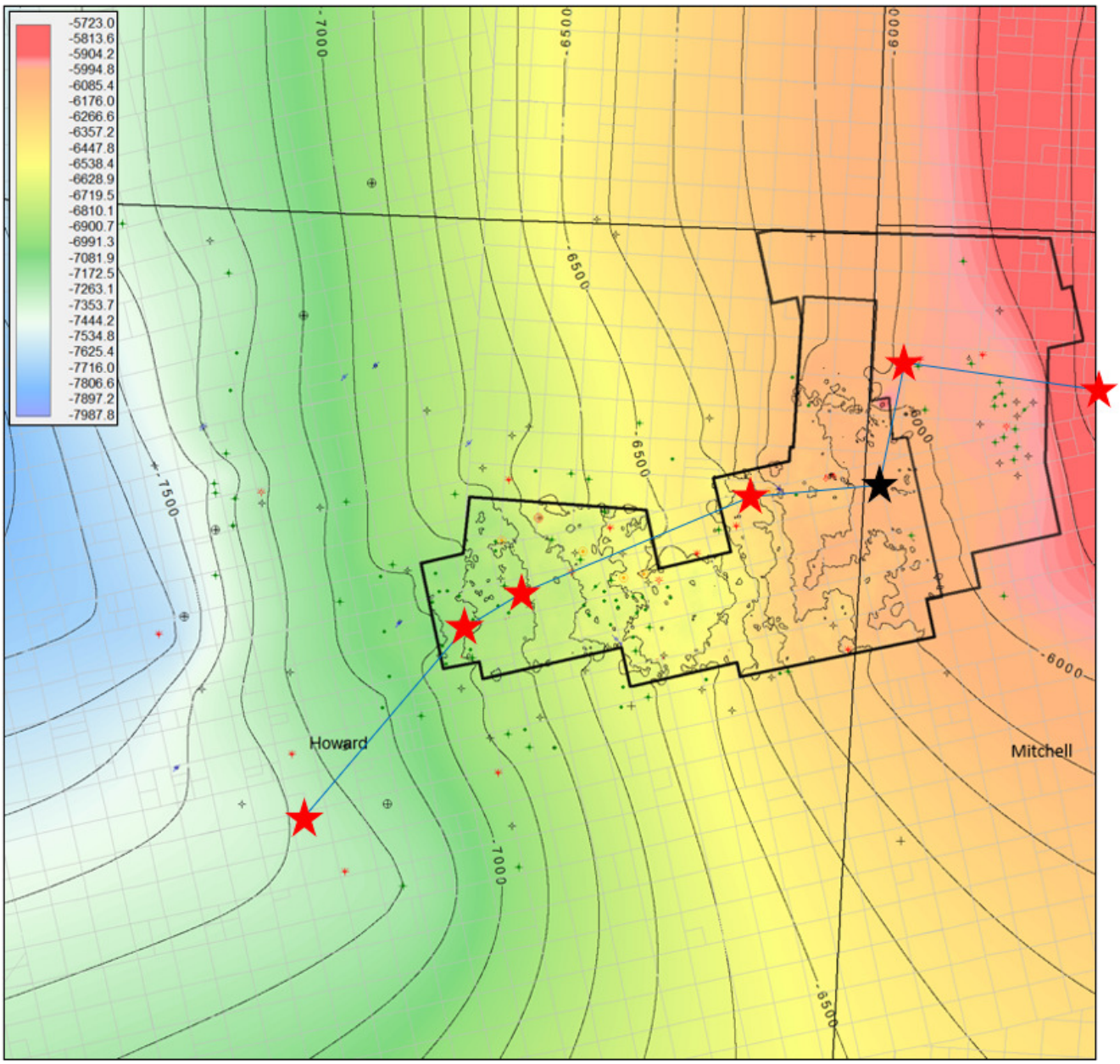

Figure 27 – Ellenburger structure map in subsea feet. The black star represents the Mongoose AGI No. 1 location and red stars represent the remaining six wells used in the model. The blue line indicates the cross-section reference map.

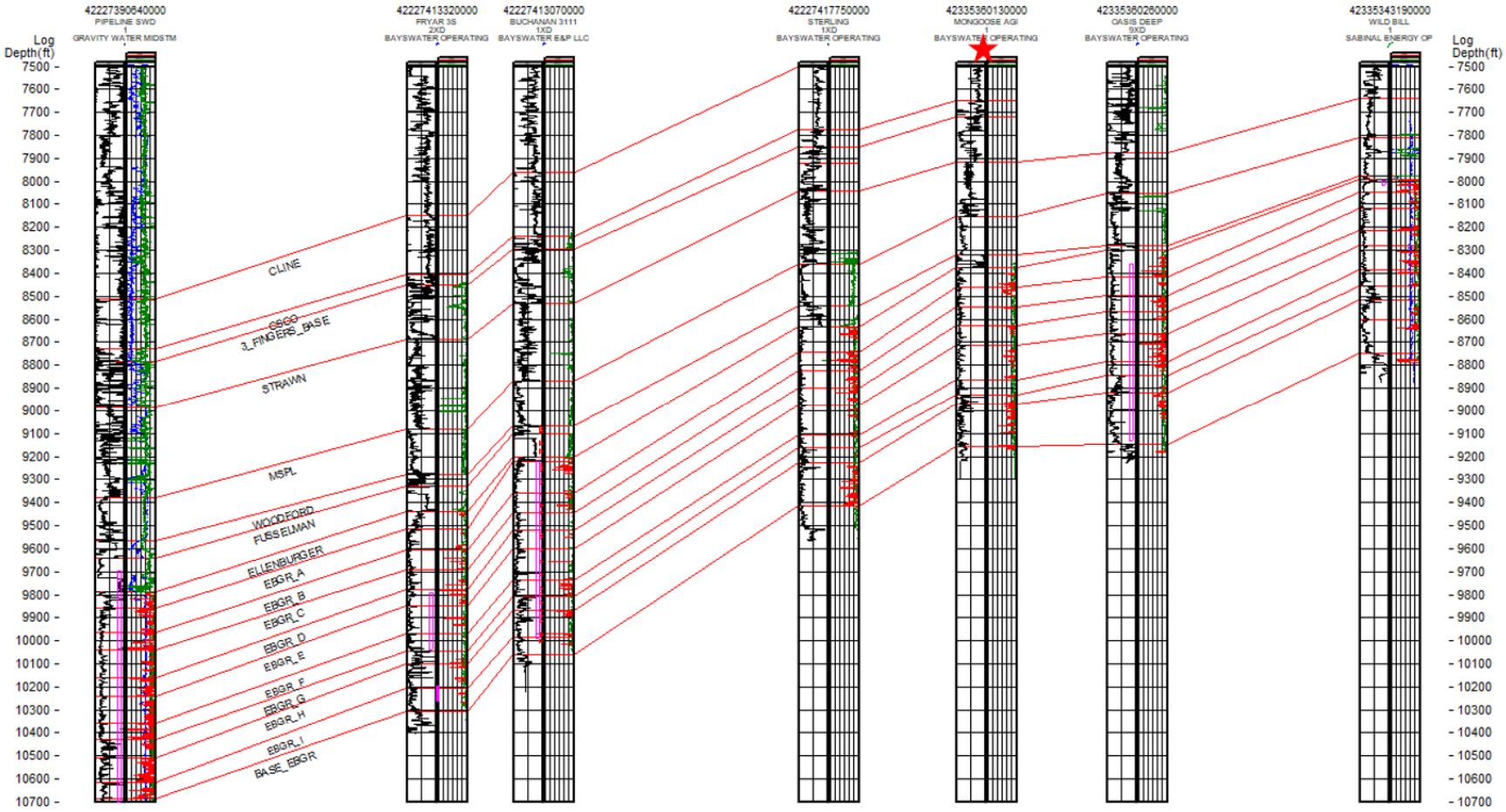

Figure 28 – Structural cross section depicting the Ellenburger.

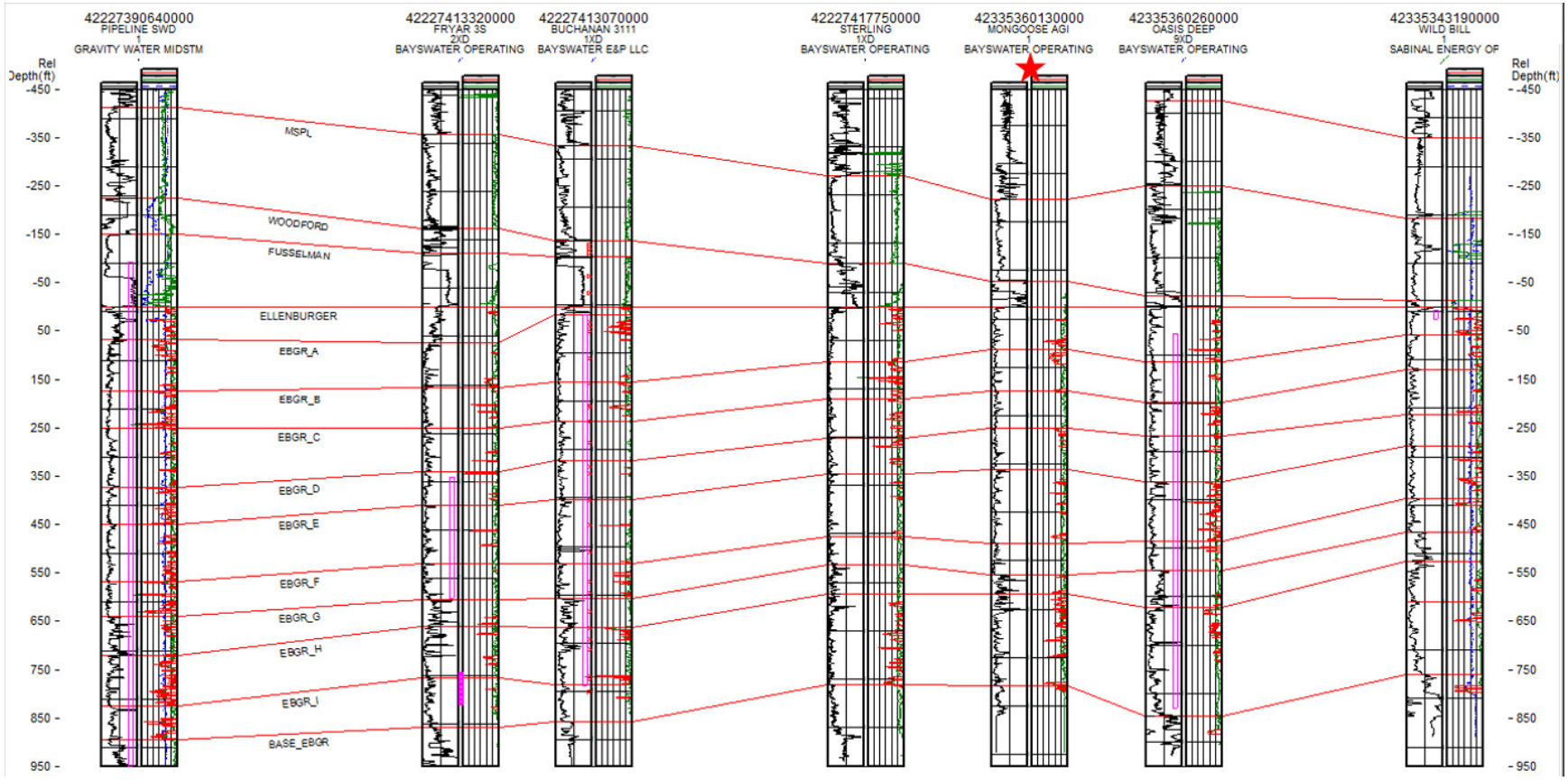

Figure 29 – Stratigraphic cross section flattened on the Ellenburger.

2.5 Injection and Confinement Summary

The lithologic and petrophysical characteristics of the Ellenburger formation at the Mongoose location indicate that it has the necessary qualities to accept the proposed injection fluids, including sufficient thickness, porosity, permeability, and lateral continuity. The Woodford Shale formation at the same well location has low permeability and is of adequate thickness and lateral continuity to act as the upper confining zone. Below the injection interval, the Precambrian formation has low permeability and low porosity, making it unsuitable for fluid migration and serving as the lower confining zone.

A thorough study of the area of review has been conducted to identify any potential subsurface features that could impact the ability of the injection and confinement units to retain the injectate within the desired injection interval. Fortunately, no faults or other hazardous geologic conditions have been identified in the area. Therefore, the conditions in this area are ideal for injection and containment.

2.6 Groundwater Hydrology

The Mongoose is located within Mitchell County, home to a population of approximately 8,400 residents, and is serviced by the Lone Wolf Groundwater Conservation District, which consists solely of Mitchell County. This conservation district has an area of roughly 900 square miles. Much of the county's economy is derived from agriculture and oil production, both water-intensive operations. Groundwater usage within the county is estimated to be 13,391 acre-feet on a yearly basis (Lone Wolf Groundwater Conservation District, 2019).

Surface Water

Mitchell County lies within the Colorado River basin, as the Colorado runs through the county. Drainage from both the east and west flow centrally towards the Colorado River, which splits the county in half. The estimated supply of surface water is 395 acre-feet (Lone Wolf Groundwater Conservation District, 2019).

Groundwater

There are multiple units where groundwater is available within Mitchell County, although only the Dockum Group provides significant amounts of water. Table 6 discusses water-bearing units in the county, and Figure 30 shows a generalized reference to structure and formation relationships.

Table 6 – Geologic Units and Their Water-Bearing Characteristics in Mitchell County (Shamburger Jr., 1967)

System	Series	Group	Formation	Approximate thickness (feet)	Lithology	Water-bearing characteristics
Quaternary	Pleistocene and Recent		Alluvium	0-100	Fine to coarse sand, and small to large gravel, with occasional clay and caliche beds.	Above the regional water table east of Colorado River, but yields up to 20 gpm of good quality water in southwestern Mitchell County.
Tertiary	Pliocene		Ogallala	0-100	Fine to coarse sand, gravel, caliche, and zones of clay.	Above the water table east of Colorado River, but yields up to 20 gpm of good quality water to wells in northwestern Mitchell County.
Cretaceous	Comanche	Fredericksburg		0-220	Predominantly limestone. 15 to 25 feet of sandy yellow marl at base overlain by chalk and shaly limestone. Very dense, massive, fossiliferous limestone in the upper part.	Upper limestones contain in places small to moderate supplies of potable but hard water in solutional openings developed along fracture systems; recharge to the openings occurs through numerous sinks.
		Trinity		0-100	White to purplish quartz sand, fine to medium grained, moderately to loosely consolidated, with occasional lenses of quartz gravel at the base.	Yields small to large quantities of potable but hard water, the amount depends on saturated thickness which ranges from 100 percent under interior limestone areas to a few feet in parts of the outcrop; yields of several hundred gallons per minute are reported.
Triassic		Dockum	Chinle	0-640	Predominantly red to maroon and purplish clay and shale, interbedded with thin, tight, cross-bedded, yellow-brown to reddish-white sandstone.	Sandstones contain generally small quantities of moderately to highly mineralized water; used principally for livestock.
			Santa Rosa	0-330	Basal conglomerate overlain by brown to gray, micaceous and carbonaceous, cross-bedded sand alternating with beds of red and gray clay.	Sands and gravels contain moderate to large quantities of fresh water east of the Colorado River, with yields up to 1,000 gpm reported; west of Colorado River capacity of sand is reportedly substantial but water is generally not potable.
Permain	Guadalupe and Ochoa				Fine-grained, red to brown sandstone; dense red silty shale with occasional gypsum or anhydrite beds.	Yield small quantities of moderately to highly mineralized water to livestock and domestic wells.

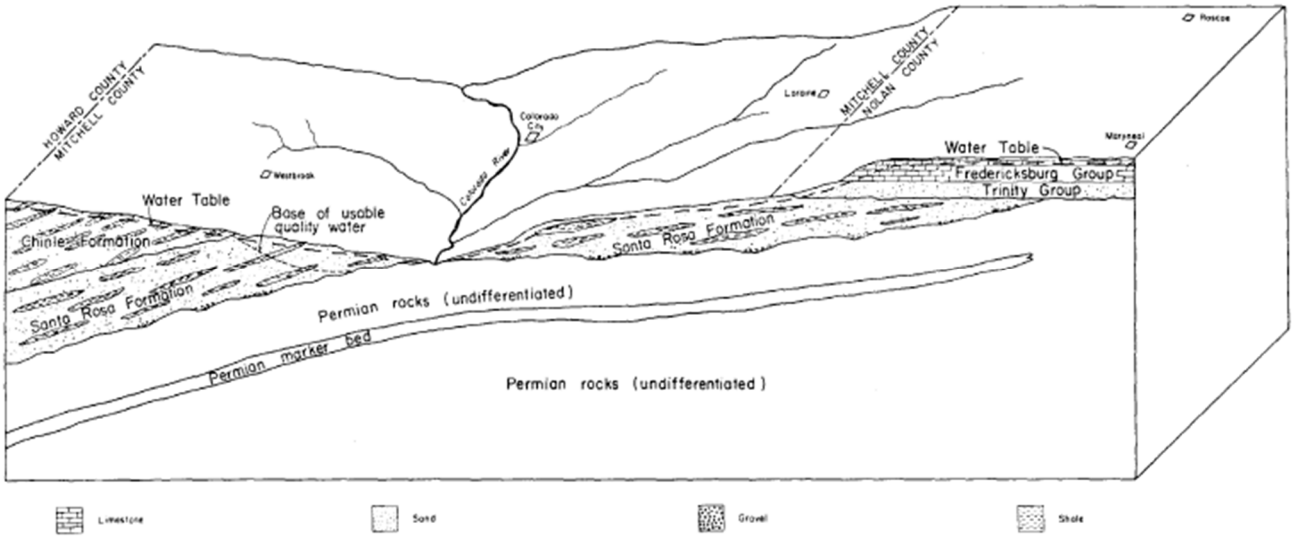

Figure 30 – General Geologic Structure and Formation Relationships in Mitchell and Western Nolan Counties (Shamburger Jr., 1967)

Permian

Permian age strata underlies much of the area and outcrops in the southeast of Mitchell County and along the Colorado River and its tributaries. These strata consist primarily of "red beds," dense red silty shales. Water wells in the Permian strata are typically less than 100 ft deep, yielding small amounts of moderately to highly mineralized water usable only for livestock (Shamburger Jr., 1967).

Dockum Aquifer

The Triassic Age Dockum group comprised by the Santa Rosa sandstone and the Chinle formation are the main sources of ground water within the county. An overview map of the extent of the Dockum Aquifer is shown in Figure 31, with outcrops depicted in solid color. The Chinle is further divided into the Tecovas formation, the Trujillo sandstone, and the Cooper Canyon formation, although the Tecovas and Cooper Canyon are generally unimportant and yield only small amounts of highly mineralized water.

The Santa Rosa sandstone lies unconformably atop the Permian age strata at the base of the Dockum Group and is one of the major sources of water for Mitchell County. It is comprised of a basal conglomerate overlain by alternating beds of red and gray micaceous shale, sand, and gravel reaching up to 130 ft in thickness (Bradley & Kalaswad, 2001). The Trujillo sandstone overlies the Tecovas, which in turn overlies the Santa Rosa, and is a cross-bedded unit composed of sandstones and conglomerates. The Santa Rosa and Trujillo sandstones are regarded as the main producers of water in the Dockum Group in Mitchell County (Lone Wolf Groundwater Conservation District, 2019). The Dockum Group was likely deposited from sediments into "fluvial, deltaic, and lacustrine environments within a closed continental basin" (Bradley & Kalaswad, 2001). The base of the Santa Rosa is typically considered the lower extent of fresh water in the area. Water levels in wells throughout the county vary between 15 ft and 215 ft below ground level (Shamburger Jr., 1967), and the aquifer is considered confined to partially confined (Bradley & Kalaswad, 2001).

Recharge of the aquifer is provided by rainwater infiltration through outcrops in the county and is estimated to be 18,108 acre-feet per year. Groundwater in the Dockum aquifer system flows towards the central Colorado River. A potentiometric surface map of the Santa Rosa sandstone, the lower Dockum member, is depicted in Figure 32. Although no values of porosity have been determined empirically, a conservative value of 10% is assumed for effective aquifer porosity (Lone Wolf Groundwater Conservation District, 2019).

Groundwater quality is generally considered poor with TDS and other constituents exceeding secondary drinking water standards (Bradley & Kalaswad, 2001). As a typical assumption, water quality west of the Colorado River within the aquifer is poor and unsuitable for municipal use, while east of the river water quality is less mineralized and is of suitable quality for municipal purposes (Lone Wolf Groundwater Conservation District, 2019). For example, a well tested 10 miles northwest of Colorado City contained chloride at 560 milligrams per liter (mg/L), sulfate at 337 mg/L, and TDS at 1,893 mg/L, all of which are above limits set by the Texas Commission on Environmental Quality (TCEQ) for use in municipal water supplies. In contrast, a well 8 miles east of Colorado City contained

chloride at 34 mg/L, sulfate at 73 mg/L, and TDS at 418 mg/L (Lone Wolf Groundwater Conservation District, 2019). A map showing TDS values for the Dockum Aquifer is shown in Figure 33.

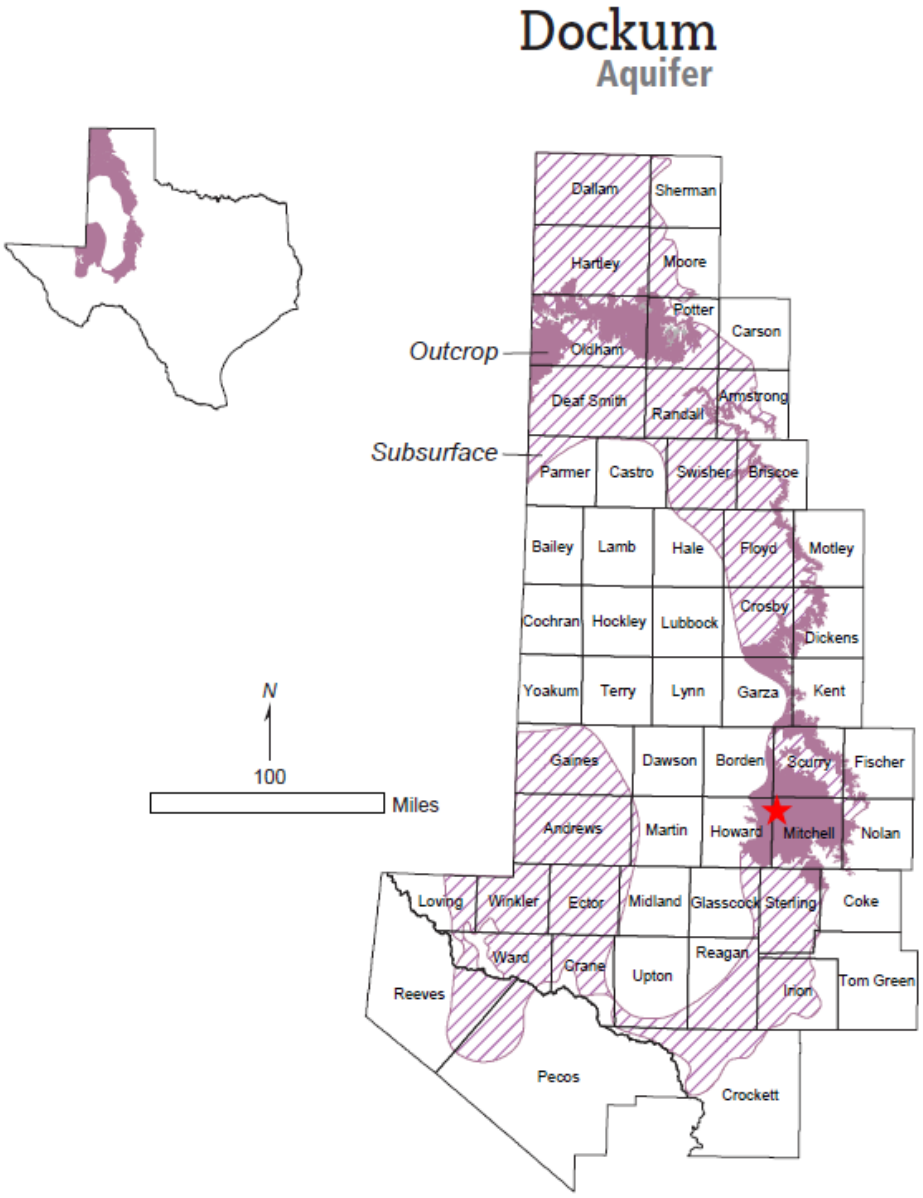

Figure 31 – Location of the Dockum Aquifer. The solid shading signifies outcrops at the surface, the hatched signifies confined subcrops, and the red star signifies the Mongoose AGI No. 1 location (George, Mace, & Petrossian, 2011).

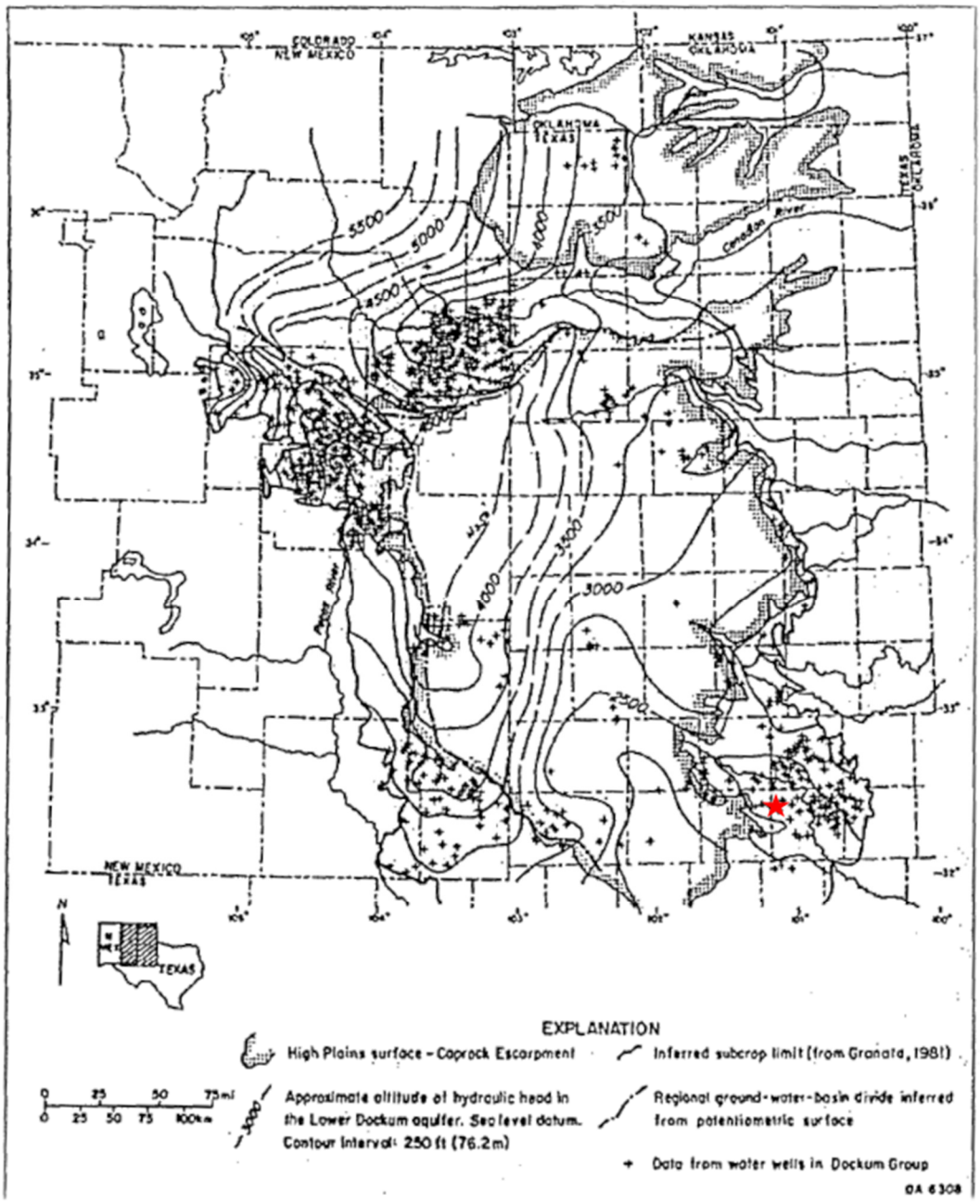

Figure 32 – Potentiometric Surface Map of the Lower Dockum (Santa Rosa) Group Groundwater. The red star shows the Mongoose AGI No. 1 location (Dutton & Simpkins, 1986).

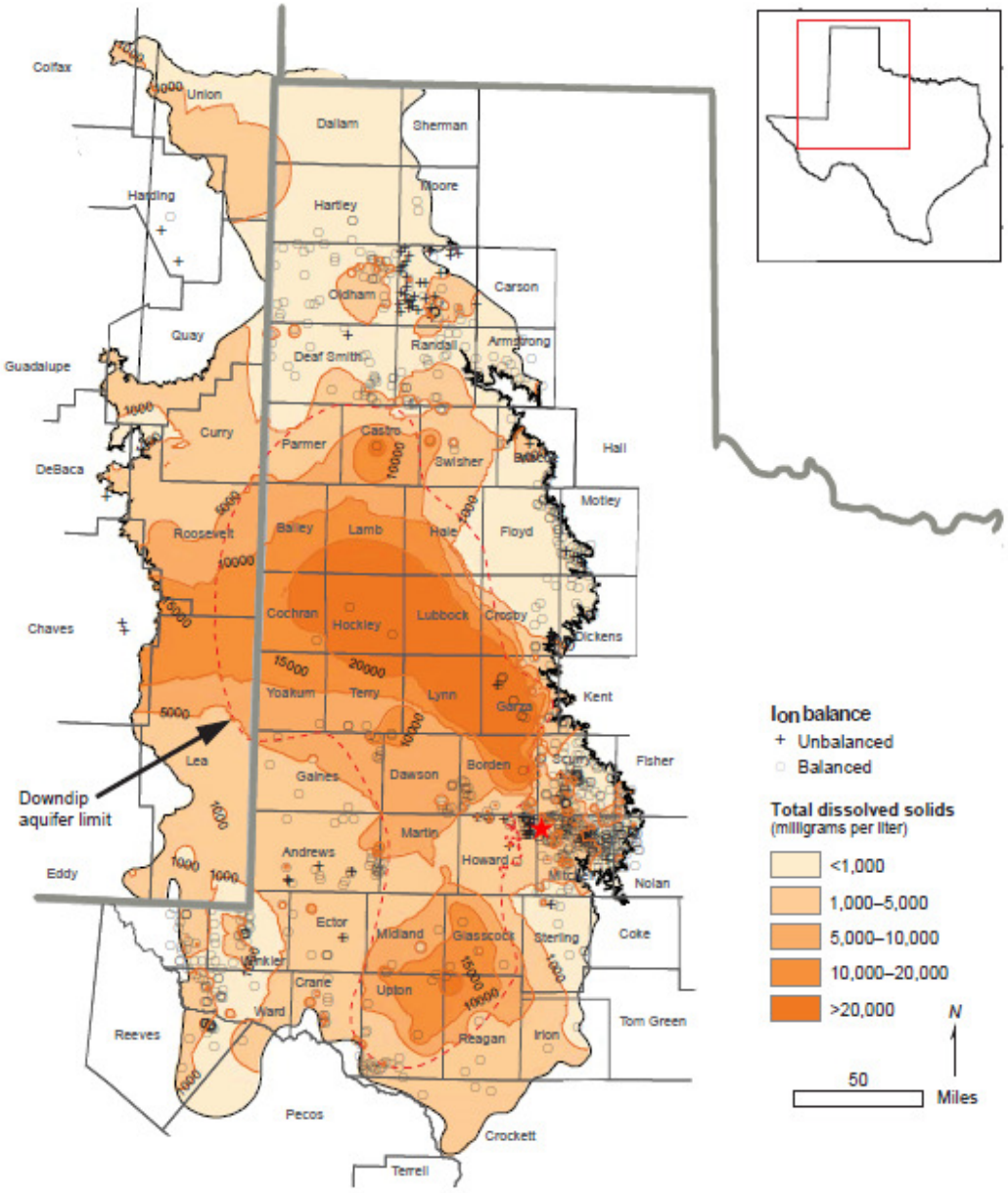

Figure 33 – Total Dissolved Solids in the Dockum Aquifer. The red star shows the Mongoose AGI No. 1 location (George, Mace, and Petrossian, 2011).

Ogallala Formation

The Tertiary age Ogallala formation occurs in the northern extents of Mitchell County. In the eastern part of the county, Ogallala sediments are generally above the water table and not a source of groundwater; however, they do provide an effective means of recharge to the underlying Santa Rosa formation. In the western part of the county, the Ogallala is up to 100 ft thick of unconsolidated sand and gravel and provides small quantities of usable water for domestic and livestock wells (Lone Wolf Groundwater Conservation District, 2019).

2.7 Description of the Injection Process

2.7.1 Current Operations

The Mongoose Amine Treating Facility and the associated Mongoose well began operating in August of 2023. The maximum rate during the injection period is expected to be 377.2 MT/yr (19.5MMscf/D). The TAG is 41.2% CO_2, which equates to 155.3 MT/yr of CO_2 each year. The current composition of the TAG stream is:

Table 7 – Gas Composition at the Plant Outlet

Component	Mole Percent
Carbon Dioxide	41.2%
Hydrogen Sulfide	58.8%

The Mongoose Amine Treating Facility is designed to dehydrate, treat, and compress the natural gas produced from the surrounding acreage in Mitchell County. The gas is dehydrated to remove the water content, and treated to remove the CO_2 and H_2S. The compressed rich gas stream is then transported via pipeline to a separate facility for processing to separate the natural gas liquids from the methane. The TAG is then directly routed from the Plant's amine unit to the Mongoose. The Plant is manned 24 hours per day, 7 days per week.

2.8 Reservoir Characterization Modeling

The modeling software used to evaluate this project was Computer Modelling Group's GEM 2023.2 (GEM) simulator. Computer Modelling Group (CMG) has put together one of the most accurate and technically sound reservoir simulation software packages for conventional, unconventional, and secondary recovery. GEM utilizes equation-of-state (EOS) algorithms along with some of the most advanced computational methods to evaluate compositional, chemical, and geochemical processes and characteristics to produce highly accurate and reliable simulation models for carbon injection and storage. The GEM model is recognized by the EPA for use in area of review delineation modeling as listed in the Class VI Well Area of Review Evaluation and Corrective Action Guidance document.

The Ellenberger formation is the target formation for the Mongoose. The Petrel software package was utilized to create the geologic model of the target formation. Within the Petrel platform, the porosity and permeability distributions were established for the model. The geologic structure was then imported into GEM for simulation purposes.

In Petrel, the structure's construction involved the utilization of nine contour tops, which were layered sequentially. These contour tops, identified as "Ellenberger A" through "Ellenberger I," collectively define the structure's configuration, Ellenberger A being the shallowest and Ellenberger I being the deepest structure package. To accurately represent the formation's true structure, true vertical depth subsea was used to account for the differing overburden depths associated with the

wells used in contour delineation. The distinction between true vertical depth (TVD) and true vertical depth subsea (TVDSS) is taken into consideration when inputting pressure and temperature gradients into the GEM model.

Porosity estimates were determined using openhole porosity logs from seven offset wells within the Ellenberger formation. These logs were used within Petrel to distribute porosity and permeability spatially. Permeability was found by using the two-function porosity-permeability curve developed from regional and local core data within the Ellenberger formation.

The reservoir is assumed to be at hydrostatic equilibrium and initially saturated with 100% brine. An infinite-acting reservoir was created to simulate boundary conditions. The gas injectate is composed of H_2S and CO_2 based on initial estimates from the source, as shown in Table 8. However, the precise gas composition may vary slightly as the Plant is still in its commissioning phase. Initial estimates anticipate the injectate composition to be 58.8% H_2S and 41.2% CO_2. Once a steady-state operating composition is determined, the MRV plan will be updated if there is a material difference. Based on the initial gas samples, the modeled percentages in the injectate for the 40-year injection period of the Mongoose is 58.8% H_2S and 41.2% CO_2.

Table 8 – Modeled Initial Gas Composition

Component	Expected Composition (mol %)	Modeled Composition (mol %)
Hydrogen Sulfide (H_2S)	58.8	58.8
Carbon Dioxide (CO_2)	41.2	41.2

Core data from literature review was used to determine residual gas saturation (Keelan and Pugh, 1975) and relative permeability curves between carbon dioxide and the connate brine within the Ellenberger dolomitic carbonates (Bennion and Bachu, 2010). The Corey-Brooks method was used to create relative permeability curves. The key inputs used in the model include a Corey exponent for brine of 2.27, a Corey exponent for gas of 2.56, gas permeability at irreducible brine saturation of 10%, an irreducible water saturation of 39.7%, and a maximum residual gas saturation of 30%. The relative permeability curves used for the GEM model are shown in Figure 34.

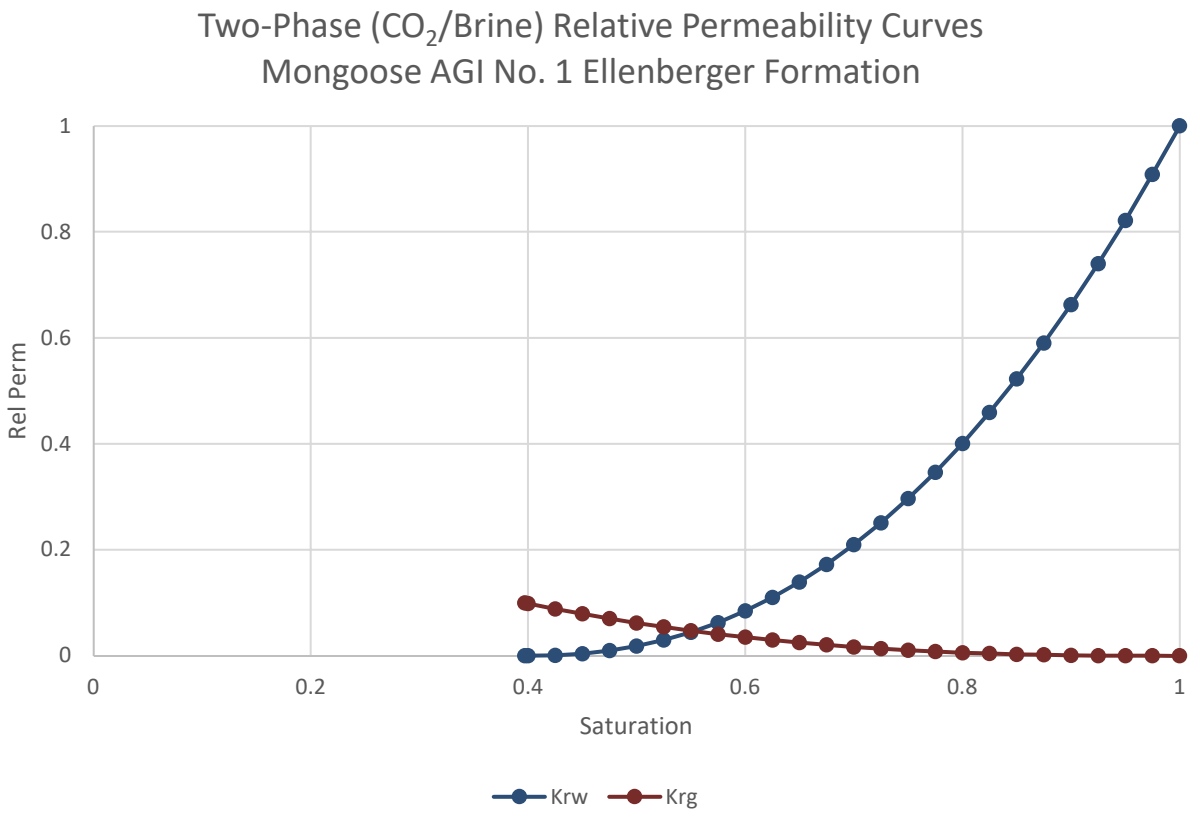

Figure 34 – Two-Phase Relative Permeability Curves Used in the GEM Model

The grid contains 135 blocks in the x-direction (east-west) and 77 blocks in the y-direction (north-south), resulting in a total of 10,395 grid blocks per layer. Each grid block spans dimensions of 1,000 ft by 1,000 ft. This configuration yields a grid size measuring 135,000 ft by 77,000 ft, equating to just under 373 square miles in area. The grid cells in the vicinity of the Mongoose, within a radius of 2.5 miles, have been refined to dimensions of 250 ft by 250 ft in all layers. This refinement is employed to ensure a more accurate representation of the plume.

In the model, each layer is characterized by heterogeneous permeability and porosity values. These values are derived from the geostatistical distribution of properties, using porosity logs implemented in Petrel as a basis. The model encompasses a total of 79 layers, each featuring varying thicknesses, with an average of approximately 10 ft per layer. As previously mentioned, the structure of the Ellenberger formation was formed using nine contour packages. The summarized property values for each of these packages are displayed in Table 9.

Table 9 – GEM Model Layer Package Properties

Contour Package	No. of Layers	Top (TVD ft)	Thickness (ft)	Perm. (mD)	Porosity
Ellenberger A	9	8,369	101	49.1	5.2%
Ellenberger B	9	8,470	76	65.1	6.0%
Ellenberger C	8	8,546	75	38.5	4.2%
Ellenberger D	9	8,621	86	39.2	4.9%
Ellenberger E	15	8,707	153	48	4.8%
Ellenberger F	6	8,860	63	32.5	4.4%
Ellenberger G	4	8,923	39	16.5	3.2%
Ellenberger H	8	8,962	82	76.9	5.5%
Ellenberger I	11	9,044	112	66	3.4%

2.8.1 Simulation Modeling

The primary objectives of the model simulation were as follows:

1. Estimate the maximum areal extent and density drift of the acid gas plume after injection.
2. Assess the impact of offset SWD well injection on density drift of the plume.
3. Determine the ability of the target formation to handle the required injection rate without fracturing the injection zone.
4. Assess the likelihood of the acid gas plume migrating into potential leak pathways.

The reservoir is assumed to be an aquifer filled with 100% brine. The salinity of the formation is estimated to be 47,427 ppm (U.S. Geological Survey National Produced Waters Geochemical Database, ver. 2.3), typical for the region and formation. The acid gas stream is primarily composed of CO_2 and H_2S as stated previously. Core data was used to help generate relative permeability curves. From the literature reviews as previously discussed, cores that most closely represent the vuggy dolomitic carbonate seen in this region were identified, and the Corey-Brooks equations were used to develop the curves (Bennion and Bachu, 2010). A low and conservative residual gas saturation based on the cores from literature review was then used to estimate the size of the plume (Keelan and Pugh, 1975). The initial reservoir pressure is 3,903 psig, which is equivalent to a 0.465 psi/ft pressure gradient and was determined from offset injection well analysis. The fracture gradient of the injection zone was estimated to be 0.664 psi/ft, which was determined using Eaton's equation. A 10% safety factor was then applied to this number, putting the maximum bottomhole pressure allowed in the model at 0.598 psi/ft, which is equivalent to 5,007 psig.

The model considers the injection volumes of offset SWD wells close to the Mongoose. Nine such wells were identified within a 19-mile radius. Historical injection rates of eight of the nine of these wells currently injecting into the Ellenberger were provided by the operators and were input into

the model. All but one of the SWD wells in the model are currently permitted and injecting. The SWD well that has not yet started injection and has no historical injection data is conservatively assumed to inject at its maximum permitted rate for 30 years and to start at the same time as the Mongoose begins injection. Projected injection rates were assumed to be the maximum permitted injection rates and ended after 30 years of life for all nine offset SWDs. This simulation includes the effect of water injection on the density drift of the plume and the bottomhole pressure of the Mongoose. The SWDs included in the model are listed in Table 10.

Table 10 – Offset SWD Wells Included in GEM Model

API Number	Well Name	Well Number
42-227-41332	Fryar 3S	2XD
42-227-41307	Buchanan 3111	1XD
42-227-39064	Pipeline SWD	1
42-335-34319	Wild Bill	1WD
42-227-41775	Sterling	1XD
42-335-36026	Oasis Deep	9XD
42-227-39098	846 SWD	2
42-227-39119	N. Midway SWD	1
42-227-40310	Hull SWD	1

The model runs for a total of 175.33 years, comprising 15.33 years of historical SWD well injection prior to the commencement of acid gas injection. This is followed by 40 years of active acid gas injection through the Mongoose, succeeded by an additional 120 years of density drift. The model begins in September 2008, aligning with the start of historical injection data for the first offset SWD well. The remainder of the SWD wells turn on between then and the start of the acid gas injection, which begins in January 2024. Throughout the entire 40-year injection period, an injection rate of 19.5 MMscf/D is assumed to model the maximum available rate, yielding a more cautious estimate of the plume size. After the 40-year injection period, when the Mongoose ceases injection, all nine offset SWD wells have been shut in—as they began injecting before the Mongoose and were assumed to stop injecting after 30 years.

The maximum plume extent during the 40-year injection period is shown in Figure 35. The final extent after 120 years of density drift after injection ceases is shown in Figure 36. Both figures show the entire grid with the included offset SWD wells. Due to the large nature of the model, a zoomed-in view of the plume extent during the 40-year injection period is shown in Figure 37 and the final extent after 120 years of density drift after injection ceases is shown in Figure 38.

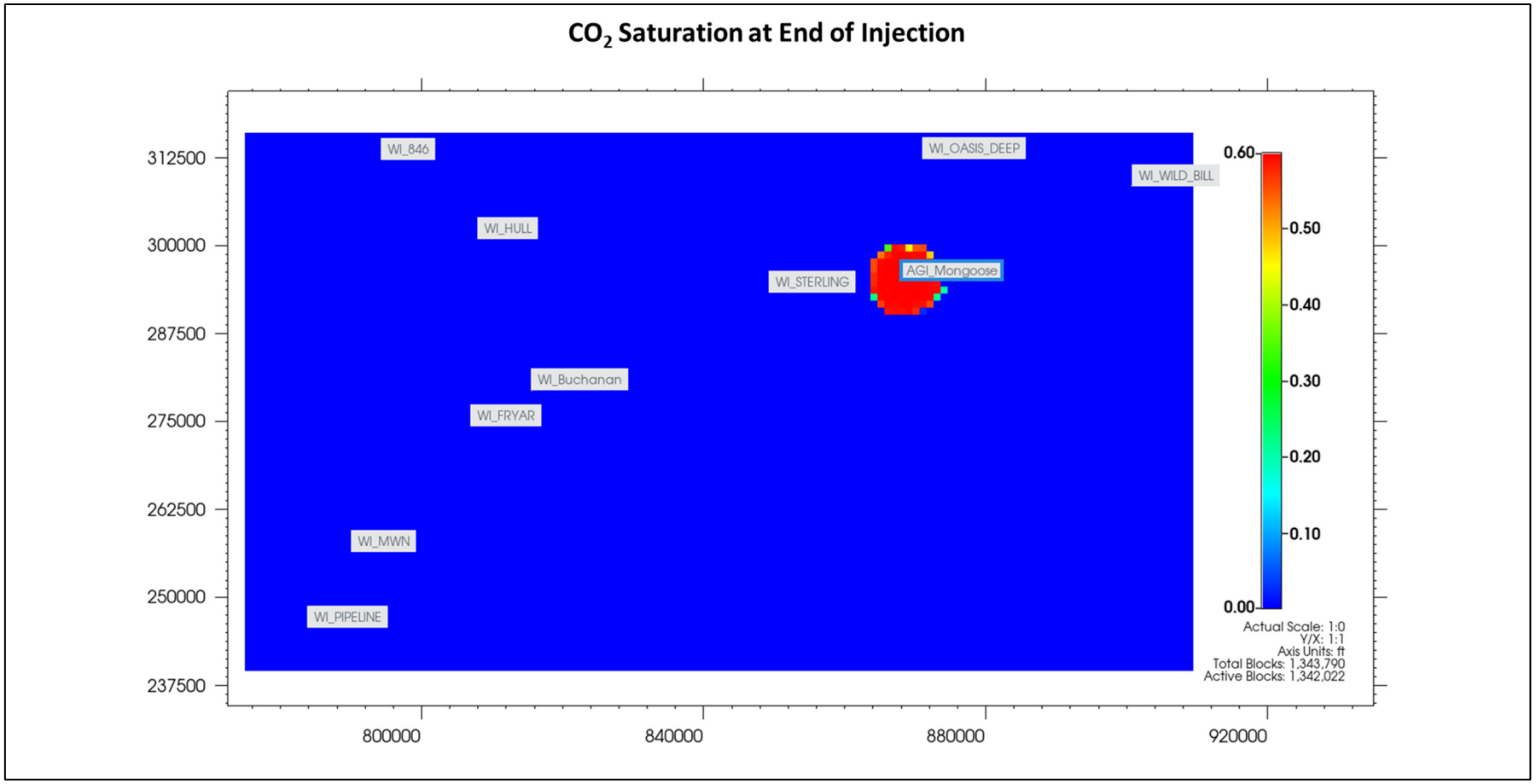

Figure 35 – Areal View of Gas Saturation Plume at Shut-in (End of Injection)

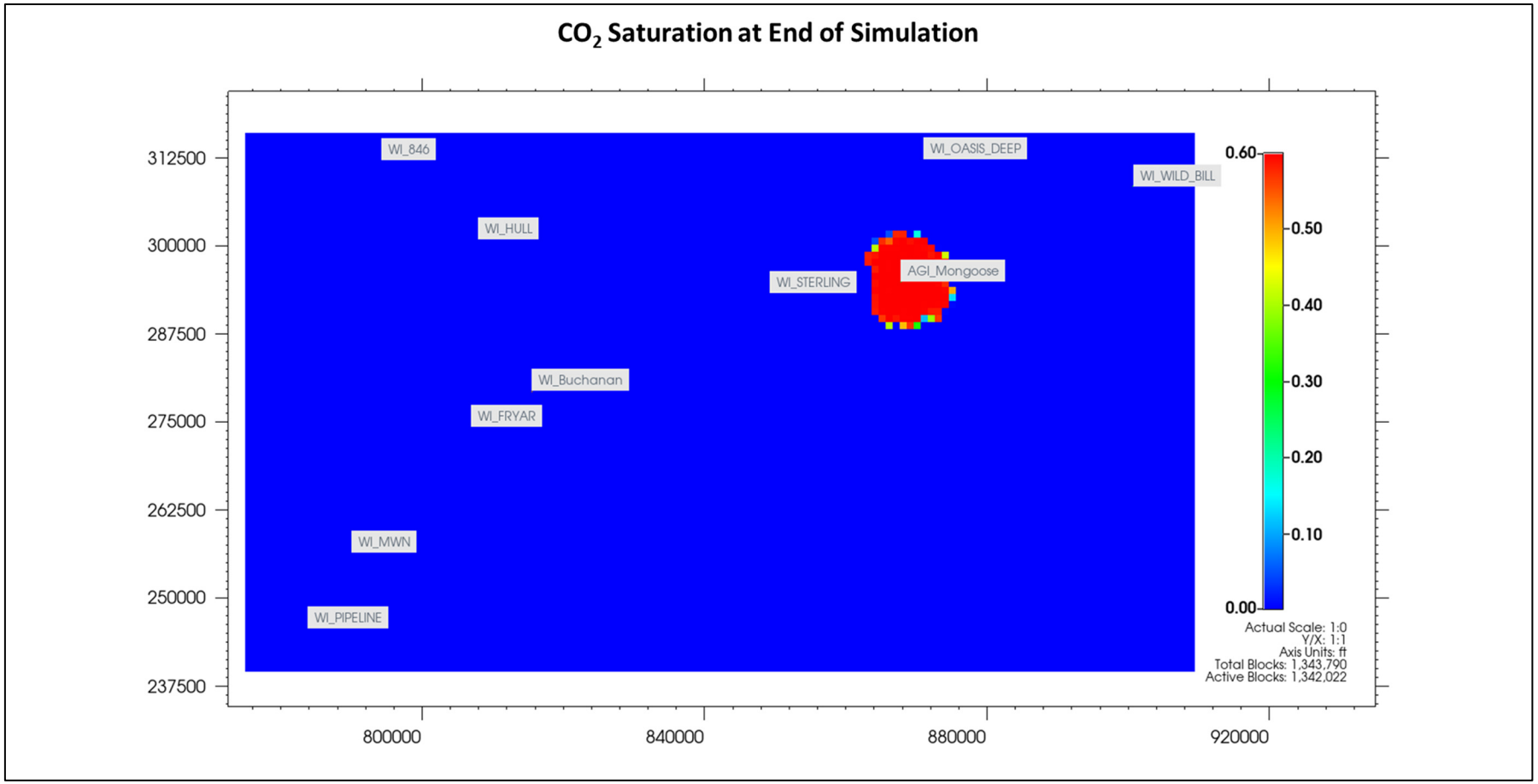

Figure 36 – Areal View of Saturation Plume at 120 Years After Shut-in (End of Simulation)

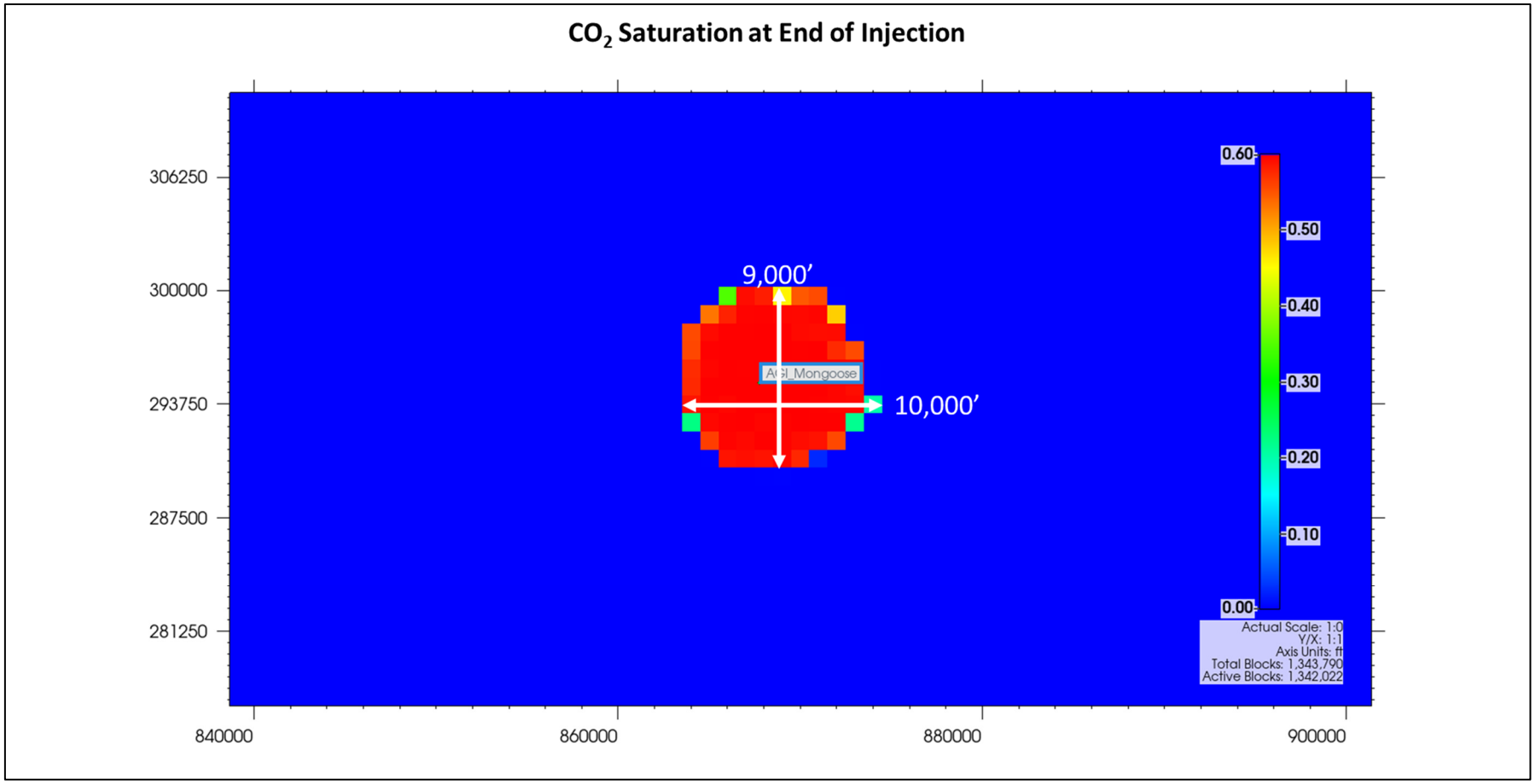

Figure 37 – Zoomed-In Areal View of Gas Saturation Plume at Shut-in (End of Injection)

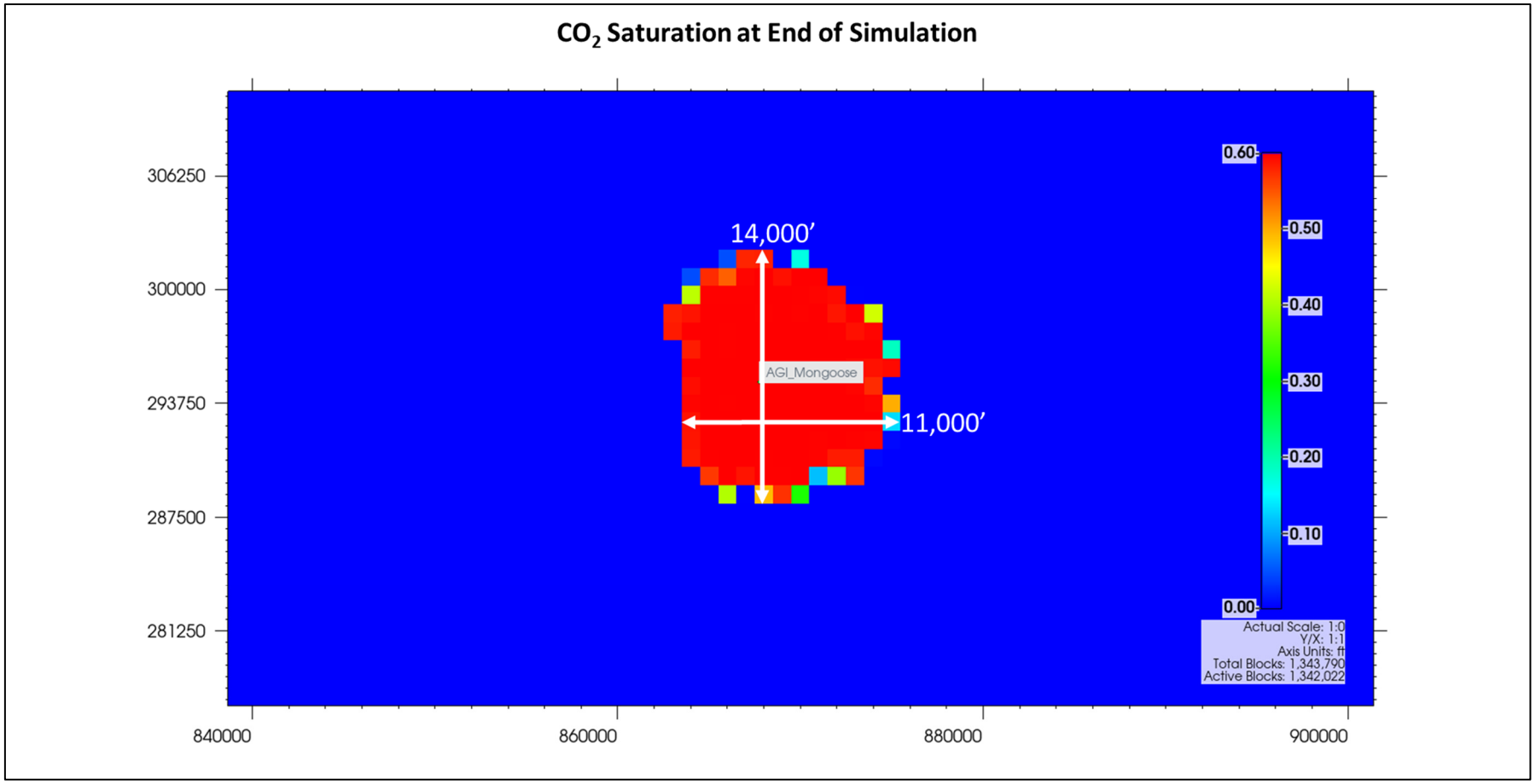

Figure 38 – Zoomed Areal View of Saturation Plume at 120 Years After Shut-in (End of Simulation)

The cross-sectional view of the Mongoose shows the extent of the plume from a side-view angle cutting through the formation at the wellbore. Figure 39 shows the maximum plume extent during the 40-year injection period. During this time, gas is injected into the permeable layers of the formation and travels predominantly laterally. Figure 40 shows the final extent of the plume after 120 years of migration. At this point in time, the effects of residual gas saturation and migration due to density drift are clearly shown. At least 30% of injected gas that travels into each grid cell is trapped as the gas travels mostly vertically, as it is less dense than the formation brine, until an impermeable layer is reached. Both figures are shown in a north-to-south view.

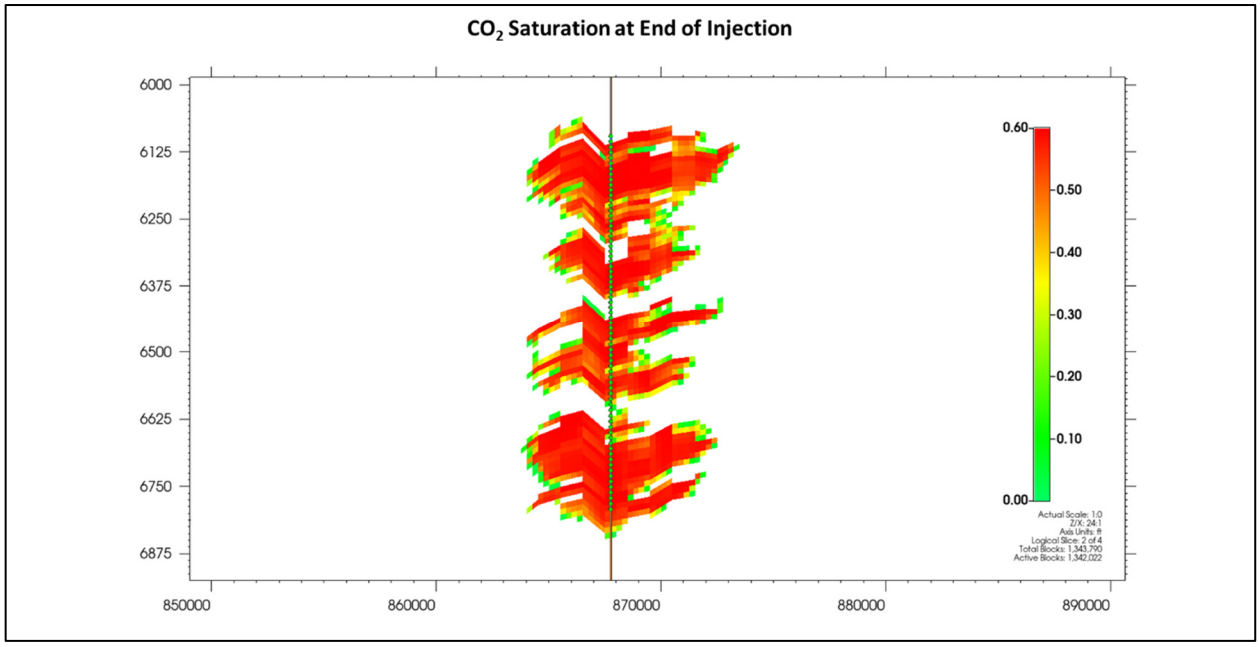

Figure 39 – North-South Cross-Sectional View of Gas Saturation Plume at Shut-in (End of Injection)

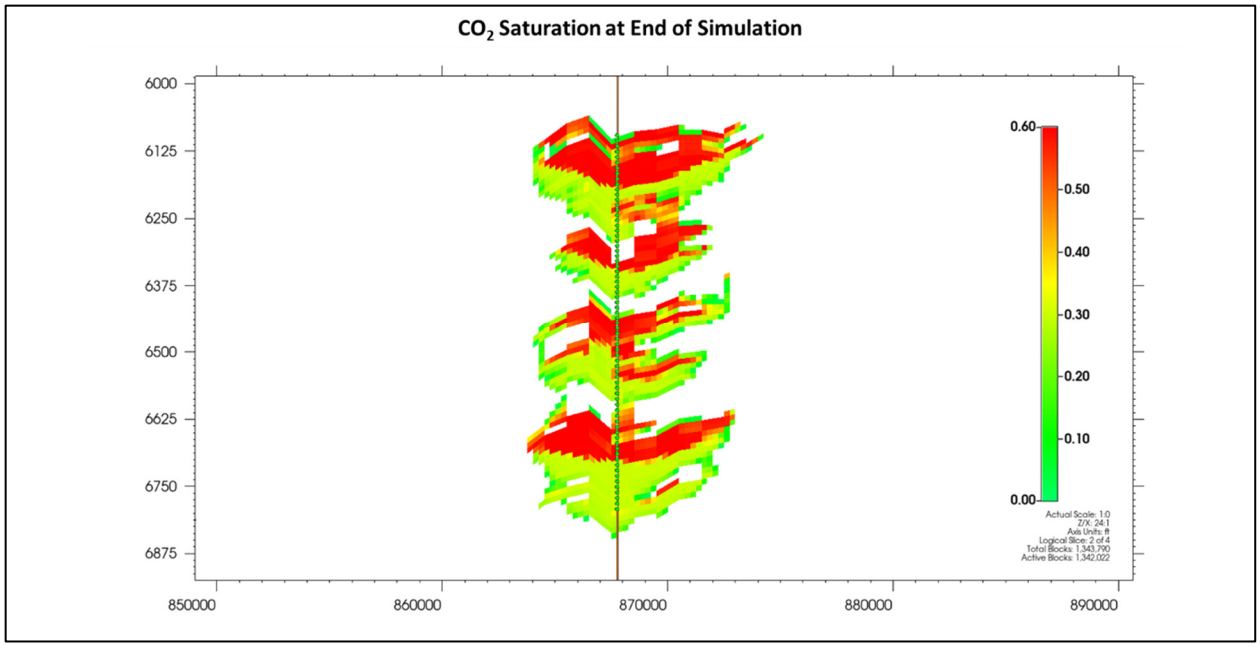

Figure 40 –North-South Cross-Sectional View of Gas Saturation Plume at 120 Years After Shut-in (End of Simulation)

Figure 41 shows the surface injection rate, bottomhole pressures, and surface pressures over the injection period and the period of density drift after injection ceases. The bottomhole pressure increases the most as the injection rate begins, reaching a maximum pressure of 4,453 psig, then slightly decreases and remains constant. This buildup of 550 psig keeps the bottomhole pressure below the fracture pressure of 5,007 psig. The maximum surface pressure associated with the maximum bottomhole pressure reached is 2,008 psig, well below the maximum allowable 2,500 psig per the TRRC UIC permit for this well. At roughly 30 years into injection for the Mongoose, all SWD wells included in the model have ceased injection. Due to the shut-in of offset SWD wells, the pressure effects within the formation are felt by the Mongoose. When this occurs, the bottomhole pressure decreases by 50 psig and surface pressure decreases by 40 psig. Bottomhole and wellhead pressures over time are in Table 11.

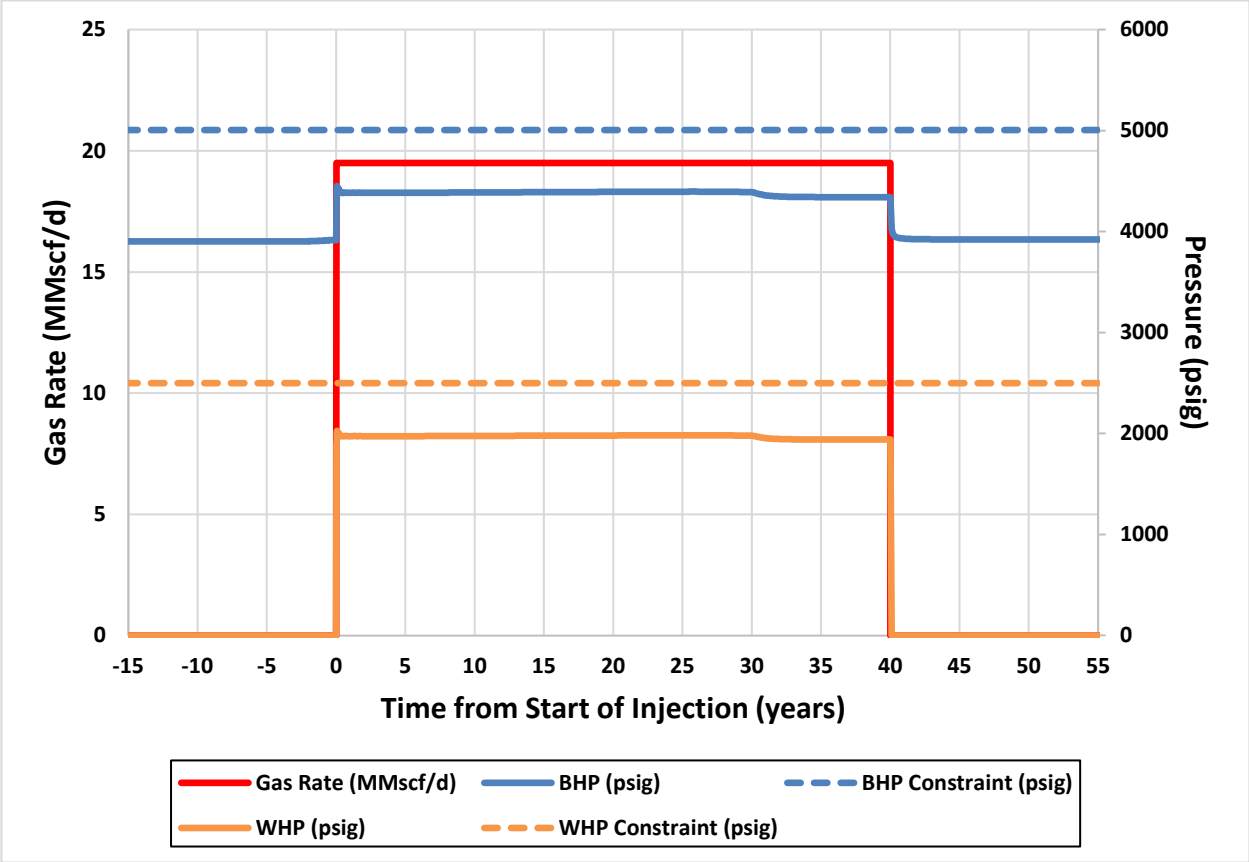

Figure 41 – Well Injection Rate and Bottomhole and Surface Pressures Over Time

Table 11 – Bottomhole and Wellhead Pressures Over Time from Start of Injection

Time from Start of Injection (years)	BHP (psig)	WHP (psig)
0	3,916	-
10	4,389	1,977
20	4,394	1,982
30	4,393	1,980
40	4,343	1,942
50	3,923	-
120	3,919	-

SECTION 3 – DELINEATION OF MONITORING AREA

This section discusses the delineation of both the maximum monitoring area (MMA) and active monitoring area (AMA) as described in 40 CFR **§98.448(a)(1)**.

3.1 Maximum Monitoring Area

The MMA is defined as equal to or greater than the area expected to contain the free-phase CO_2 plume until the plume has stabilized, plus an all-around buffer zone of at least half a mile. Numerical simulation was used to predict the size and drift of the plume. With CMG's GEM software package, reservoir modeling was used to determine the areal extent and density drift of the plume. The model considers the following:

- Offset well logs to estimate geologic properties
- Petrophysical analysis to calculate the heterogeneity of the rock
- Geological interpretations to determine faulting and geologic structure
- Offset injection history to adequately predict the density drift of the plume

Bayswater's expected gas composition was used in the model. The acid gas injectate is estimated at a molar composition of 58.8% H_2S and 41.2% CO_2, with trace amounts of other constituents. Upon the Plant achieving stable operations, a representative injectate sample will be collected and analyzed by a third-party laboratory. If the actual gas analysis varies materially from the injectate composition herein, an update to this MRV plan will be provided. As discussed in *Section 2*, the gas will be injected into the Ellenberger formation. The geomodel was created based on the rock properties of the Ellenberger.

The plume boundary was defined by the weighted average gas saturation in the aquifer. A value of 3% gas saturation was used to determine the boundary of the plume. When injection ceases in Year 40, the areal expanse of the plume will be 2,192 acres. The maximum distance between the wellbore and the edge of the plume is approximately 1.25 miles to the southeast. After 120 additional years of density drift, the areal extent of the plume is 3,280 acres with a maximum distance to the edge of the plume of approximately 1.5 miles to the southeast.

Figure 42 shows the plume boundary at the end of injection, the stabilized plume boundary, and the MMA. The MMA is depicted in this figure by taking the stabilized plume boundary after 120 years of density drift, and adding an all-around buffer zone of one half mile.

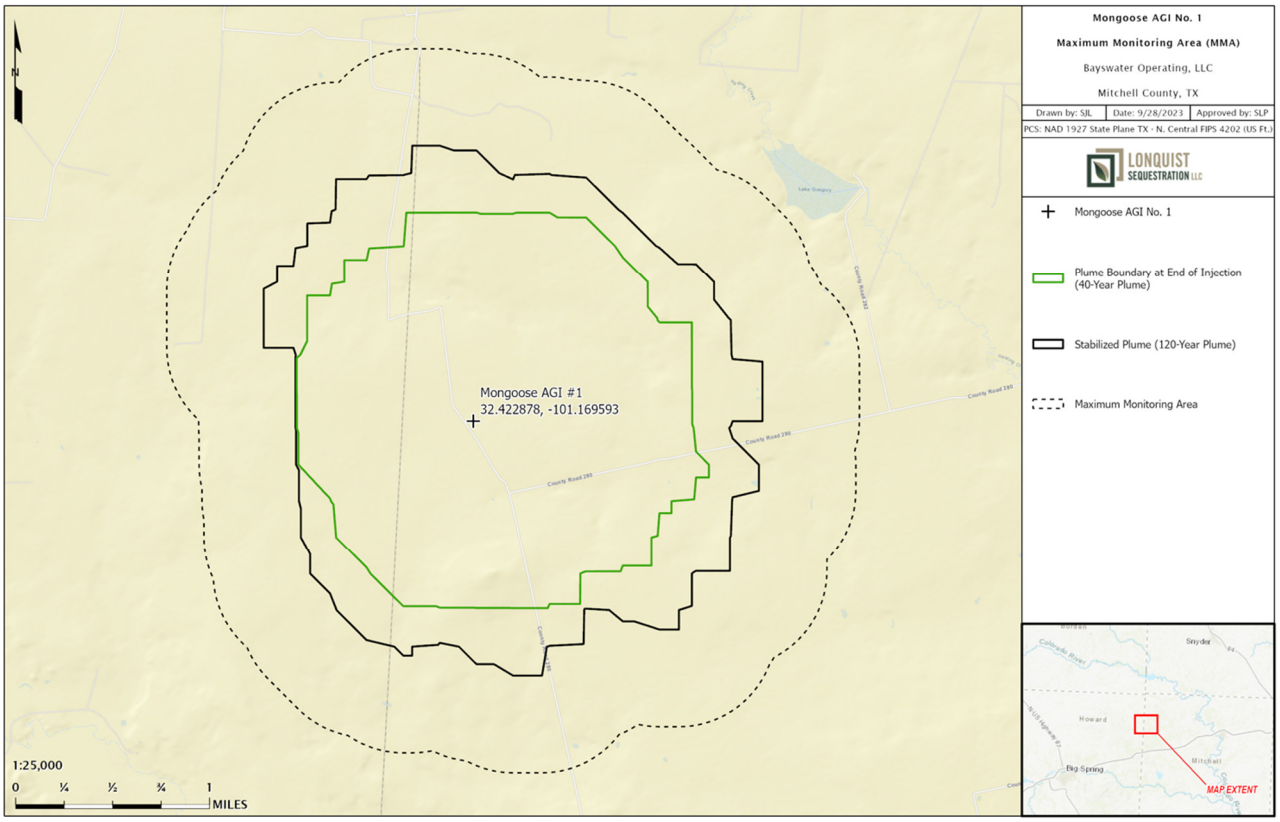

Figure 42 – Plume Boundary at End of Injection, Stabilized Plume Boundary, and Maximum Monitoring Area

3.2 Active Monitoring Area

The initial AMA will cover a 12-year period, which equates to almost one third of the expected injection lifecycle. This provides Bayswater sufficient time to develop its asset base, achieve steady operations, and evaluate any potential modifications to the MRV plan.

The AMA will be established by superimposing the area based on a half-mile buffer around the anticipated plume location after 12 years of injection (2036), with the area of the projected free-phase CO_2 plume at five additional years (2041). In this case, the plume boundary in 2041 is within the plume in 2036 plus a half-mile buffer. By 2036, a revised MRV plan will be submitted to define a new AMA. Figure 43 shows the area covered by the AMA.

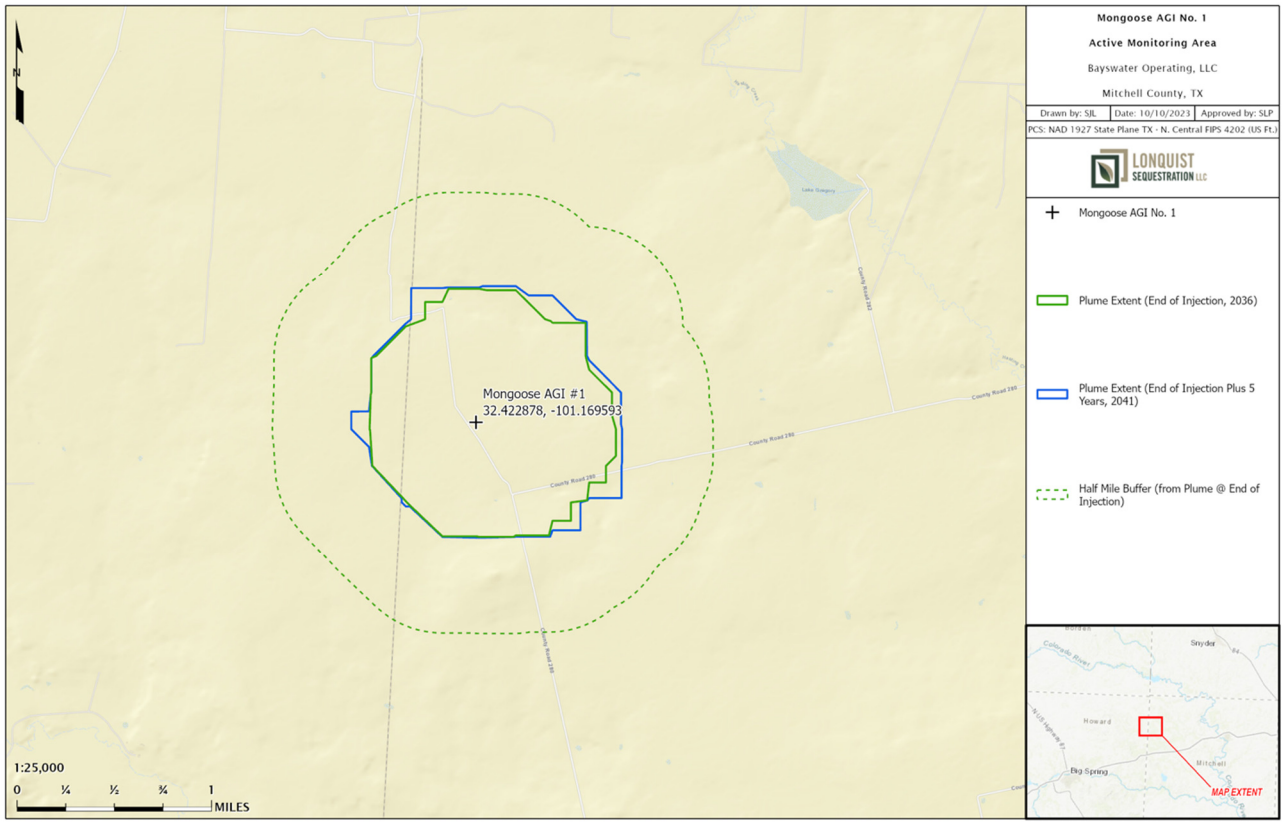

Figure 43 – Active Monitoring Area

SECTION 4 – POTENTIAL PATHWAYS FOR LEAKAGE

This section identifies the potential pathways for CO_2 to leak to the surface within the MMA. Also included are the likelihood, magnitude, and timing of such leakage. The potential leakage pathways are:

- Leakage from surface equipment
- Leakage through existing wells within the MMA
- Leakage through faults and fractures
- Leakage through the confining layer
- Leakage from natural or induced seismicity

Table 12 – Potential Leakage Pathway Risk Assessment

Potential Leakage Pathway	Likelihood		Magnitude	Timing
Surface Equipment	Possible during injection operations.	Low	Low. Automated systems will detect leaks and execute shut-down procedures.	During active injection period. Thereafter the well will be plugged.
Existing wells within the MMA	Unlikely. Two artificial penetrations were drilled into the gross injection interval. These wells were plugged in accordancee TRRC requirements.	Low	Low. Vertical migration of CO_2 would likely enter a shallower hydrocarbon production zone.	During active injection.
Faults and fractures	Unlikely. There are no faults within the modeled area. Bayswater monitors the area for seismic activity.	Low	Low. Vertical migration of CO_2 would likely enter a shallower hydrocarbon production zone.	During active injection.
Upper confining layer	Unlikely. The lateral continuity of the Woodford Shale blanketing the Ellenburger is recognized as a very competent seal. There is 7,825' of overburden between the Injection Interval and the base of the USDW.	Low	Low. Vertical migration of CO_2 would likely enter a shallower hydrocarbon production zone.	During active injection.
Natural or induced seismicity	Unlikely. There have been no seismic events of 3.0 magnitude or greater detected. There is over 7,825' of overburden between the Injection Interval and the base of the USDW.	Low	Low. Vertical migration of CO_2 would likely enter a shallower hydrocarbon production zone.	During active injection.

Magnitude Assessment Description
Low - catergorized as little to no impact to safety, health and the environment and the costs to mitigate are minimal.
Medium - potential risks to the USDW and for surface releases does exist, but circumstances can be easily remediated.
High - danger to the USDW and significant surface release may exist, and if occurs this would require significant costs to remediate.

4.1 Leakage from Surface Equipment

The Plant and Mongoose are newly designed and constructed facilities for treating and injecting acid gas with the fundamental objective of ensuring maximum safety for the public, the employees, and the environment. These are depicted in Figures 44 and 45. The facilities have been designed to minimize leakage and failure points, following applicable National Association of Corrosion Engineers (NACE) and American Petroleum Institute (API) standards and best practices. Monitors for H_2S are installed at key locations around the Plant as depicted on the site plan in Appendix B-2. These devices are continuously monitored by the Supervisory Control and Data Acquisition (SCADA) system and will alarm at set points based on H_2S exposure limits set by the Occupational Safety and Health Administration (OSHA). These exposure limits are incorporated in the gas dispersion model provided to the TRRC with the Class II AGI application. OSHA sets the detection or exposure limits at 15 ppm as the High Alarm and the High- High Alarm or Facility Shutdown limit at 40 ppm.

The facilities have been designed and constructed with important safety systems to provide safe operations. These systems include emergency shutdown (ESD) valves, with high- and low-pressure shutoff settings to isolate the Plant and the Mongoose well. Bayswater has installed a flare stack to safely depressure piping and equipment if an event occurs. These valves, gas monitors, and the gas flow meter are called out in the detailed site plan in Appendix B-2. Data from this flow meter will be used in the calculations of the total mass of CO_2 (in metric tons) in the CO_2 stream injected each year, per 40 CFR **§98.444(b)**.

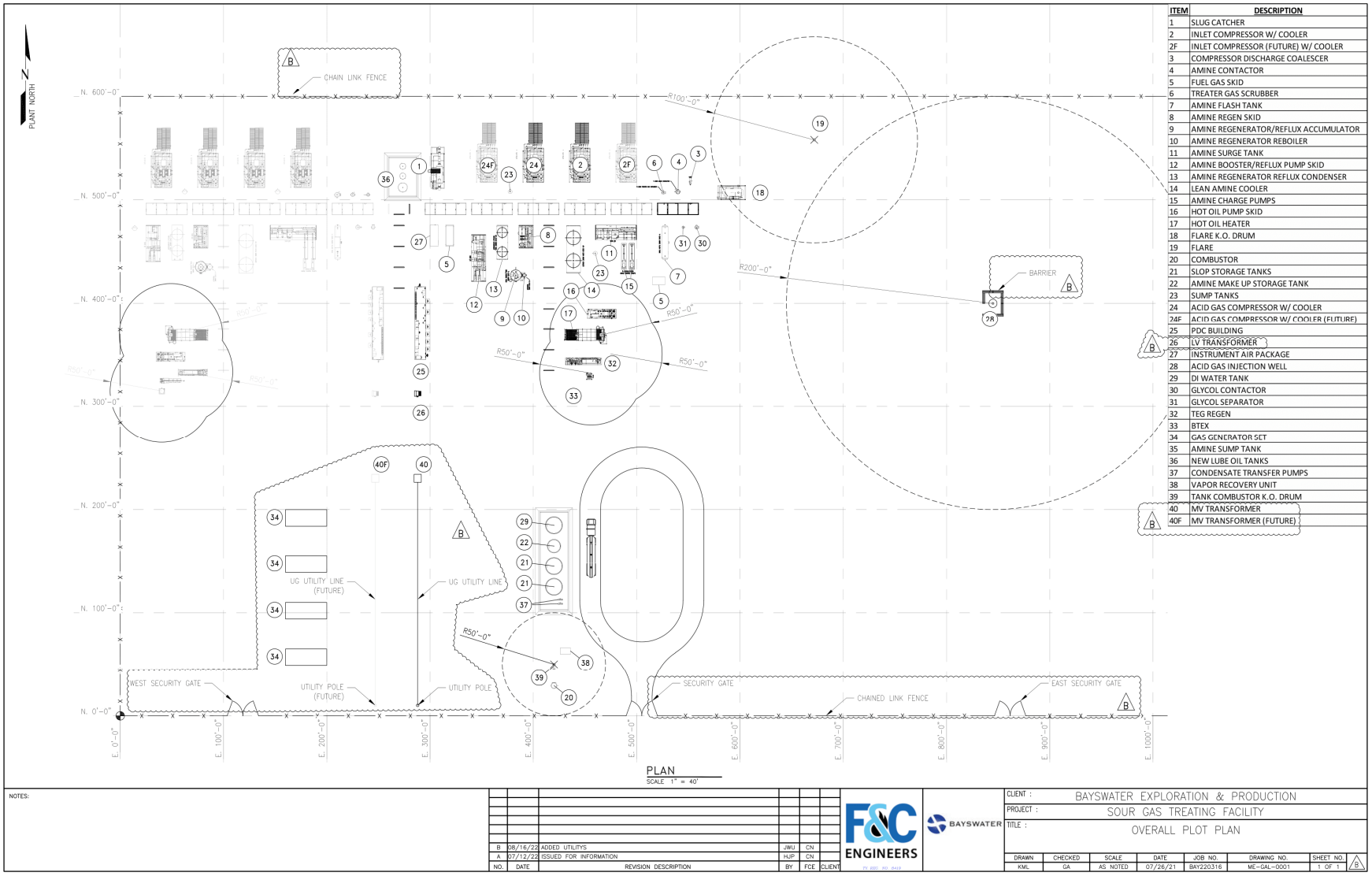

ITEM	DESCRIPTION
1	SLUG CATCHER
2	INLET COMPRESSOR W/ COOLER
2F	INLET COMPRESSOR (FUTURE) W/ COOLER
3	COMPRESSOR DISCHARGE COALESCER
4	AMINE CONTACTOR
5	FUEL GAS SKID
6	TREATER GAS SCRUBBER
7	AMINE FLASH TANK
8	AMINE REGEN SKID
9	AMINE REGENERATOR/REFLUX ACCUMULATOR
10	AMINE REGENERATOR REBOILER
11	AMINE SURGE TANK
12	AMINE BOOSTER/REFLUX PUMP SKID
13	AMINE REGENERATOR REFLUX CONDENSER
14	LEAN AMINE COOLER
15	AMINE CHARGE PUMPS
16	HOT OIL PUMP SKID
17	HOT OIL HEATER
18	FLARE K.O. DRUM
19	FLARE
20	COMBUSTOR
21	SLOP STORAGE TANKS
22	AMINE MAKE UP STORAGE TANK
23	SUMP TANKS
24	ACID GAS COMPRESSOR W/ COOLER
24F	ACID GAS COMPRESSOR W/ COOLER (FUTURE)
25	PDC BUILDING
26	LV TRANSFORMER
27	INSTRUMENT AIR PACKAGE
28	ACID GAS INJECTION WELL
29	DI WATER TANK
30	GLYCOL CONTACTOR
31	GLYCOL SEPARATOR
32	TEG REGEN
33	BTEX
34	GAS GENERATOR SET
35	AMINE SUMP TANK
36	NEW LUBE OIL TANKS
37	CONDENSATE TRANSFER PUMPS
38	VAPOR RECOVERY UNIT
39	TANK COMBUSTOR K.O. DRUM
40	MV TRANSFORMER
40F	MV TRANSFORMER (FUTURE)

Figure 44 – Site Plan

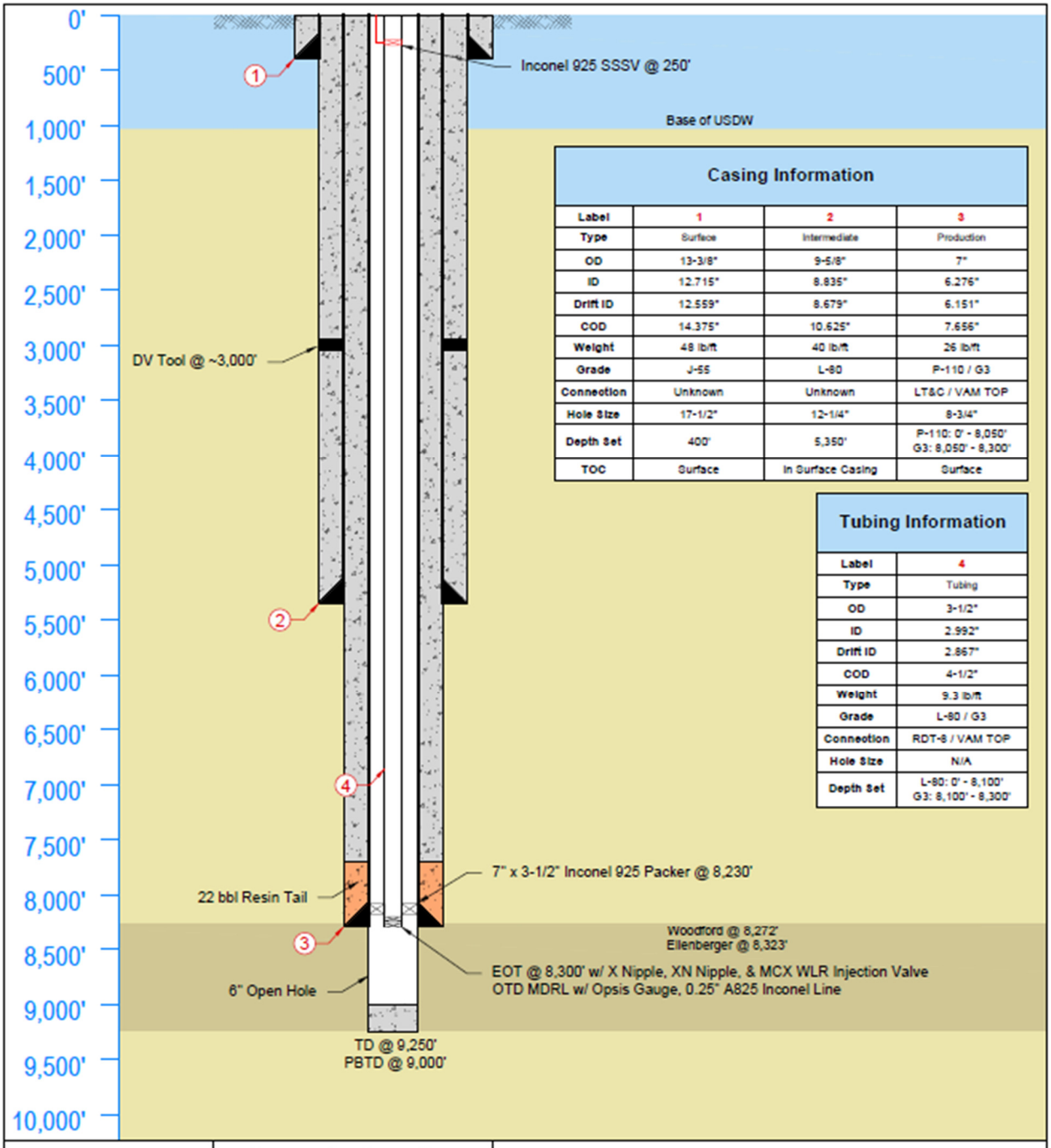

Figure 45 – Mongoose AGI No. 1 Wellbore Schematic

With the level of monitoring implemented at the Plant, a release of CO_2 would be quickly identified, and the safety systems and protocols would minimize the release volume. The acid gas stream injected into the well could include trace amounts of methane, nitrogen, and other compounds. The CO_2 injected into the AGI well is from the amine treater in the Plant adjacent to the Mongoose. Bayswater will increase its future injection volumes from its own gas production and possibly other sources. However, the gas composition is not expected to materially change due to the consistency of the surrounding production. If any leakage were to be detected, the volume of CO_2 released would be quantified based on the operating conditions at the time of release, as stated in *Section 7* in accordance with 40 CFR **§98.448(a)(5)**. Bayswater concludes that the leakage of CO_2 through the surface equipment is unlikely.

4.2 Leakage Through Existing Wells Within the MMA

The Mongoose was designed to prevent migration from the injection interval to the surface through a special casing and cementing design as depicted in the schematic provided in Figure 45. Mechanical integrity tests (MITs), required under Statewide Rule (SWR) **§3.46** [40 CFR **§146.23 (b)(3)**], will take place every 5 years to verify that the well and wellhead can contain the appropriate operating pressures. If the MIT were to indicate a leak, the well would be isolated and the leak mitigated to prevent leakage of the injectate to the atmosphere.

A map of all oil and gas wells within the MMA is shown in Figure 46. The MMA review map and a summary of all wells in the MMA is provided in *Appendix C*. Figure 47 highlights that only two wells penetrate the MMA's gross injection zone. These wells were non-productive and have been plugged and abandoned in accordance with TRRC requirements. Bayswater will perform baseline soil gas sampling prior to the implementation of the MRV plan and subsequent injection records. In addition, annual soil gas samples will be taken in the area adjacent to artificial penetrations and analyzed by a third-party lab. The results, should they indicate an issue with the sequestered CO_2 will be presented in the annual report to the GHGRP.

The summary of all oil and gas wells in *Appendix C* also provides the total depth (TD) of all wells within the MMA. Those wells that are shallower and do not penetrate the injection zone are isolated by the Woodford Shale as discussed in *Section 2.2.2*. The Woodford Shale provides 50 feet or more of contiguous low permeable shale and its presence in offset wells within the MMA indicates lateral continuity, migration of the fluid above the injection zone into shallower offset artificial penetrations is unlikely.

Bayswater is the operator of many of the shallower offset oil and gas wells within the MMA and frequently performs gas analysis on their production volumes. If a material variance in the quantity of CO_2 produced is indicated, Bayswater would investigate to determine the affected well(s), the root cause of the CO_2 increase to formulate a resolution plan and utilize the gas analysis variance to calculate any adjustments to reported volumes.

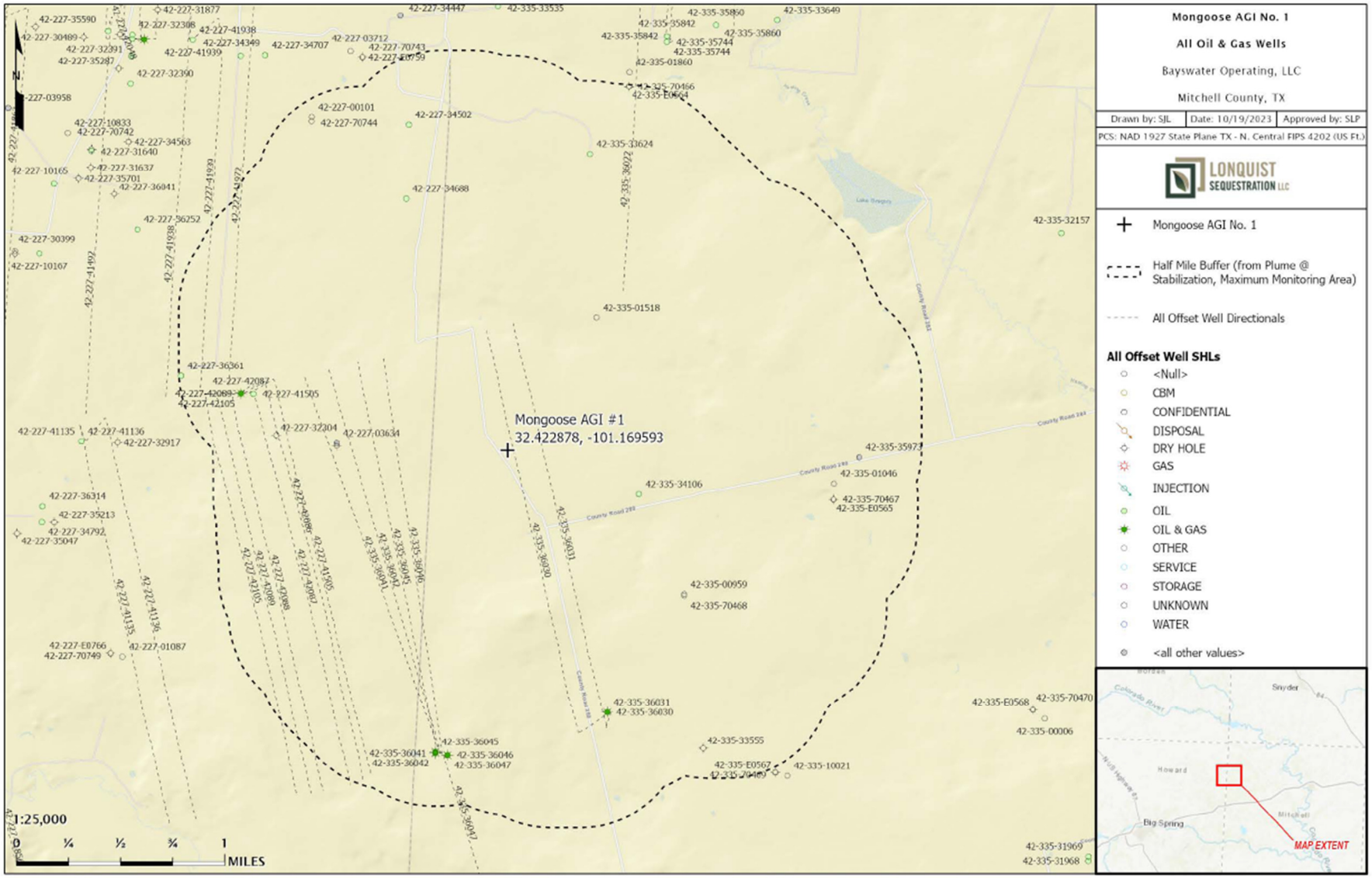

Figure 46 – All Oil and Gas Wells Within the MMA

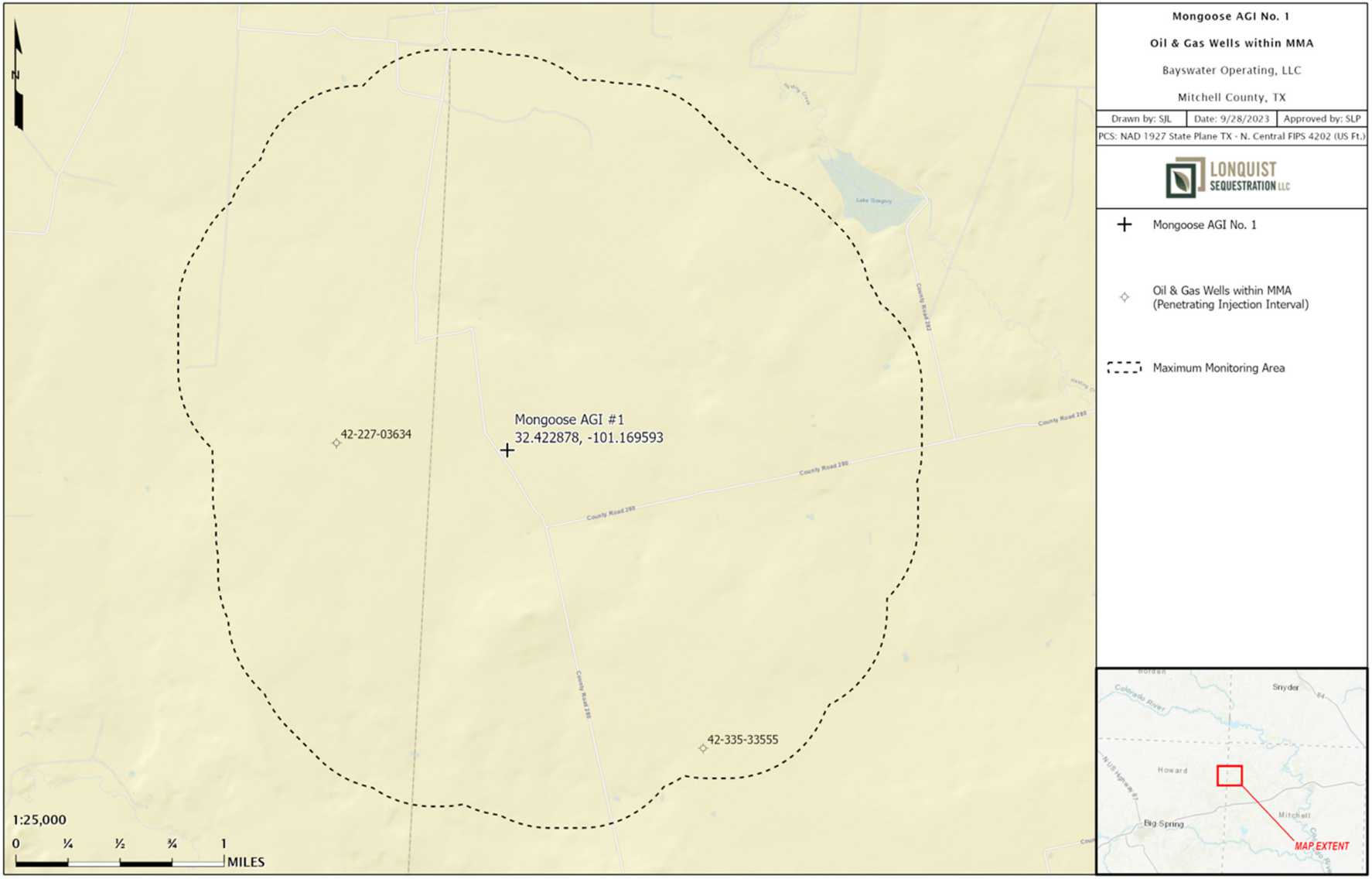

Figure 47 – Oil and Gas Wells Penetrating the Gross Injection Interval Within the MMA

4.2.1 Future Drilling

Potential leak pathways caused by future drilling in the area are not expected to occur. The deeper formations, Cambrian, have proven to date to be nonproductive in this area. Furthermore, any drilling permits issued by the TRRC in the area of the Mongoose will include a list of formations for which operators are required to comply with TRRC Rule 13 (entitled Casing, Cementing, Drilling, Well Control, and Completion Requirements), 16 TAC **§3.13**. The Mongoose drilling permit, provided in *Appendix A*, serves as an example. The Ellenburger is among the formations listed for which operators in Mitchell County and District 8 (where the Mongoose is located) are required to comply with TRCC Rule 13. The rule requires oil and gas operators to set steel casing and cement either (1) across and above all formations permitted for injection under TRRC Rule 9, or (2) immediately above all formations permitted for injection under Rule 46, for any well proposed within a quarter-mile radius of an injection well. In this instance, any new well permitted and drilled to the injection zone and located within a quarter-mile radius of the Mongoose will be required under TRRC Rule 13 to set steel casing and cement above the well's injection zone. Additionally, Rule 13 requires operators to case and cement across and above all potential flow zones and zones with corrosive formation fluids. The TRRC maintains a list of such known zones by TRRC district and county and provides that list with each drilling permit issued (also provided in the permit in *Appendix A*).

4.2.2 Groundwater Wells

A groundwater well search results found three wells within the MMA, as identified by the Texas Water Development Board. A field investigation was performed to validate the existence and location of these wells. However, none of the wells listed in the database could be located. An exhaustive search of well records was performed and no completion reports and/or plugging records were found. The result is there are no groundwater wells to monitor as none exist within the MMA.

The surface, intermediate, and production casing strings in the Mongoose, as shown in Figure 45, are designed to protect the shallow freshwater aquifers, consistent with applicable TRRC regulations and the GAU letter issued for this location (and included in *Appendix A*). The wellbore casings and specialty cements also prevent CO_2 leakage to the surface along the borehole. Bayswater concludes that leakage of the sequestered CO_2 to the groundwater aquifer is unlikely.

4.3 Leakage Through Faults and Fractures

No faults were interpreted at the Ellenburger level within the 3D seismic coverage in the area of the Mongoose. This includes areas well outside of the simulated plume boundary. Therefore, there is little to no risk of injectate leakage through faults in the region.

In the event of an unmapped fault existing within the plume boundary, any displacement caused by it would be too small to be detected through 3D seismic resolution. This displacement would be even smaller than the thickness of the Woodford Shale, effectively keeping it juxtaposed and preventing any vertical migration.

Porosity development within the injection intervals is primarily attributed to fractures and aerial exposure. However, these fractures are limited and do not extend into the upper confining unit, which helps mitigate the risk of migration through fractures outside of the designated injection interval.

4.4 Leakage Through the Confining Layer

The overlying Woodford formation acts as a competent sealing formation for the proposed Ellenburger injection interval. The Woodford contains ideal properties that will allow it to maintain sealing properties through the injection process. This is validated through the permeability and threshold entry pressure tests performed through the core analysis detailed in *Section 2*. If, in the most unlikely circumstance, the Woodford seal is compromised, additional tight Mississippian lime of roughly 168 ft lies above the Woodford Shale which would also act as an additional sealing interval. Additional confining strata that include salt, shale, and tight carbonates are present between the Mississippian lime and USDW, which would alleviate any threat of migration of the injection into the USDW.

4.5 Leakage from Natural or Induced Seismicity

The Mongoose is situated within the Eastern Shelf region, an area that has experienced a few minor seismic events along the edges of the 9.08-kilometer (km) radius recommended by the TRRC. Analyzing historical seismic data available on the USGS's Advanced National Seismic System website (spanning from 1971 until now) and the Bureau of Economic Geology's TexNet catalog (ranging from 2017 forward), as depicted in Figure 48, reveals that the closest seismic occurrence (unspecified whether natural or induced) took place just within the 9.08 km radius.

All seismic events depicted on the map were recorded at depths exceeding 20,000 ft, indicating their occurrence within the Precambrian basement rock. Additionally, none of the events had a magnitude of 3.0 or greater. Notably, the 3D seismic assessment did not indicate the presence of any faults or fracture zones. This absence suggests that any deep-seated seismic activities are unlikely to compromise the integrity of the upper confining unit. Consequently, the risks associated with injectate migration beyond the injection interval are unlikely.

Stringent operating procedures will be programmed into the SCADA and control systems to ensure that operating pressures stay below the fracture gradient of both the injection and confining intervals. Moreover, a combination of continuous well monitoring and monitoring of the TexNet site for activity will promptly identify any irregularities in the operations linked to seismic events.

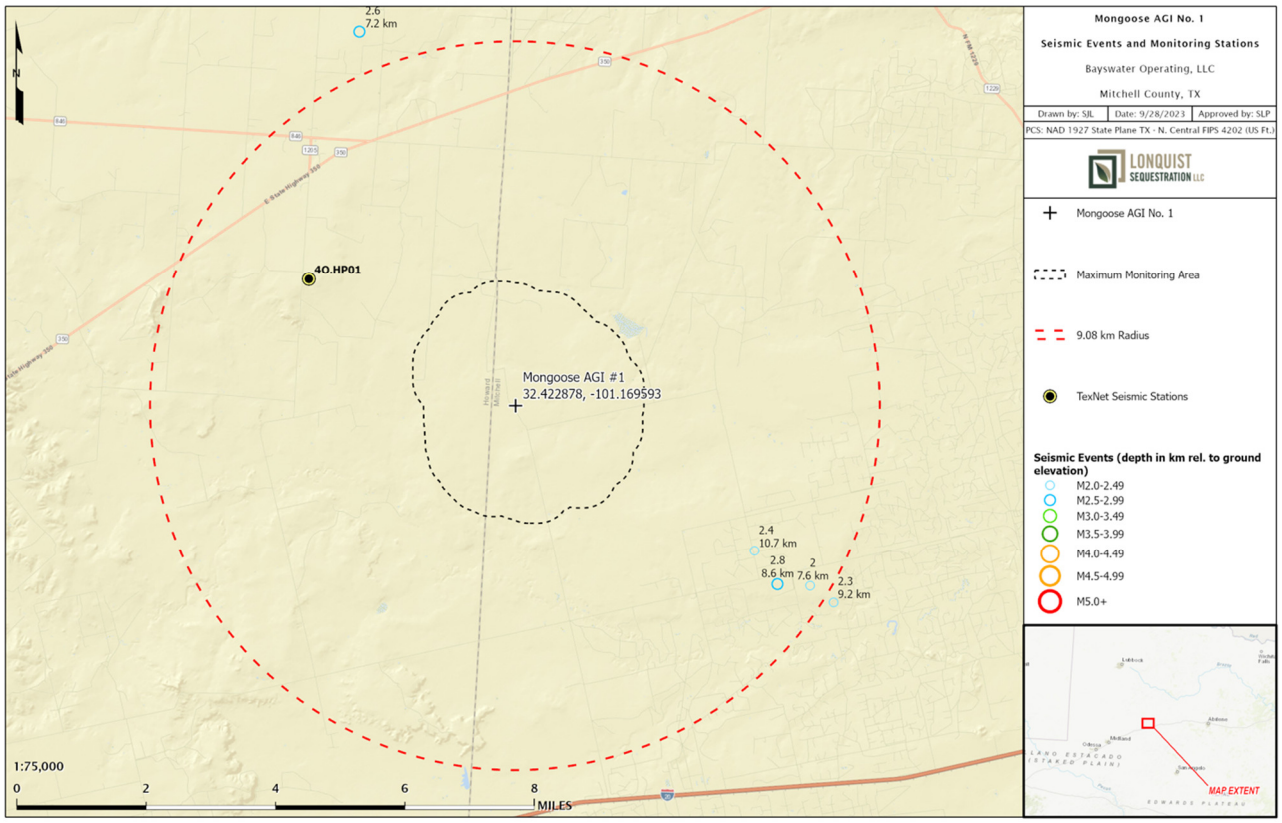

Figure 48 – Seismicity Review (TexNet – 08/04/2023)

SECTION 5 – MONITORING FOR LEAKAGE

This section discusses the strategy that Bayswater will employ for detecting and quantifying surface leakage of CO_2 through the pathways identified in *Section 4*, to meet the requirements of 40 CFR **§98.448(a)(3)**. As the injectate stream contains both H_2S and CO_2, the H_2S will be a proxy for CO_2 leakage and therefore the monitoring systems in place to detect H_2S will also indicate a release of CO_2. Table 13 summarizes the monitoring of the following potential leakage pathways to the surface. Monitoring will occur during the planned 40-year injection period or cessation of injection operations, plus a proposed 120-year post-injection period until the plume has stabilized.

- Leakage from surface equipment
- Leakage through existing and future wells within the MMA
- Leakage through faults, fractures, or confining seals
- Leakage through natural or induced seismicity

Table 13 – Summary of Leakage Monitoring Methods

Leakage Pathway	Monitoring Method
Leakage from surface equipment	Fixed H_2S monitors throughout the AGI facility
	Visual inspections
	SCADA continuous monitoring of the AGI facility
Leakage through existing wells	SCADA continuous monitoring of the AGI well
	Monitor CO_2 levels in Above Zone producing wells
	Mechanical Integrity Tests (MIT) of the AGI Well every 5 years
	Visual inspections
	Annual soil gas sampling at well locations that penetrate the Upper Confining Zone within the AMA
Leakage through groundwater wells	Annual groundwater samples from monitoring wells
Leakage from future wells	Compliance with TRRC Rule 13 Regulations
Leakage through faults and fractures	SCADA continuous monitoring at the AGI well (volumes and pressures)
	Monitor CO_2 levels in Above Zone producing wells
Leakage through the confining layer	SCADA continuous monitoring at the AGI well (volumes and pressures)
	Monitor CO_2 levels in Above Zone producing wells
Leakage from natural or induced seismicity	Monitor CO_2 levels in Above Zone producing wells
	Monitor existing TexNet station

5.1 Leakage from Surface Equipment

The Plant and the Mongoose were designed to operate in a manner that will reduce to the lowest factor the possibility of an escape of CO_2 and H_2S. Leakage from surface equipment is unlikely and would quickly be detected and addressed. The facility design minimizes leak points through the equipment used, and key areas are constructed with materials that are NACE and API compliant. A baseline atmospheric CO_2 concentration will be established during the commissioning of the Plant. Ambient H_2S monitors are located at the Plant and near the Mongoose for local alarm and are connected to the SCADA system for continuous monitoring.

The Plant is continuously monitored through automated systems. Details surrounding these systems can be found in *Appendix B*. The locations of H_2S detectors and Emergency Shutdowns are identified throughout the facility on the Appendix B-2 Site Plan. In addition, field personnel conduct routine visual field inspections of gauges, and gas monitoring equipment. The effectiveness of the internal and external corrosion control program is monitored through the periodic inspection of the corrosion coupons and inspection of the cathodic protection system. These inspections and the automated systems allow Bayswater to detect and respond to any leakage situation quickly. The surface equipment will be monitored for the injection and post-injection period. Should leakage be detected during active injection operations, the volume of CO_2 released will be calculated based on operating conditions at the time of the event, per 40 CFR **§98.448(a)(5)** and **§98.444(d)**.

Pressures, temperatures, and flow rates through the surface equipment are continuously monitored during operations. If a release occurred from surface equipment, the amount of CO_2 released would be quantified based on the operating conditions, including pressure, flow rate, percentage of CO_2 in the injectate, size of the leak-point opening, and duration of the leak. In the unlikely event a leak occurs, Bayswater will quantify the leak per the strategies discussed in *Section 7*.

5.2 Leakage Through Existing and Future Wells Within the MMA

Bayswater continuously monitors and collects injection volumes, pressures, and temperatures through their SCADA systems, for the Mongoose. This data is reviewed by qualified personnel and will follow response and reporting procedures when data exceeds acceptable performance limits. A change of injection or annular pressure would indicate the presence of a possible leak and be thoroughly investigated. In addition, an MIT will be performed every 5 years, as required by the TRRC and UIC. A failed MIT would also indicate the potential of a leak. Upon a negative MIT, the well would be isolated and the leak mitigated.

As discussed previously, Rule 13 ensures that new wells in the field would be constructed with proper materials and practices to prevent migration from the injection interval.

In addition to the fixed monitors described previously, Bayswater will also establish an in-field soil gas monitoring program to detect CO_2 leakage within the AMA. This would include sample collection and testing for CO_2 and H_2S at the AGI well site and near one of the identified artificial penetrations of the injection interval within the AMA. The samples will be analyzed by a qualified third party and used to establish a monitoring baseline. Prior to approval and implementation of

the MRV plan and through the post-injection site care period, Bayswater will have these monitoring systems in place.

There are currently only two wells that have been identified within the AMA that penetrate the Upper Confining Zone. As both wells have been plugged and abandoned in compliance with TRRC requirements, Bayswater believes a leak event is unlikely. Bayswater will perform soil gas sampling and analysis proximate to the Mongoose and one of the abandoned artificial penetrations by May 20, 2024. Thereafter, soil gas samples will be taken annually and analyzed by a third-party lab, and the results will be included in the annual report.

Bayswater is the operator of record for many oil and gas producing wells with the AMA. These wells will be used as a proxy for an above-zone monitoring well. If any CO_2, migrates up-hole, the CO_2 would likely end up in this formation. Since gas analysis is performed on a regular basis on the hydrocarbons produced from this formation, any material variance from historical data would indicate the potential of an issue needing further investigation. In the unlikely event a leak occurs, Bayswater will quantify the leak per the strategies discussed in *Section 7*, or as may be applicable provided in 40 CFR **§98.443** and **§98.444(d)** based on the actual leakage circumstance. It is not the intent of Bayswater to produce any of the CO_2 in this scenario but to use this as an indication of an event warranting further investigation.

5.2.1.1 Groundwater Quality Monitoring

As explained in *Section 4.2.2,* there are no groundwater wells within the MMA. Therefore, there are no groundwater wells to monitor.

5.3 Leakage Through Faults, Fractures, or Confining Seals

Bayswater continuously monitors the operations of the Mongoose well through automated systems. Any deviation from normal operating conditions indicating movement into a potential pathway, such as a fault or breakthrough of the confining seal, would trigger an alert due to a change in the injection pressure. Any such alert would be reviewed by field personnel and appropriate action would be taken, including shutting in the well, if necessary.

Bayswater will also monitor production from their oil and gas wells that do not penetrate the injection zone for any material variance in CO_2 content in the produced gas stream. Since gas analysis is very consistent over time, any material variance in the CO_2 content would be an early indicator of a potential issue. Should the CO_2 migrate vertically, the magnitude risk of this event is very low, as the reservoir provides an ideal containment given the Upper Confining Zone has successfully held hydrocarbons in place. In the unlikely event a leak occurs, Bayswater will quantify the leak per the strategies discussed in *Section 7*, or as may be applicable provided in 40 CFR **§98.443** and **§98.444(d)** based on the actual leakage circumstance.

5.4 Leakage Through Natural or Induced Seismicity

While the likelihood of a natural or induced seismicity event is extremely low, Bayswater plans to use the nearest TexNet seismic monitoring station to monitor the area of the Mongoose well. This station is approximately 3.5 miles west-northwest of the well location, as shown in Figure 49. This is a sufficient distance to allow for accurate and detailed monitoring of the seismic activity surrounding the Bayswater facility. Bayswater will monitor this station for any seismic activity that occurs in the area. If a seismic event of 3.0 magnitude or greater is detected, Bayswater will review the injection volumes and pressures of the AGI well to determine if any significant changes have occurred that would indicate potential leakage. In the unlikely event a leak occurs, Bayswater will quantify the leak per the strategies discussed in *Section 7*.

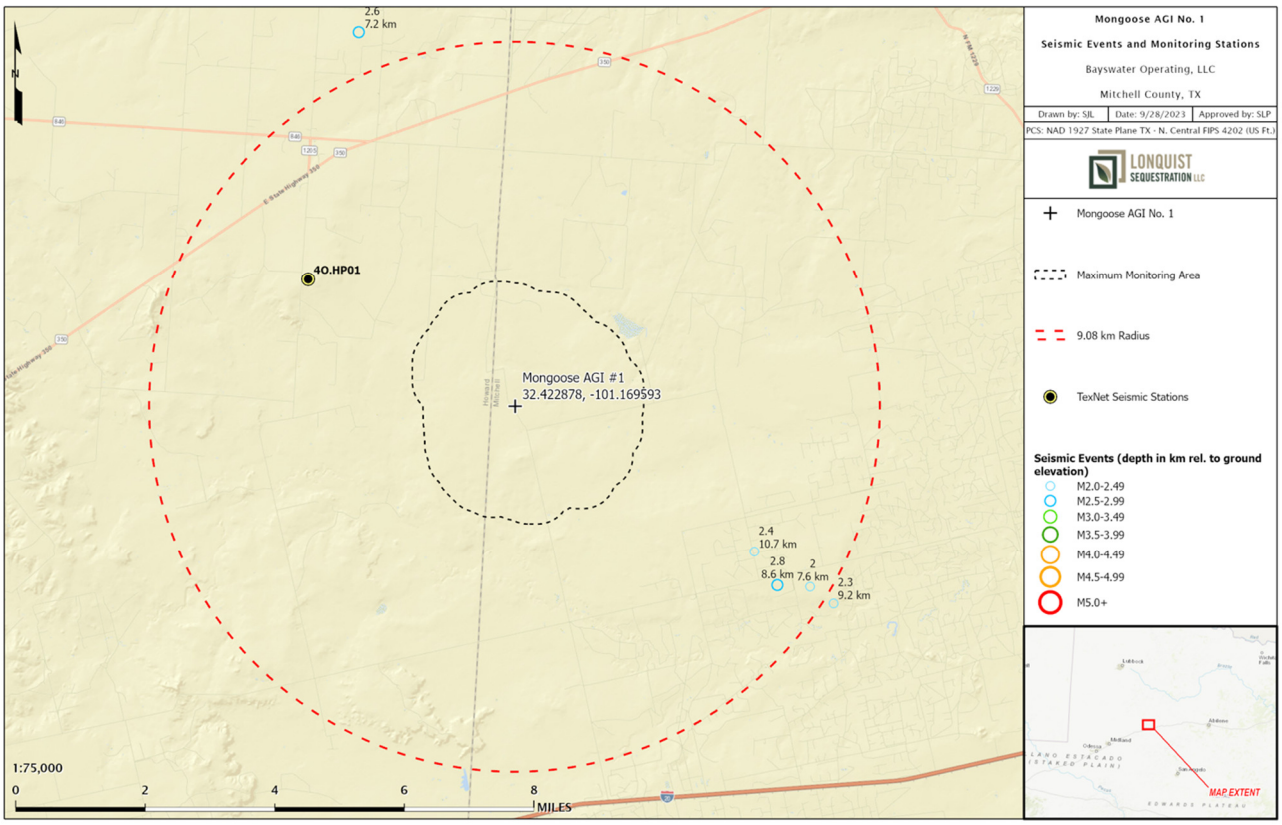

Figure 49 – Seismic Events and Monitoring Station

SECTION 6 – BASELINE DETERMINATIONS

This section identifies the strategies Bayswater will undertake to establish the expected baselines for monitoring CO_2 surface leakage per 40 CFR **§98.448(a)(4).** Bayswater will use the existing SCADA monitoring systems to identify changes from the expected performance that may indicate leakage of injectate and a corresponding amount of CO_2.

6.1 Visual Inspections

Regular inspections will be conducted by field personnel at the Plant and the Mongoose. These inspections will aid in identifying and addressing possible issues to minimize the risk of leakage. If any issues are identified, such as vapor clouds or ice formations, corrective actions will be taken in a prudent and safe manner to address such issues.

6.2 CO_2/H_2S Detection

In addition to the fixed gas monitors at the well site, Bayswater will perform an annual soil gas sampling program to detect any CO_2 leakage proximate to select artificial penetrations of the Upper Confining Zone within the AMA. The baseline determination will include atmospheric H_2S measurements at the AGI well and soil gas sampling near the AGI well and one of the abandoned artificial penetrations within the AMA.

These soil gas sample probes will be inserted below the surface. The probes have special material inserts that collect the gas samples over a 21-day period. These inserts are then removed and sent to a third-party lab to be analyzed for CO_2, H_2S, and trace contaminants typically found in a hydrocarbon gas stream. This initial sample collection is scheduled to be completed by May 20, 2024; a sufficient time period prior to the implementation of the MRV plan and will establish baseline values for future reference.

6.3 Operational Data

Upon starting injection operations, baseline measurements of injection volumes and pressures will be recorded. Any significant deviations over time will be analyzed for indication of leakage of acid gas and the corresponding component of CO_2.

6.4 Continuous Monitoring

The total mass of CO_2 emitted by surface leakage and equipment leaks will not be measured directly, as the injection stream for this project is well beyond the Occupational Safety and Health Administration (OSHA) Permissible Exposure Limit (PEL) 8-hour Time Weighted Average (TWA) of 5,000 ppm. Direct leak surveys are dangerous and present a hazard to personnel due to the presence of H_2S in the gas stream. Continuous monitoring systems will trigger an alarm if there is a release. The mass of the CO_2 released would be calculated based on the operating conditions,

including pressure, flow rate, percentage of CO_2, size of the leak-point opening, and duration. This method is consistent with 40 CFR **§98.448(a)(5)** and **§98.444(d)**, allowing the operator to calculate site-specific variables used in the mass balance equation.

In the case of a de-pressuring event, the acid gas stream will be diverted to a flare stack to be safely processed and vented. The event will be reported as required for the operation of the well.

SECTION 7 – SITE-SPECIFIC CONSIDERATIONS FOR MASS BALANCE EQUATION

This section identifies how Bayswater will calculate the mass of CO_2 injected, emitted, and sequestered. This also includes site-specific variables for calculating the CO_2 emissions from equipment leaks and vented emissions of CO_2 between the injection flow meter and the injection well, per 40 CFR **§98.448(a)(5)**.

7.1 Mass of CO_2 Received

Per 40 CFR **§98.443**, the mass of CO_2 received must be calculated using the specified CO_2 received equations "unless you follow the procedures in 40 CFR **§98.444(a)(4**)." 40 CFR **§98.444(a)(4)** states that "if the CO_2 you receive is wholly injected and is not mixed with any other supply of CO_2, you may report the annual mass of CO_2 injected that you determined following the requirements under paragraph (b) of this section as the total annual mass of CO_2 received instead of using Equation RR-1 or RR-2 of this subpart to calculate CO_2 received." The CO_2 received for this injection well is wholly injected and not mixed with any other supply; the annual mass of CO_2 injected will equal the amount received. Any future streams would be metered separately before being combined into the calculated stream.

7.2 Mass of CO_2 Injected

Per 40 CFR **§98.444(b)**, since the flow rate of CO_2 injected will be measured with a volumetric flow meter, the total annual mass of CO_2, in metric tons, will be calculated by multiplying the volumetric flow at standard conditions by the CO_2 concentration in the flow and the density of CO_2 at standard conditions, according to Equation RR-5:

$$CO_{2,u} = \sum_{p=1}^{4} Q_{p,u} * D * C_{CO_{2,p,u}}$$

Where:

$CO_{2,u}$ = Annual CO_2 mass injected (metric tons) as measured by flow meter u

$Q_{p,u}$ = Quarterly volumetric flow rate measurement for flow meter u in quarter p at standard conditions (standard cubic meters per quarter)

D = Density of CO_2 at standard conditions (metric tons per standard cubic meter): 0.0018682

$C_{CO2,p,u}$ = CO_2 concentration measurement in flow for flow meter u in quarter p (vol. percent CO_2, expressed as a decimal fraction)

p = Quarter of the year

u = Flow meter

7.3 Mass of CO_2 Produced

The Mongoose is not part of an enhanced oil recovery project; therefore, no CO_2 will be produced.

7.4 Mass of CO_2 Emitted by Surface Leakage

The mass of CO_2 emitted by surface leakage and equipment leaks will not be measured directly as the injection stream for this well contains high concentrations of H_2S. Direct leak surveys are dangerous and present a hazard to personnel. Because no venting is expected to occur, the calculations would be based on the unusual event that a blowdown is required and those emissions sent to a flare stack and reported as a part of the required GHG reporting for the Plant. Any leakage would be detected and managed as an upset event. Continuous monitoring systems should trigger an alarm upon a release of CO_2 and H_2S. The mass of the CO_2 released would be calculated for the operating conditions, including pressure, flow rate, size of the leak-point opening, and duration of the leak. This method is consistent with 40 CFR **§98.448(a)(5)**, allowing the operator to calculate site-specific variables used in the mass balance equation.

In the unlikely event that CO_2 was released because of surface leakage, the mass emitted would be calculated for each surface pathway according to methods outlined in the plan and totaled using Equation RR-10 as follows:

$$CO_{2E} = \sum_{x=1}^{X} CO_{2,x}$$

Where:

CO_{2E} = Total annual CO_2 mass emitted by surface leakage (metric tons) in the reporting year

$CO_{2,x}$ = Annual CO_2 mass emitted (metric tons) at leakage pathway x in the reporting year

X = Leakage pathway

Calculation methods using equations from Subpart W will be used to calculate CO_2 emissions due to any surface leakage between the flow meter used to measure injection quantity and the injection wellhead.

As discussed previously, the potential for pathways for all previously mentioned forms of leakage are unlikely. Given the possibility of uncertainty around the cause of a leakage pathway that is mentioned above, Bayswater believes the most appropriate method to quantify the mass of CO_2 released will be determined on a case-by-case basis. Any mass of CO_2 detected leaking to the surface will be quantified by using industry proven engineering methods including, but not limited to, engineering analysis on surface and subsurface measurement data, dynamic reservoir modeling, and history-matching of the sequestering reservoir performance, among others. In the unlikely event that a leak occurs, it will be addressed, quantified, and documented within the appropriate timeline. Any records of leakage events will be kept and stored as stated in *Section 10*.

7.5 Mass of CO_2 Sequestered

The mass of CO_2 sequestered in subsurface geologic formations will be calculated based on Equation RR-12. Since the Mongoose has commenced operations, Bayswater will begin collecting data for reporting under this plan based on the approval of this MRV plan and any applicable stipulations therein. The calculation of sequestered volumes utilizes the following equation as this well will not actively produce oil, natural gas, or any other fluids:

$$CO_2 = CO_{2I} - CO_{2E} - CO_{2FI}$$

Where:

CO_2 = Total annual CO_2 mass sequestered in subsurface geologic formations (metric tons) at the facility in the reporting year

CO_{2I} = Total annual CO_2 mass injected (metric tons) in the well or group of wells covered by this source category in the reporting year

CO_{2E} = Total annual CO_2 mass emitted (metric tons) by surface leakage in the reporting year

CO_{2FI} = Total annual CO_2 mass emitted (metric tons) from equipment leaks and vented emissions of CO_2 from equipment located on the surface, between the flow meter used to measure injection quantity and the injection wellhead, for which a calculation procedure is provided in subpart W of this part

CO_{2FI} will be calculated in accordance with Subpart W reporting of GHGs. Because no venting is expected to occur, the calculations would be based on an unusual event that a blowdown is required and those emissions are sent to a flare stack and reported as part of the required GHG reporting for the Plant.

- Calculation methods from Subpart W will be used to calculate CO_2 emissions from equipment located on the surface, between the flow meter used to measure injection quantity and the injection wellhead.

SECTION 8 – IMPLEMENTATION SCHEDULE FOR MRV PLAN

The Mongoose is a new injection well currently reporting under the TRRC Class II regulations. Bayswater is submitting this MRV application to the GHGRP to comply with the requirements of Subpart RR. The MRV plan will be implemented upon receiving EPA approval. The Annual Subpart RR Report will be filed on March 31 of the year following the reporting year.

SECTION 9 – QUALITY ASSURANCE

This section identifies how Bayswater plans to manage quality assurance and control to meet the requirements of 40 CFR **§98.444.**

9.1 Monitoring QA/QC

CO_2 Injected

- The flow rate of the CO_2 being injected will be measured with a volumetric flow meter, consistent with applicable industry standards. These flow rates will be compiled quarterly.
- The composition of the injectate stream will be measured upstream of the volumetric flow meter with a continuous gas composition analyzer or representative sampling consistent with applicable industry standards.
- The gas composition measurements of the injected stream will be averaged quarterly.
- The gas measurement equipment will be calibrated per the requirements of 40 CFR **§98.444(e)** and **§98.3(i)**.

CO_2 Emissions from Leaks and Vented Emissions

- Gas monitors within the Mongoose facility will be operated continuously, except for maintenance and calibration.
- Gas monitors will be calibrated according to the requirements of 40 CFR **§98.444(e)** and **§98.3(i)**.
- Calculation methods from Subpart W will be used to calculate CO_2 emissions from equipment located on the surface, between the flow meter used to measure injection quantity and the injection wellhead.

Measurement Devices

- Flow meters will be continuously operated except for maintenance and calibration.
- Flow meters will be calibrated according to 40 CFR **§98.3(i).**
- Flow meters will be operated and maintained in accordance with applicable standards as published by a consensus-based standards organization.

All measured volumes of CO_2 will be converted to standard cubic meters at a temperature of 60°F and an absolute pressure of 1 atmosphere.

9.2 Missing Data

In accordance with 40 CFR **§98.445**, Bayswater will use the following procedures to estimate missing data if unable to collect the data needed for the mass balance calculations:

- If a quarterly quantity of CO_2 injected is missing, the amount will be estimated using a representative quantity of CO_2 injected from the nearest previous period at a similar injection pressure.

- Fugitive CO_2 emissions from equipment leaks from facility surface equipment will be estimated and reported per the procedures specified in Subpart W of 40 CFR **§98.**

9.3 MRV Plan Revisions

If any changes outlined in 40 CFR **§98.448(d)** occur, Bayswater will revise and submit an amended MRV plan within 180 days to the Administrator for approval.

SECTION 10 – RECORDS RETENTION

Bayswater will retain records as required by 40 CFR **§98.3(g)**. These records will be retained for at least 3 years and include the following:

- Quarterly records of the CO_2 injected
  - Volumetric flow at standard conditions
  - Volumetric flow at operating conditions
  - Operating temperature and pressure
  - Concentration of the CO_2 stream
- Annual records of the information used to calculate the CO_2 emitted by surface leakage from leakage pathways.
- Annual records of the information used to calculate CO_2 emitted from equipment leaks and vented emissions of CO_2 from equipment located on the surface, between the flow meter used to measure injection quantity and the injection wellhead.

SECTION 11 - REFERENCES

Adams, D. C., & Keller, G. R. (1996). Precambrian Basement Geology of the Permian Basin Region of West Texas and Eastern New Mexico: A Geophysical Perspective1. *AAPG*.

Aird, P. (2019). *Deepwater Geology & Geoscience*. Retrieved from ScienceDirect: https://www.sciencedirect.com/topics/engineering/overburden-stress

Bradley, R. G., & Kalaswad, S. (2001). *Chapter 12: Dockum Aquifer in West Texas.* Texas Water Development Board.

Bennion, B., & Bachu, S. (2010). Drainage and Imbibition CO_2/Brine Relative Permeability Curves at Reservoir Conditions for Carbonate Formations. *SPE Annual Technical Conference and Exhibition.*

Comer, J. B. (1991). Stratigraphic Analysis of the Upper Devonian Woodford Formation, Permian Basin, West Texas asn Southeatern New Mexico. *BEG*.

Conselman, F. B. (1954). Preliminary Report on the Geology of the Cambrian Trend of West Central Texas. *Abilene Geologic Society*.

Domede, P. S. (2017). *Mechanical behaviour of granite. A compilation, analysis and correlation of data from around the world*. Retrieved from https://hal.insa-toulouse.fr/hal-01743870/document

Dutton, A. R., & Simpkins, W. W. (1986). *Hydrogeochemistry and Water Resources of the Triassic Lower Dockum Group in the Texas Panhandle and Eastern New Mexico.* Austin Tx: Bureau of Economic Geology.

Fanchi, J. R. (2010). Integrated Reservoir Asset Management .

Galley, J. (1958). Oil and Geology in the Permian Basin of Texas and New Mexico. *Basin or Areal Analysis or Evaluation*.

Gunn, R. D. (1982). Desmoinesian Depostional Systems in the Knox Baylor Trough. *North Texas Geological Society*.

Hendricks, L. (1964). STRATIGRAPHIC SUMMARY OF THE ELLENBURGER GROUP OF NORTH TEXAS. *Tulsa Geological Society Digest, Volume 32*.

Hornhach, M. J. (2016). Ellenburger wastwater injection and seismicity in North Texas. *Physics of the Earth and Planetary Interiors*.

Jesse G. White, P. P. (2014). Reconstruction of Paleoenvironments through Integrative Sedimentology and Ichnology of the Pennsylvanian Strawn Formation. *AAPG Southwest Section Annual Convention, Midland, Texas*.

Keelan, K., & Pugh, V. (1975). Trapped-Gas Saturations in Carbonate Formations. *SPE J. 15: 149–160.*

Kerans, C. (1990). Depositional Systems and Karst Geology of the Ellenburger Group (Lower Ordovician), Subsurface West Texas. *Bureau of Economic Geology*.

Lone Wolf Groundwater Conservation District. (2019). *Management Plan 2019-2024.* Colorado City, Tx.

Loucks, R. (2003). REVIEW OF THE LOWER ORDOVICIAN ELLENBURGER GROUP OF THE PERMIAN BASIN, WEST TEXAS. *Bureau of Economic Geology*.

Loucks, R. (2006). *Review of the Lower Ordovician Ellenburger Group of the Permian Basin, West Texas.* Austin, Tx: Bureau of Economic Geology.

Mason, C. C. (1961). GROUND-WATER GEOLOGY OF THE HICKORYSANDSTONE MEMBER OF THE RILEY FORMATION. McCULLOCH COUNTY. TEXAS. *TEXAS BOARD OF WATER ENGINEERS*.

Merrill, M., Slucher, E., Roberts -Ashby, T., Warwick, P., Blondes, M., Freeman, P., . . . Lohr, C. (2015). Geologic Framework for the National Assessment of Carbon Dioxide Storage Resources–Permian and Palo Duro Basins and Bend Arch-Fort Worth Basin. *USGS*.

Popova, O. (2020). Permian Basin Part 1 Wolfcamp, Bone Spring, Delaware shale plays of the Delaware Basin Geology Review. *USDOE*.

Powers, R. B. (1989). *Petroleum Exploration Plays and Resource Estimates, 1989, On shore United States -- Region 5, West Texas and Eastern New Mexico.* USGS.

Sanchez, T., Loughry, D., & Coringrato, V. (2019). Evaluating the Ellenburger Reservoir for Salt Water Disposal in the Midland Basin: An Assessment of Porosity Distribution Beyond the Scale of Karsts. *Unconventional Resources Technology Conference* (pp. 1-17). Denver: URTeC. doi:10.15530/urtec-2019-600

Scanlon, B. R., Reedy, R. C., Male, F., & Walsh, M. (n.d.). *Water Issues Related to Transitioning from Conventional to Unconventional Oil Production in the Permian Basin.* Austin: Bureau of Economic Geology.

Shamburger Jr., V. M. (1967). *Report 50: Ground-Water Resources of Mitchell and Western Nolan Counties, Texas.* Austin, Tx: Texas Water Development Board.

Snee, J.-E. L., & Zoback, M. D. (2018). State of stress in the Permian Basin, Texas and New Mexico: Implications for induced seismicity. *The Leading Edge*, 810-819.

Waite, L. (2021, October 25). Geology of the Permian Basin. UT Dallas Geoscience Permian Basin Research Lab.

Zerwer, N. Y. (1997). Stress Regimes in the Gulf Coast, Offshore Louisiana:. *AAPG Bulletin*, 293-307.